

# **Development of a Process for the Cleavage of a Mucin Fusion Protein by Enterokinase**

A Dissertation submitted to the

Technical Faculty

of the

Bielefeld University

For the degree of

Doctor of Natural Sciences (Dr. rer. nat.)

by

Tina Kubitzki

From

Muehlhausen / Thuringia, Germany

Bielefeld 2008



Presented 2008

Prof. Dr. Thomas Noll

---

First Referee

Prof. Dr. Christian Wandrey

---

Second Referee

30<sup>th</sup> March 2009

---

Date of Examination



*“Die Wissenschaft, richtig verstanden, heilt den Menschen von seinem Stolz;  
denn sie zeigt ihm seine Grenzen.  
(Albert Schweitzer)*

To my family  
And all the people who significantly influenced my personality



## Acknowledgments

The experimental work for the presented dissertation was carried out between October 2005 and September 2008 at the Institute of Biotechnology II of the Research Centre Juelich GmbH; Germany.

***This is a good time to thank a number of people, who supported me throughout this time and beyond...***

Prof. Dr. T. Noll for the design of this project, for always having time, although being far away in Bielefeld, for helpful suggestions and the interest in my work;

Prof. Dr. C. Wandrey for the opportunity to work on this project, for the excellent working conditions at the institute, for interesting discussions, helpful suggestions, the interest in the course of my work, and for functioning as co-referee;

Dr. S. Lütz for good supervision of the every-day work, the helpful and interesting discussions, as well as the motivation and personal support;

Ursula Mackfeld for her never-ending enthusiasm, even in hopeless times, her ideas and outstanding work in the laboratory;

Daniel Minör for his excellent work during his diploma thesis, the good cooperation with "Horst", for the challenging questions asked, and for the amazing atmosphere at work;

Meike Priehn und Elisabeth Zieger for the interest in my work and their engagement in learning something new;

Lilia Härter und Heike Offermann for their precious work in the organization of our laboratories, their continuous help in technical concerns and beyond this, and for their motivation;

my colleagues of room 126, especially Brigitte Osterath and Falk Hildebrand, for the interesting conversations and discussions, for the good working atmosphere, and for bringing laughter into a challenging time;

all other colleagues of the "Technical Biocatalysis" group for the excellent working atmosphere, for the constant will to help either in technical or theoretical questions, and for the fun throughout work;

## ACKNOWLEDGEMENT

---

Esther Knieps-Grünhagen and Petra Geilenkirchen for a lot of support with analytical questions;

all other colleagues of the Bioseparation group for fruitful discussions;

Dr. M. Oldiges for his support and the good cooperation with regard to microbial fermentation, for helpful discussions and suggestions as well as the interest in my work;

all members of the Fermentation group, especially Jochem Gätgens and Bianca Klein, for their help whenever it was needed,

Marianne Hess for her outstanding work in organizing the institute from the inside, and her readiness to help others;

the remaining members of the IBT-2 for their work making a smooth working routine possible, for the good working atmosphere and the wonderful time;

the colleagues of the IBT-1, especially Conny Gätgens, for her friendliness and kindness in sharing her laboratory and for smiling every day;

furthermore, members of the IMET for the good cooperation and the exchange of equipment;

the colleagues of the mechanical and electronic workshop for their creativity and the constant contribution to comfortable working;

Lisa Collins-Racie for the supply of the recombinant *E. coli* for enterokinase production;

and most important my family for their endless motivation and support and their imperturbable belief in me.



# Contents

<b><u>ABSTRACT</u></b>	<b><u>I</u></b>
<b><u>ZUSAMMENFASSUNG</u></b>	<b><u>II</u></b>
<b><u>ABBREVIATIONS</u></b>	<b><u>III</u></b>
<b><u>SYMBOLS</u></b>	<b><u>IV</u></b>
<b><u>1 INTRODUCTION</u></b>	<b><u>- 1 -</u></b>
1.1 ENTEROKINASE	- 1 -
1.2 FUSION PROTEINS	- 6 -
1.3 THE TARGET PROTEIN MUC1	- 10 -
<b><u>2 AIM OF THE PROJECT</u></b>	<b><u>- 17 -</u></b>
<b><u>3 INVESTIGATIONS CONCERNING MUC1-IGG2A FC</u></b>	<b><u>- 19 -</u></b>
3.1 THEORETICAL BACKGROUND	- 19 -
3.2 ISOLATION AND PURIFICATION OF MUC1-IGG2A FC	- 20 -
3.3 STABILITY OF MUC1-IGG2A FC	- 23 -
3.4 SUMMARY: MUC1-IGG2A FC	- 24 -
<b><u>4 ENTEROKINASE PRODUCTION</u></b>	<b><u>- 25 -</u></b>
4.1 THEORETICAL BACKGROUND	- 25 -
4.2 FERMENTATION OF ESCHERICHIA COLI	- 28 -
4.3 PRODUCT ISOLATION AND PURIFICATION	- 38 -
4.4 NEW EXPRESSION PLASMID	- 43 -
4.5 SUMMARY: ENTEROKINASE PRODUCTION	- 46 -
<b><u>5 ENZYME CHARACTERIZATION</u></b>	<b><u>- 49 -</u></b>
5.1 THEORETICAL BACKGROUND	- 49 -
5.2 SYNTHETIC SUBSTRATE GD <sub>4</sub> K-2NA	- 50 -
5.3 MUC1-IGG2A FC AS SUBSTRATE	- 53 -
5.4 SUMMARY: ENZYME CHARACTERIZATION	- 55 -

---

<b>6</b>	<b><u>IMMOBILIZATION OF ENTEROKINASE</u></b>	<b>- 57 -</b>
6.1	THEORETICAL BACKGROUND	- 57 -
6.2	IMMOBILIZATION ON POROUS BEADS	- 59 -
6.3	IMMOBILIZATION ON MAGNETIC PARTICLES	- 63 -
6.4	REACTION PARAMETERS OF IMMOBILIZED ENTEROKINASE	- 66 -
6.5	FUSION PROTEIN CLEAVAGE BY IMMOBILIZED ENTEROKINASE	- 67 -
6.6	REACTION KINETICS FOR MUC1-IGG2A FC CLEAVAGE BY IMMOBILIZED ENTEROKINASE	- 69 -
6.7	SUMMARY: IMMOBILIZATION	- 73 -
<b>7</b>	<b><u>APPLICATION OF THE IMMOBILIZED ENTEROKINASE IN FUSION PROTEIN CLEAVAGE</u></b>	<b>- 75 -</b>
7.1	THEORETICAL BACKGROUND	- 75 -
7.2	CONTINUOUS PROCESS	- 76 -
7.3	REPETITIVE BATCH EXPERIMENTS	- 78 -
7.4	SUMMARY: APPLICATION OF IMMOBILIZED ENTEROKINASE	- 82 -
<b>8</b>	<b><u>PRODUCT PURIFICATION</u></b>	<b>- 83 -</b>
8.1	IMPROVEMENT OF THE PURIFICATION PROCEDURE	- 83 -
8.2	SUMMARY: PRODUCT PURIFICATION	- 86 -
<b>9</b>	<b><u>CONCLUSION AND OUTLOOK</u></b>	<b>- 87 -</b>
9.1	SUPPLY OF THE REACTING PROTEINS	- 87 -
9.2	IMMOBILIZATION OF ENTEROKINASE	- 88 -
9.3	COMPARISON OF CSTR AND REPEATED UTILIZATION OF IMMOBILIZED ENTEROKINASE	- 89 -
9.4	COMPARISON OF SOLUBLE AND IMMOBILIZED ENTEROKINASE IN FUSION PROTEIN CLEAVAGE	- 91 -
9.5	PRODUCT PURIFICATION	- 94 -
9.6	OUTLOOK	- 95 -
<b>10</b>	<b><u>MATERIALS AND METHODS</u></b>	<b>- 97 -</b>
10.1	MATERIALS	- 97 -
10.2	METHODS	- 100 -

<b><u>11 APPENDIX</u></b>	<b>- 117 -</b>
<b>11.1 PERFUSION CULTURES OF CHO-K1</b>	<b>- 117 -</b>
<b>11.2 CHROMATOGRAMS OF PURIFIED PROTEINS BY IEC</b>	<b>- 119 -</b>
<b>11.3 IMMUNOBLOTTING FOR MUC1-IGG2A FC</b>	<b>- 120 -</b>
<b>11.4 ELISA FOR MUC1-IGG2A FC</b>	<b>- 122 -</b>
<b>11.5 THE CHALLENGE OF ANALYTICAL PROTEIN SEPARATION</b>	<b>- 124 -</b>
<b><u>12 REFERENCES</u></b>	<b>- 127 -</b>
<b><u>13 CURRICULUM VITAE</u></b>	<b>- 133 -</b>

## List of Figures

Figure 1-1	Activation of dietary proteins starting with trypsinogen by enterokinase.....	- 2 -
Figure 1-2	Catalytic triade. ....	- 3 -
Figure 1-3	Reaction mechanism of a serine protease. ....	- 4 -
Figure 1-4	Structure of enterokinase. ....	- 5 -
Figure 1-5	Target markets for new biopharmaceuticals.....	- 7 -
Figure 1-6	Pathway of O-linked glycosylation of MUC1 by the mammary gland for normal and malignant cells. ....	- 13 -
Figure 3-1	Protein structure of the fusion protein MUC1-IgG2a Fc.....	- 19 -
Figure 3-2	Detectable MUC1-IgG2a Fc after the first purification step using filtration. ....	- 21 -
Figure 3-3	Second purification step for MUC1-IgG2a Fc using ion exchange chromatography.....	- 22 -
Figure 3-4	Received fractions of MUC1-IgG2a Fc with the corresponding chromatogram (left) and the specific purity after IEC (right).....	- 22 -
Figure 3-5	Stability of MUC1-IgG2a Fc at pH 8 (representative SDS-PAGE). ....	- 23 -
Figure 4-1	Schematic drawing of the growth behavior of microorganisms in a batch fermentation...	- 26 -
Figure 4-2	Fermentation strategies: batch fermentation (left) and fed-batch fermentation (right) [16].....	- 27 -
Figure 4-3	Growth behavior of the expression strains <i>E. coli</i> K12 and <i>E. coli</i> BL21 in the pre-culture.....	- 29 -
Figure 4-4	Growth behavior of the expression strains <i>E. coli</i> K12 and <i>E. coli</i> BL21 in the main culture....	- 30 -
Figure 4-5	Glucose concentration during the fermentation process.....	- 34 -
Figure 4-6	Acetate formation of the expression hosts during fermentation. ....	- 36 -
Figure 4-7	Structure of the fusion protein DsbA/EK <sub>L</sub> for the production of the catalytic subunit of enterokinase. ....	- 38 -
Figure 4-8	Batch binding chamber used for the isolation of enterokinase by affinity chromatography.....	- 39 -
Figure 4-9	SDS-PAGE of isolated enterokinase using different technical setups.....	- 40 -
Figure 4-10	Enterokinase yields received by using an improved downstream process involving the use of a batch binding chamber for enzyme isolation ( <sup>a</sup> [18]). ....	- 41 -
Figure 4-11	Purification of isolated enterokinase using ion exchange chromatography. ....	- 42 -
Figure 4-12	Comparison of the two expression systems for the production of enterokinase.....	- 43 -
Figure 4-13	Results for isolation and purification of enterokinase using the new expression system...	- 44 -
Figure 4-14	Comparison of the final production processes for enterokinase.....	- 47 -
Figure 5-1	Determination of reaction parameters for the synthetic substrate GD <sub>4</sub> K-2NA.....	- 51 -
Figure 5-2	Determination of reaction parameters for MUC1-IgG2a Fc as substrate.....	- 54 -
Figure 6-1	Immobilization techniques. ....	- 58 -
Figure 6-2	Loading capacity of activated Sepabeads <sup>®</sup> EC-HA203.....	- 59 -
Figure 6-3	Influence of bound enzyme to enzyme activity.....	- 60 -
Figure 6-4	Immobilization of enterokinase on activated porous material. ....	- 61 -
Figure 6-5	Storage stability of enterokinase immobilized on Sepabeads <sup>®</sup> EC-HA203.....	- 62 -

LIST OF FIGURES

Figure 6-6	Half-life time and remaining activity of enterokinase immobilized on magnetic microspheres activated with glutardialdehyde. ....	63 -
Figure 6-7	Remaining activity (A) and half-life time (B) of enterokinase immobilized on paramagnetic microspheres activated with EDCA.....	65 -
Figure 6-8	Reaction parameters of immobilized enterokinase compared to the free enzyme. ....	66 -
Figure 6-9	Cleavage of MUC1-IgG2a Fc by free enterokinase. ....	67 -
Figure 6-10	Incubation of MUC1-IgG2a Fc in presence of the carrier material. ....	68 -
Figure 6-11	Cleavage reactions of MUC1-IgG2a Fc using enterokinase immobilized on different carrier. .	69 -
Figure 6-12	Reaction parameters for the cleavage of MUC1-IgG2a Fc by immobilized enterokinase (iEK). ....	70 -
Figure 6-13	Influence of immobilization on substrate surplus inhibition.....	71 -
Figure 7-1	Comparison of CSTR and batch reactor. ....	76 -
Figure 7-2	Continuous reactor setup for the cleavage of MUC1-IgG2a Fc by immobilized enterokinase..	77 -
Figure 7-3	Application of immobilized enterokinase (iEK) in repetitive fusion protein cleavage. ....	78 -
Figure 7-4	Repeated fusion protein cleavage by immobilized enterokinase (iEK) in the absence and presence of magnesium.....	81 -
Figure 8-1	Techniques applied for the purification of MUC1.....	84 -
Figure 8-2	SDS-PAGE of the obtained lyophilisates containing MUC1.....	85 -
Figure 8-3	Lyophilized MUC1 with a purity of 94 %.....	86 -
Figure 10-1	Simplified scheme of the expression vector for the fusion protein MUC1-IgG2a Fc. ....	100 -
Figure 10-2	Simplified scheme of the expression plasmids for enterokinase production as fusion protein DsbA/EK <sub>L</sub> . ....	101 -
Figure 10-3	Summary of the fermentation procedure for the production of enterokinase. ....	103 -
Figure 10-4	Batch binding cell containing Ni <sup>2+</sup> -IDA sepharose for the purification of the fusion proteins DsbA/EK <sub>L</sub> and DsbA-EK-H6. ....	106 -
Figure 10-5	Technical drawing of the 2-membrane module used for the isolation and purification of MUC1-IgG2a Fc from the cell culture medium.....	110 -
Figure 10-6	Size marker used for protein identification. ....	111 -
Figure 10-7	Example for data analysis of the ELISA.....	112 -
Figure 10-8	Applied analytical method for investigating the cleavage reaction of MUC1-IgG2a Fc using enterokinase.....	114 -
Figure 10-9	Reactor scheme for continuous cleavage reaction of MUC1-IgG2a Fc by immobilized enterokinase.....	115 -
Figure 11-1	Chromatograms received after ion exchange chromatography using HiPrep 16/10 QFF sepharose.....	119 -
Figure 11-2	Stacking scheme of blotting chamber for the transfer of proteins from SDS-gel to PVDF membrane. ....	120 -

## List of Tables

Table 1-1	Enzyme Nomenclature. Main enzyme classes and examples for the catalyzed reactions (modified) [60].	- 1 -
Table 1-2	Approved biopharmaceuticals produced as fusion proteins in industrial scale (added) [111].	- 9 -
Table 3-1	Concentrated MUC1-IgG Fc solutions received from different perfusion cultures of CHO-K1 cells after the first purification step.	- 20 -
Table 4-1	Selected methods for cell disruption.	- 28 -
Table 4-2	Growth rates $\mu$ of the expression hosts reached during batch phase.	- 31 -
Table 4-3	Final values for OD and CDW received in the main culture.	- 32 -
Table 4-4	Biomass yield in correlation with the utilized glucose and resulting biomass production rate.	- 33 -
Table 4-5	Rate of glucose consumption during batch fermentation.	- 33 -
Table 4-6	Rate of glucose consumption during fed-batch phase.	- 35 -
Table 4-7	Final acetate concentrations measured during large scale fermentation.	- 37 -
Table 4-8	Activity and amount of isolated enterokinase produced by different expression hosts using varying purification procedures.	- 41 -
Table 7-1	Process parameters for the repeated utilization of immobilized enterokinase.	- 79 -
Table 7-2	Process parameters of the repeated utilization of immobilized enterokinase in the presence or absence of $Mg^{2+}$ .	- 80 -
Table 8-1	MUC1 content and purity degree of the obtained lyophilisates.	- 85 -
Table 9-1	Comparison of the continuous process and the repeated utilization of immobilized enterokinase.	- 91 -
Table 9-2	Comparison of the reaction processes for the cleavage of MUC1-IgG2a Fc using soluble or immobilized enterokinase.	- 93 -
Table 10-1	Composition of the used media for the fermentation of Escherichia coli.	- 102 -
Table 10-2	Buffer compositions for affinity chromatography.	- 106 -
Table 10-3	Reaction setups for activity determination of enterokinase.	- 108 -
Table 11-1	Properties of proteins involved in the cleavage reaction.	- 124 -

## Abstract

In today's pharmacological industry, fusion proteins are used for the production of recombinant proteins of therapeutic interest. However, to obtain the therapeutically important protein in its monomeric form, the fusion partner, generally a signal peptide for translocation, needs to be removed using either chemicals or enzymes. In the latter case, the cleavage of fusion proteins can be conducted with higher specificity and under milder reaction conditions.

One of the biocatalysts used in laboratory scale is the serine protease enterokinase. In this study, enterokinase was applied in the cleavage of MUC1-IgG2a Fc for the generation of MUC1, a potential target in cancer immunotherapy.

To make enterokinase an attractive candidate for industrial fusion protein cleavage, the process for biocatalyst production by recombinant *E. coli* was optimized with regard to fermentation conditions and used isolation and purification techniques. By the application of a newly developed batch-binding chamber, the downstream process was simplified and the process time could be reduced by half. Furthermore, the yield of isolated biocatalyst was increased 8-fold for an inducible expression system and 14-fold with constitutive protein expression.

The enzymatic cleavage reaction needs to be economically feasible making an efficient utilization of the biocatalyst necessary. Therefore, different carrier materials for enzyme immobilization have been investigated, of which two – the porous Sepabeads® EC-HA203 and non-porous magnetic particles – gave promising results. Remaining activities for immobilized enterokinase of 60 % could be achieved with an additional stabilizing effect when using the porous material. Enterokinase immobilized on Sepabeads® EC-HA203 was successfully applied in fusion protein cleavage receiving the desired protein MUC1, compared to the non-porous support.

Finally, enterokinase immobilized on porous support was applied in the preparative cleavage of MUC1-IgG2a Fc either in a continuous process or in repetitive utilization. According to the received process parameters, the repeated application of the enzyme-support preparation proved to be the more efficient method in fusion protein cleavage. Immobilized enterokinase was re-used 15 to 18 times for cleaving MUC1-IgG2a Fc increasing the total turnover number 419-fold compared to a single application of the biocatalyst.

## Zusammenfassung

In der heutigen pharmazeutischen Industrie werden Fusionsproteine für die Herstellung von therapeutisch wichtigen, rekombinanten Proteinen eingesetzt. Um jedoch das eigentliche Zielprotein in aktiver Form zu erhalten, muss zunächst der Fusionspartner, meist ein Signalpeptid für Translokation, durch eine chemische oder enzymatische Reaktion entfernt werden. Letzteres erlaubt eine sehr spezifische Spaltung des Fusionsproteins unter milden Reaktionsbedingungen.

Ein im Labormaßstab eingesetzter Biokatalysator ist die Serinprotease Enterokinase. In dieser Arbeit wird Enterokinase für die Spaltung von MUC1-IgG2a Fc verwendet, um MUC1, ein potentielles Zielprotein für die Immuntherapie in der Krebsbehandlung, herzustellen.

Damit Enterokinase zu einem attraktiven Kandidaten für die industrielle Spaltung von Fusionsproteinen wird, fand eine Optimierung des Prozesses für die Biokatalysatorproduktion durch rekombinanten *E. coli* in Bezug auf die Fermentationsbedingungen und die eingesetzten Isolations- und Aufreinigungsmethoden statt. Durch eine neuartige Anbindungszelle wurde die Aufarbeitung vereinfacht und die Prozesszeit halbiert. Des Weiteren konnte die Ausbeute an isoliertem Biokatalysator um das 8fache durch ein induziertes Expressionssystem und um das 14fache durch konstitutive Expression gesteigert werden.

Um eine enzymatische Spaltungsreaktion wirtschaftlicher zu machen, muss der Biokatalysator effizienter in die Reaktion eingebracht werden. Aus diesem Grund wurden verschiedene Trägermaterialien für die Immobilisierung des Enzyms untersucht, wobei zwei – die porösen Sepabeads® EC-HA203 und die nicht porösen Magnetpartikel – viel versprechende Ergebnisse zeigten. Es konnten Restaktivitäten von 60 % und eine zusätzliche Stabilisierung der Enterokinase bei Verwendung des porösen Trägers erzielt werden. MUC1-IgG2a Fc wurde erfolgreich durch auf Sepabeads® EC-HA203 immobilisierte Enterokinase gespalten. Es zeigte sich, dass poröse Stoffe eher für die Immobilisierung von einem kleinen Biokatalysator, der anschließend für die Spaltung von großen Fusionsproteinen verwendet wird, geeignet sind. Abschließend wurde das Immobilisat sowohl in einem kontinuierlichen Prozess als auch in wiederholten Spaltungsreaktionen von MUC1-IgG2a Fc eingesetzt. Die erhaltenen Prozessparameter zeigen, dass die mehrmalige Anwendung des Immobilisats eine sehr effiziente Methode zur Spaltung des Fusionsproteins darstellt. Die immobilisierte Enterokinase wurde zwischen 15 und 18mal wieder verwendet, wodurch die Katalysatorausnutzung um das 419fache, verglichen mit einer einzelnen Reaktion, gesteigert werden konnte.



## Abbreviations

$\mu$	Specific growth rate
2-MCE	2-mercaptoethanol
2NA	2-naphthylamine
AIDS	Autoimmune deficiency syndrome
AP	Alkaline phosphatase
Asp (G)	Aspartic acid
BCIP/NBT	5-Bromo-4-chloro-3-indolyl phosphate/Nitro blue tetrazolium
BSA	Bovine serum albumin
BWB	Blocking/washing buffer
CAT-hANF	Chloramphenicol transferase-atrial natriuretic factor
CDW	Cell dry weight
CE	Capillary electrophoresis
CHO	Chinese hamster ovary
CMV	Cytomegalovirus
CV	Column volume
DF-3	Murine monoclonal antibody to MUC1
DsbA	Thioredoxin homologue
EC-EA	Enzyme carrier – ethylamino
EC-HA	Enzyme carrier – hexamethylamino
EDCA	N-(3-dimethylaminopropyl)-N'-ethyl-carbodiimide hydrochloride
EDTA	Ethylene diamine tetraacetic acid
EK	Enterokinase
ELISA	Enzyme-linked immunosorbent assay
FPLC	Fast protein liquid chromatography
Fuc	Fucose
Gal	Galactose
GalNAc	N-Acetylgalactosamine
GD <sub>4</sub> K-2NA	Gly-Asp-Asp-Asp-Asp-Lys-2-naphthylamide
Glc	Glucose
GlcA	Glucuronic acid
GlcNAc	N-acetylglucosamine
Gly (G)	Glycine
GMP	Good manufacturing practice
hEPO	Human erythropoetin
hGCSF	Human granulocyte stimulating factor
hGh	Human growth hormone
His (H)	Histidine
His-Tag	Poly-histidine sequence
HIV	Human immunodeficiency virus
HMFG-1 / HMFG-2	Human milk fat globulin antibody
IEC	Ion exchange chromatography
iEK	immobilized enterokinase
IgG2a Fc	Immunoglobulin G 2a Fc region
Ile (I)	Isoleucine
IMAC	Immobilized metal affinity chromatography
IPTG	Isopropylthiogalactoside
LB	Lysogeny broth ( <i>Luria-Bertani medium</i> )
Lys (K)	Lysine
mAb	Monoclonal antibody
Man	Mannose
MUC1	Mucin 1
Neu5Ac	Sialic acid

Ni <sup>2+</sup> -IDA	Nickel-loaded sepharose
PBS	Phosphate buffered saline
PEM	Polymorphic epithelial mucin
PhRMA	Pharmaceutical Research and Manufacturers of America
pNPP	4-nitrophenyl phosphate disodium salt hexahydrate
PVDF membrane	Polyvinylidene difluoride membrane
RP-HPLC	Reversed phase – high performance liquid chromatography
rpm	Rounds per minutes
SDS-PAGE	Sodium dodecyl sulfate polyacrylamide gel electrophoresis
SEC	Size exclusion chromatography
Ser (S)	Serine
SM-3	Anti-MUC1 core monoclonal antibody
Thr (T)	Threonine
TNF- $\alpha$	Tumor necrosis factor alpha
Xyl	Xylose

## Symbols

$p$	Percentage	%
$\mu_{\max}$	Maximum specific growth rate	$\text{h}^{-1}$
$c$	Concentration	$\mu\text{M}$ , $\text{mM}$
$K_s$	Saturation constant	$\text{g}\cdot\text{L}^{-1}$
$m$	Mass	$\mu\text{g}$ , $\text{mg}$
$M$	Molar mass	$\text{kDa}$
OD	Optical density	-
$S_l$	Concentration of the limiting substrate	$\text{g}\cdot\text{L}^{-1}$
$T$	Temperature	$^{\circ}\text{C}$
$t$	Time	min, h
$ttn$	total turnover number	-
$U$	Units of enzyme activity	$\mu\text{mol}\cdot\text{min}^{-1}$
$V$	Volume	$\mu\text{L}$ , $\text{mL}$ , $\text{L}$
$v/v$	Volume per volume	%
$V_R$	Reactor volume	%
$w/v$	Weight per volume	-
$Y_s$	Biomass yield in relation to utilized substrate	-
$\lambda$	Wavelength	nm

# CHAPTER 1

---

INTRODUCTION



# 1 Introduction

## 1.1 Enterokinase

### 1.1.1 Enzyme classification

By the 1950s, great progress was achieved in isolating and characterizing enzymes, making the regulation of enzyme nomenclature indispensable. In 1961, a guideline named “*Enzyme Nomenclature*” was published, which has been constantly updated. This guideline suggests two names for each enzyme: 1) a recommended name for every day use and 2) the systematic name for minimizing ambiguity. In both cases, the name was chosen according to the catalyzed reaction. In Table 1-1 the main enzyme classes, the catalyzed reactions as well as examples of enzymes belonging to the specific group are listed [1].

**Table 1-1 Enzyme Nomenclature.**  
Main enzyme classes and examples for the catalyzed reactions (modified) [1].

<i>Enzyme class</i>	<i>Catalyzed reaction</i>	<i>Example</i>	<i>Reference</i>
I. Oxidoreductases	Redox reactions	Alcohol dehydrogenase	$BH_2 + A \rightarrow B' + AH_2$
II. Transferases	Transfer of functional groups	Glycosyl transferase	$D-B + A-H \rightarrow D-H + A-B$
III. Hydrolases	Hydrolysis reaction	Enterokinase	$A-B + H_2O \rightarrow A-H + B-OH$
IV. Lyases	Group elimination (formation of double bonds)	Benzaldehyde lyase	$A-B \rightarrow A' + B'$
V. Isomerases	Isomerization reactions	Amino acid racemase	$R-A-B \rightarrow A'-B'-R$
VI. Ligases	Bond formation	Pyruvate carboxylase	$A-OH + BH \rightarrow A-B$ $ATP \rightarrow ADP + P_i$

Enterokinase belongs to the enzyme class III; enzymes that catalyze the hydrolysis of peptide bonds. The catalysis of this reaction is very important for the utilization of dietary proteins.

Enterokinase belongs to the group of serine proteases which can be found in the intestinal tract being responsible for the specific cleavage of trypsinogen, the propeptide of trypsin. The developed active trypsin is further responsible for the activation of numerous enzymes of the pancreas (Figure 1-1) [2, 3]. The conversion of trypsinogen to trypsin is caused by the hydrolysis at a specific amino acid sequence (Lys<sub>(6)</sub>-Ile<sub>(7)</sub>) [4, 5]. The enterokinase shows a very strong affinity to the amino acid sequence (Asp)<sub>4</sub>-Lys, which is conserved in the amino terminus of most trypsinogens [6, 7]. This amino acid sequence is located at the N-terminus of the peptide bond to be cleaved retaining the N-terminus of the adjacent fusion partner. Thus, the biological activity of the target protein will not be influenced by the cleavage reaction [7]. Due to its high specificity for the (Asp)<sub>4</sub>-Lys sequence, the enzyme enterokinase has often been used for the *in vitro* cleavage of fusion proteins [8-12].

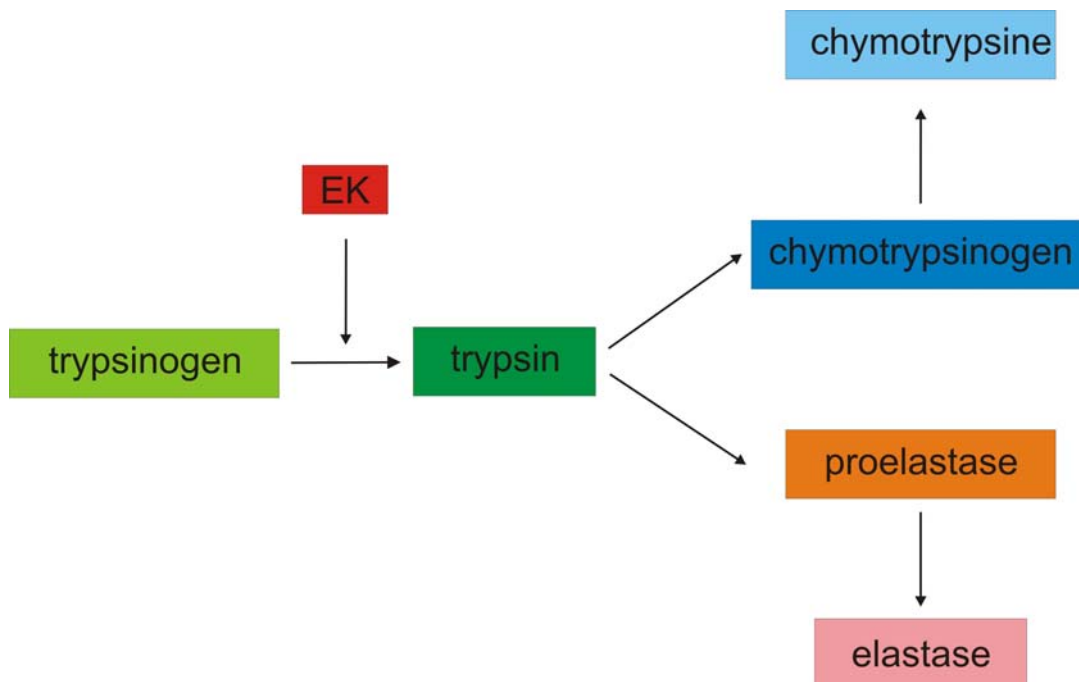
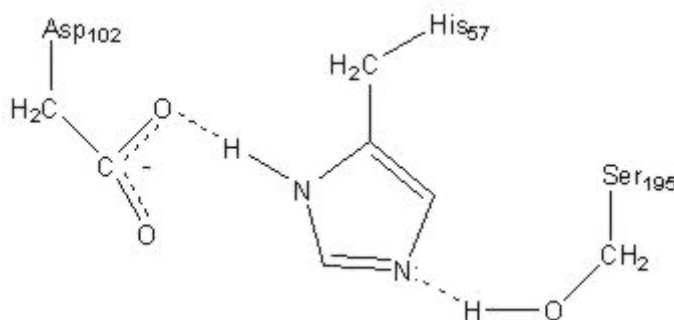


Figure 1-1 Activation of dietary proteins starting with trypsinogen by enterokinase.

### 1.1.2 Mode of action of serine proteases

All enzymes belonging to this group of proteolytic enzymes – serine proteases – have a characteristic catalytic mechanism in common. This mechanism relies on the occurrence of a reactive serine residue which belongs to the *catalytic triade* (Figure 1-2). The catalytically important amino acids His 57 and Ser 195 as well as the invariant Asp 102, present in most serine proteases, are located in the substrate binding site of the enzyme. Additionally, Asp 102 is positioned in a valley not being exposed to any solvents [13-15].



**Figure 1-2 Catalytic triade.**

The essential amino acids located in the active site of serine proteases [13].

After the substrate has bound to the substrate binding site of the serine protease, which contains the catalytic triade, the hydrolysis of the peptide bond is initiated (Figure 1-3). Since the reaction mechanism is very similar among all serine proteases, the catalytic reaction is described using the enzyme chymotrypsine.

As soon as the substrate binds to the enzyme forming the Michaelis-complex (Figure 1-3A), a nucleophilic attack of the carbonyl group by Ser 195 occurs, resulting in the formation of a tetrahedral intermediate (Figure 1-3B). Due to deprotonation of His 57, the tetrahedral intermediate disintegrates to the acyl-enzyme-intermediate (Figure 1-3C).

The amino group ( $R^2NH_2$ ) is released from the enzyme and is replaced by water of the solvent (Figure 1-3D). Due to the catalytic effectivity of the enzyme, the acyl-enzyme intermediate is easily cleaved hydrolytically. By the release of a carboxylate product, a new C-terminal part of the cleaved polypeptide chain (Figure 1-3E), the enzyme is regenerated (Figure 1-3F) [13-15].

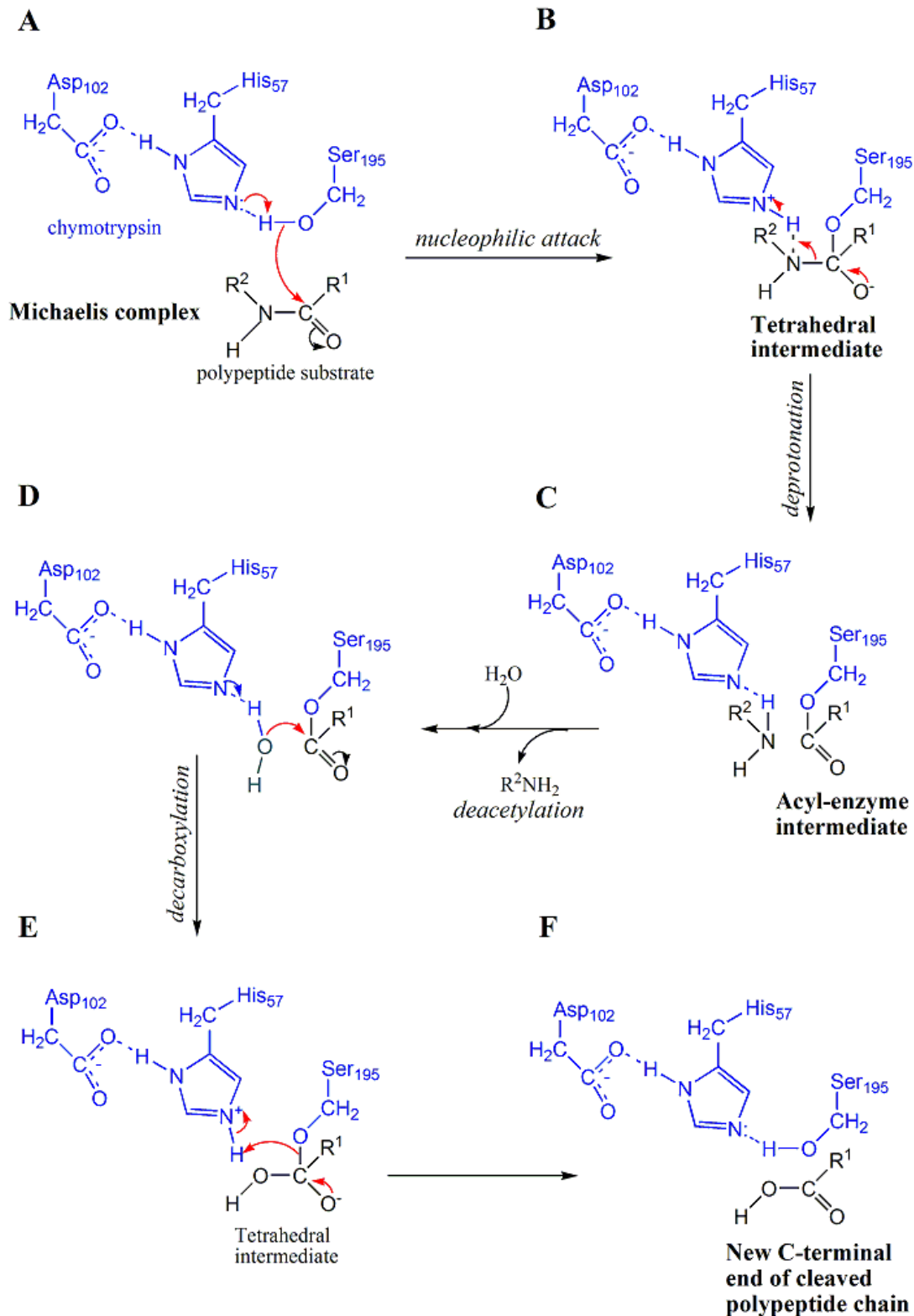


**Figure 1-3 Reaction mechanism of a serine protease.**

The catalyzed hydrolysis of a peptide bond (modified) [13].

- (A) Binding of substrate to the enzyme and formation of the Michaelis-complex
- (B) Nucleophilic attack of the carbonyl group by Ser 195 and formation of a tetrahedral intermediate
- (C) Deprotonation of His 57 and development of the acyl-enzyme-intermediate
- (D) Release of the amino group and replacement by a water molecule
- (E) Decarboxylation and formation of a second tetrahedral intermediate
- (F) Release of the carboxylate product and regeneration of the enzyme



### 1.1.3 Structure of enterokinase

The enzyme enterokinase is composed of two subunits: a 115 kDa structural subunit and a 35 kDa catalytic subunit. The structural part of the protein allows the anchoring at the surface of the duodenum and the exposure of the smaller catalytic subunit into the lumen. Both subunits are linked via disulphide bonds [16, 17]. A drawing of the enzyme structure can be seen in Figure 1-4.

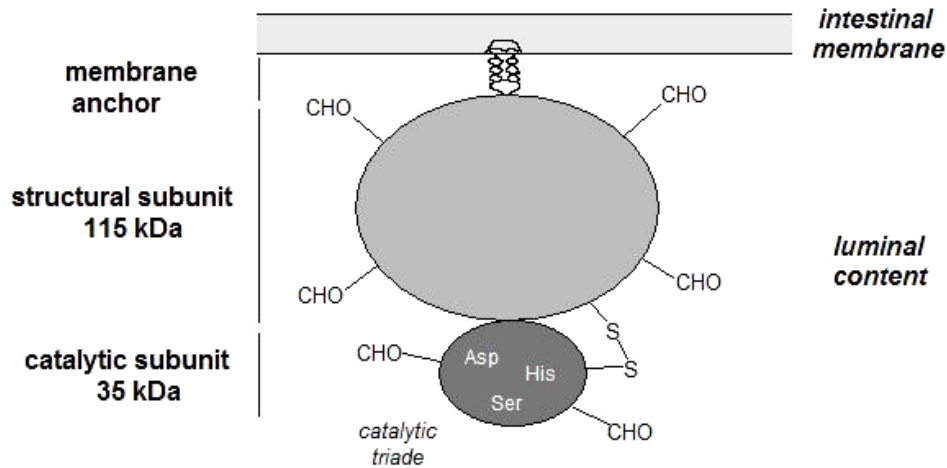


Figure 1-4 Structure of enterokinase.

### 1.1.4 Application of enterokinase in biotechnology

Due to the high affinity to the amino acid sequence (Asp)<sub>4</sub>-Lys and the retention of the biological activity of the cleaved target protein, enterokinase is often and preferably used in the *in vitro* cleavage of fusion proteins [8, 10].

In today's pharmacological industry, fusion proteins are used for the production of recombinant proteins of therapeutic interest, such as antibodies, coagulation factors, growth hormones, vaccines and insulin [5, 10, 18]. However, to gain the therapeutically important protein in a monomeric form, the fusion tag, generally a signal peptide for translocation, needs to be cleaved away. This is the critical step influencing the yield, the purity of the protein as well as the manufacturing costs. The enzymatic cleavage of fusion proteins gives higher specificity and allows milder reaction conditions compared to the chemical cleavage using e.g. cyanogen bromide. However, the industrial application of proteolytic enzymes is often limited by the high cost for the biocatalyst which adds to the costs for the downstream processing.

Several proteolytic enzymes have been used for fusion protein cleavage in laboratory scale such as factor Xa [4, 18], thrombin [4, 5, 19], urokinase [19, 20] and enterokinase. Using the enterokinase system, therapeutics for cancer treatment, such as mucin 1 [21-

23] and deacetylases [24], human growth hormones [11] and cytokines [12] have been produced so far. A main reason for the use of enterokinase in the application of fusion protein cleavage is the distinct specificity of this enzyme for a defined amino acid sequence. Thus, the risk of unspecific cleavage and the resulting destruction of the target protein can be avoided.

## **1.2 Fusion proteins**

### **1.2.1 Industrial importance**

*“Since 2000, over a quarter of all new drug approved have been biopharmaceuticals.”*

(Gary Walsh, 2003)

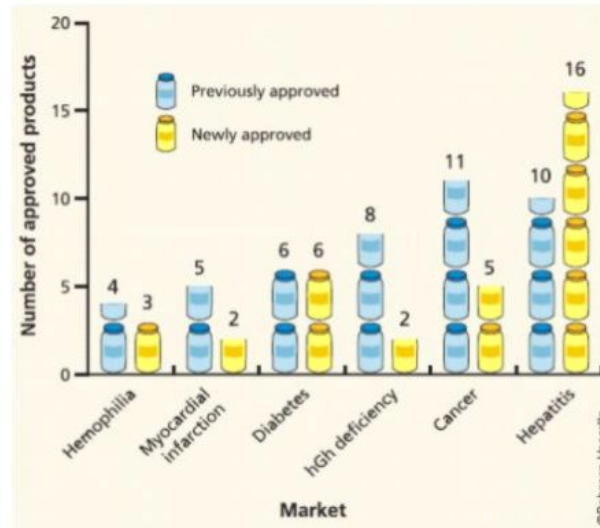
Humilin (recombinant insulin) produced by Genentech, San Francisco, CA, USA was the first human protein produced recombinantly by means of biotechnology. This was about 26 years ago. Since then, the portfolio of biopharmaceutical products involves not only recombinant forms of natural proteins and from natural sources derived biologics, but also therapeutics based on monoclonal antibodies (mAb). More than 120 pharmaceutical products have been approved in the United States and the European Union by the end of 2003, and about 500 additional products are currently undergoing clinical evaluation. As stated by Holmer in 2000, not only more than 250 million people, but also the biotechnology business have benefited from this new “era” of biotechnology products [25, 26].

Most of the new approved biopharmaceuticals are protein-based drugs, of which some are unmodified recombinant proteins, and others have undergone some type of engineering for improving their functionality. Those drugs are medicines against the major killers of the West civilization: diabetes, hemophilia, myocardial infarction and various cancers (Figure 1-5A). According to the Pharmaceutical Research and Manufacturers of America (PhRMA), representing the US drug industry, approximately 370 of the 500 candidate biopharmaceuticals undergo clinical evaluation in the United States. Around half of these drugs find their application in the treatment of cancer, others are involved in the therapy of infectious disease, autoimmune disorders, neurological disorders and AIDS/HIV-related conditions (Figure 1-5B) [25].

Several different technologies are used for the production of recombinant proteins, such as transgenic animals, transgenic plants, mammalian cells and the production using microorganisms [27]. The application of transgenic animals or plants may represent a more cost effective production system compared to mammalian or microbial cell cultures, but does still not belong to the standard techniques. One explanation for this is that the

biologically active form of most glycosylated proteins could be produced only in mammalian cells so far. This is due to the potential of mammalian cells for glycosylation and protein folding. Glycosylation can of course also be achieved in transgenic animals, but at present the used technology does not sufficiently fulfill the GMP (Good Manufacturing Practice) regulations.

A



B

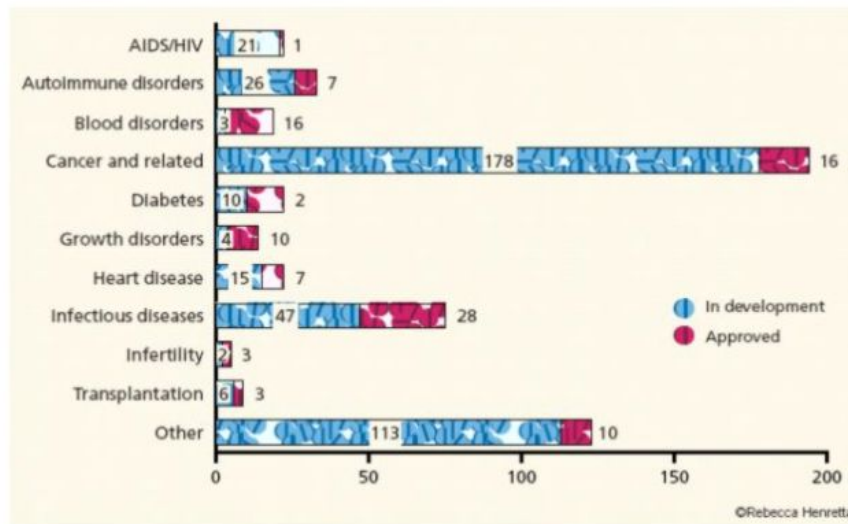


**Figure 1-5 Target markets for new biopharmaceuticals.**

A) Approved biotechnology products applied for the treatment of the major killers of the West civilization,

B) Number of drugs undergoing clinical evaluation in the United States. [25]

For industrial production it is of importance to achieve high yields and excellent purity of the desired recombinant proteins. One useful technique is the expression of the recombinant polypeptide as part of a larger fusion protein [28, 29]. The fusion of the target protein to a peptide sequence has several advantages, such as the secretion of the products from yeast [30] and *E. coli* [31] cells into the culture medium. Additionally, the fused polypeptide sequence can serve as an aid in identification and purification of the product. When using a fusion partner, this may also contribute in the correct folding of the target protein by functioning as chaperone.

The most prominent and most abundantly used fusion tag is the green fluorescent protein (GFP). It can be linked genetically to almost every protein making the visualization of many processes within a cell possible. Due to the broad range of applications, the GFP has become one of the most important tools in biological research. In 1961, the researcher Osamu Shimomura discovered the GFP in the Pacific jellyfish *Aequorea Victoria*. Later, in the early Nineties, Martin Chalfie isolated the gene for GFP making it available for modern biotechnology. The mechanism by which GFP is glowing was first described by Roger Tsien. Now in 2008, these three scientists have been awarded with the Nobel Prize for chemistry for their outstanding and significant work regarding the green fluorescent protein [32].

Although being beneficial for the production of recombinant proteins, the fusion protein approach also has several drawbacks. First, the added polypeptide sequence may hinder the protein to fold properly into a native, active state. Second, the fused peptide needs to be removed in a sensitive way, so the target protein is not damaged or destroyed [8].

Misfolding can be overcome by the treatment with a strong denaturant followed by a refolding procedure. The removal of the fusion peptide is preferably done using enzymatic reactions such as for the production of cytokines in Chinese Hamster Ovarian cells using factor  $X_a$ , in which the fusion partner IgG, used for detection and purification, is removed [12]. In a fungal expression system using *Aspergillus niger*, a glycoamylase-TNF $\alpha$  fusion protein is cleaved using enterokinase [9]. In Table 1-2, examples of approved biopharmaceuticals produced as fusion proteins are given.

**Table 1-2 Approved biopharmaceuticals produced as fusion proteins in industrial scale (added) [25].**

<i>Product</i>	<i>Company</i>	<i>Information</i>
<b>CAT-hANF</b> (chloramphenicol transferase-atrial natriuretic factor)	Glaxo Group LTD (US)	1987, GB 2180538
<b>hGh-x</b> (human growth hormone)	Eli Lilly CO	1988, CA 1291068
<b>Fc-hEPO</b> (human erythropoetin), <b>Fc-hGCSF</b> (human granulocyte colony stimulating factor)	Merck Patent GmbH (D), Sudo Yukuo (JP)	1999. WO 958662
<b>Amevive</b> (alefacept)	Biogen Idec Inc.	Approved 2003 (US)
<b><sup>a</sup>Enbrel</b>	Amgen (US), Wyeth (EU)	Approved 1998 (US), 2000 (EU)
<b>Ontak</b>	Seragen/Ligand Pharmaceuticals	Approved 1999 (US)

### 1.2.2 Glycoproteins and glycosylation mechanisms

Many cellular biomolecules have glycans attached to their structure. Those biomolecules can also be named glycoconjugates and are divided into glycoproteins, glycolipids, and proteoglycans. In case of glycoproteins, the glycan chains are covalently linked to functional groups of amino acid side chains within a protein or peptide.

Glycosylation is one mechanism of post-translational modifications, meaning the transfer of sugars by enzymes, such as glycosyltransferases. The complexity of glycosylation is caused by the number of enzymes catalyzing the reaction, which can be described as the “one enzyme-one linkage” concept proposed by Hagopian and Eylar (1986) [33]. This concept states the general rule that for each carbohydrate linkage a specific glycosyltransferase gene has to be provided. Besides the glycosyltransferases, five different parameters further affect the structural diversity of glycans:

1. the composition of the unit monosaccharide, e.g. Gal, GalNAc, Glc, GlcA, GlcNAc, Fuc, Man, Neu5Ac and Xyl,
2. the length of the glycan chain (varies between one to several hundred monosaccharide units),
3. the linkage type of the glycosidic bond between the carbohydrates and the peptide chain,
4. the anomeric configuration of the corresponding groups,
5. the branching; the number of carbohydrates connected to one monosaccharide [34, 35].

The mechanism of glycosylation can be differentiated into three main types depending on the chemical function by which the glycans are transferred. The types of transfer mechanisms are:

*O-glycosylation*: the carbohydrates are attached to the hydroxyl group of serine and threonine residues, when the protein/peptide is transported from the *cis* Golgi to the *trans* Golgi,

*N-glycosylation*: the starting sugar is bound to the carboxy amide group of an asparagine occurring in the endoplasmic reticulum and the Golgi apparatus,

*C-glycosylation*: the sugar mannose is linked to the carbon 2 of tryptophan of RNase 2 [36].

According to the glycosylation pattern, glycoproteins are divided into O-linked and N-linked glycans. Many important functions are mediated by those glycans. Thus, glycoproteins play an important role in cell-cell interaction and signaling. Moreover, glycosylation as a post-translational tool greatly influences proteins by:

- stabilizing protein structure,
- assisting in protein folding,
- shielding the protein from proteases,
- mediating protein half-life *in vivo*,
- orienting the protein on the cell surface
- participating in protein regulation by competing with other post-translational modifications [37, 38].

For the use of biopharmaceuticals in mammals, it is therefore of great importance to produce proteins with the correct glycosylation pattern to receive the biologically active form of the protein with the desired functioning.

## **1.3 The target protein MUC1**

### **1.3.1 General aspects**

MUC1 belongs to the mucin family, being an O-linked (mucin-type) glycoprotein. In humans, eight mucins have been identified, of which seven are secreted and one (MUC1) is the only membrane-anchored molecule. All proteins are produced by epithelial cells of the gastrointestinal, respiratory and genitourinary tracts, and also by the cancers that arise from these tissues.

MUC1 was the first member of the mucin family to be described and characterized. It was first isolated from human milk as a glycoprotein with a high molecular weight and a large extracellular domain [39]. There are alternative names for MUC1 existing, such as PAS-O, non-penetrating protein, DF-3 antigen, polymorphic epithelial mucin (PEM) and episialin [40]. The gene encoding MUC1 is located at chromosome 1q21-24 and the resulting protein has an apparent molecular mass of 300-600 kDa. The structure of the glycoprotein can be divided into a long (69 amino acids) cytoplasmic tail and a structural variable extracellular domain, which is almost entirely composed of between 20 to 100 tandem repeats of a 20 amino acid motif [41, 42]. Each tandem repeat contains five potential glycosylation sites, allowing the highly glycosylated MUC1 to carry typically between 60 and 200 oligosaccharide side chains. In humans, approximately 50 % of the mass of the mucin molecule are carbohydrates [40].

Extensive studies have shown that MUC1 plays a diverse role in normal cells, including the involvement in anti-adhesion processes [43-45]; it may prevent interactions between other molecules located on the opposing side of the membrane preventing adhesion and thereby maintaining the lumen. It may also inhibit adhesion and extravasation of lymphocytes in high endothelial venules. Furthermore, MUC1 was found to be involved in signal transduction [46, 47]; it protects and lubricates the tissue surface [48], modulates the immune response and regulates cellular motility [49]. Furthermore, MUC1 is an important component of the glycocalyx and functions as a barrier against microbial toxins and protector against proteolytic degradation.

MUC1 synthesized by normal cells, has a short and highly immunogenic amino acid sequence (caused by the glycosylation of specific amino acids) between the glycan side chains, which can be recognized by several monoclonal antibodies, such as HMFG-1, HMFG-2 and SM-3. The mucin molecule can be found at the apical surface of glandular epithelial cells, e.g. lactating mammary gland, pancreas, bronchus and salivary gland, and is also synthesized by many types of cancer.

### **1.3.2 MUC1 and cancer**

MUC1 as a large glycoprotein being expressed at the cell surface possesses numerous functions, but its potential role in the progression of tumors and metastasis has to be emphasized. An over-expression of tumor-associated MUC1 has been observed in many epithelial malignancies. There is also a change in the glycosylation pattern of MUC1: the N-terminal domain becomes aberrantly glycosylated with shortened carbohydrate side chains. This leads to the unmasking of the epitopes on its peptide core [50]. This could be documented for breast and ovarian cancer [51], and is also suggested to be true for lung, pancreatic and prostate cancer [46, 52]. The changed topology of MUC1 occurs also at

the basolateral surface. Differences in the number of O-glycosylation sites could be observed between mucins produced by the normal lactating mammary gland and produced by the breast cancer cell line T47D. This contributes to the different expression profiles assumed in normal and malignant cells [46].

Besides the number of glycosylation sites, there are also variations in the compositions of O-glycans added to MUC1. In mucin-type O-glycosylation, *N*-acetylgalactosamine (GalNAc) is the first sugar added to serine or threonine. In normal human mammary gland cells, galactose (Gal) is added to form the core 1 structure; a reaction catalyzed by  $\beta$ -1,3-galactosyl transferase ( $\beta$ -1,3-GalNAc transferase). The enzyme  $\beta$ -1,6-acetylglucosamine transferase ( $\beta$ -1,6-GlcNAc transferase) then catalyzes the addition of *N*-acetylglucosamine (GlcNAc) to GalNAc to form core 2. This structure is further extended to form polylactosamide side chains (Figure 1-6, left pathway).

In comparison to this, truncated side chains are found in breast cancer cells. The enzyme  $\alpha$ -2,3-sialyl transferase is suggested to compete with  $\beta$ -1,6-GlcNAc transferase for the core 1 structure as substrate. Sialic acid (SA) is added to the Gal of core 1 by  $\alpha$ -2,3-sialyl transferase, thereby inhibiting carbohydrate side chain extension (Figure 1-6, right pathway). This side chain termination may also be caused by the addition of fucose instead of sialic acid [53-55]. Therefore, normally glycosylated mucins possess core 2 based O-glycans, whereas the structure of O-glycans of mucins isolated from breast cancer cell lines were found to be core 1 based. Differences in enzyme activity of  $\beta$ -1,6-GlcNAc transferase and  $\alpha$ -2,3-sialyl transferase were found in breast cancer cell lines compared to normal epithelial cells, suggesting an explanation for the truncated carbohydrate side chains found in tumor-associated MUC1 [56].

The enzyme  $\alpha$ -2,6-sialyl transferase was found to add sialic acid to GalNAc, the first sugar linked to serine or threonine resulting also in side chain termination. The carbohydrate antigens Tn, T and sTn are preferentially expressed by malignant cells. The expression of tumor-associated carbohydrate moieties are suggested to increase the metastatic potential through interactions between sialic acid residues and components of the extracellular matrix [56].



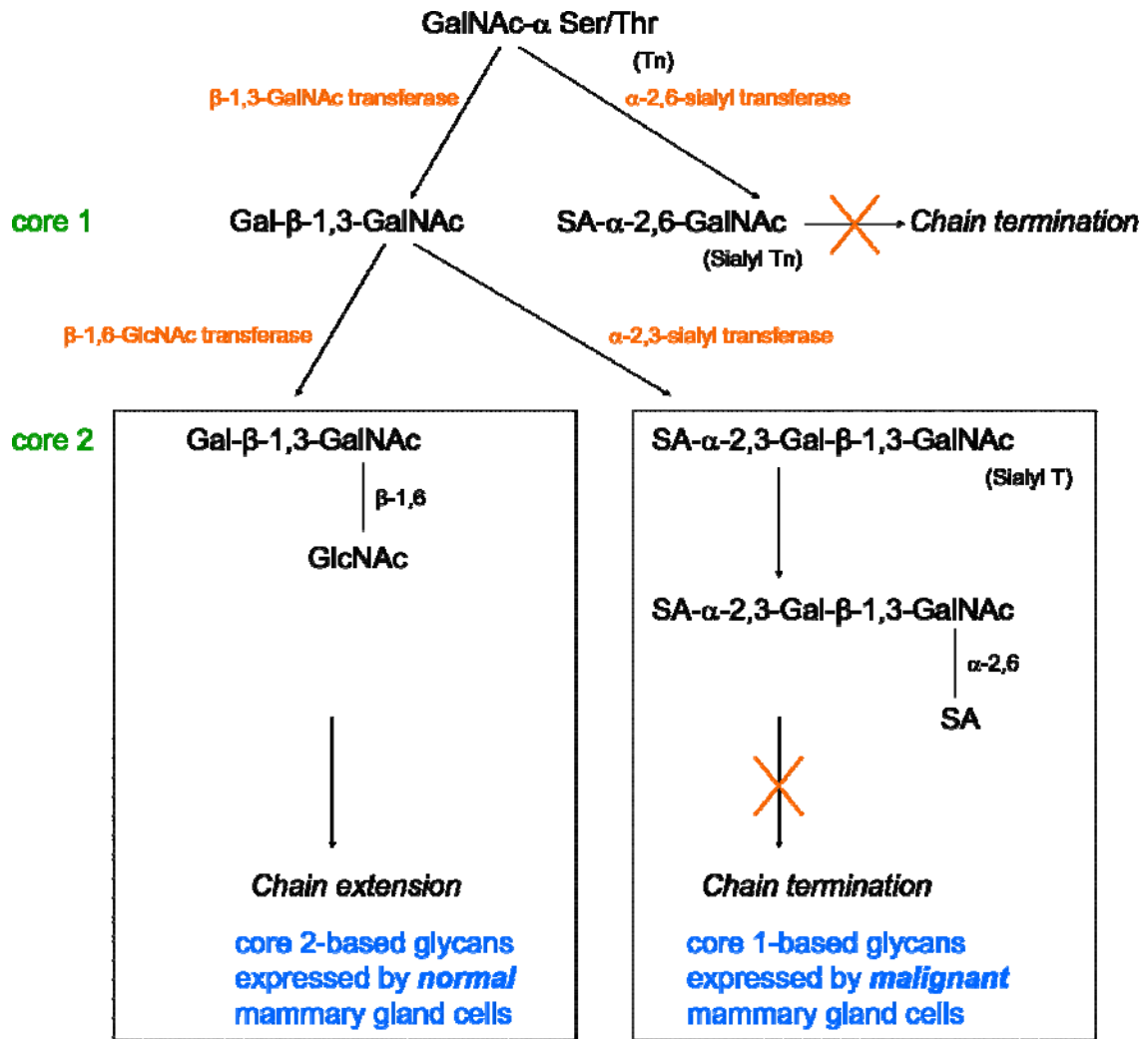


**Figure 1-6 Pathway of O-linked glycosylation of MUC1 by the mammary gland for normal and malignant cells.**  
 Core 1 glycans are converted to core 2 glycans in normal cells, whereas in cancer mucin the glycans are core 1 based with a high level of sialic acid [46, 57].

In recent studies it is suggested that MUC1 plays a role in tumorigenicity, tumor cell migration, and also in immunosuppression. The latter might be promoted by MUC1 due to enhancing the resistance to apoptosis and genotoxic agents. As mentioned before, malignant cells over-express MUC1, which is claimed to be advantageous under conditions of oxidative or other forms of stress, thus contributing to the survival of carcinoma cells [58]. Furthermore, the anti-adhesive action of MUC1 may also influence the anti-tumor response of the body. MUC1 may, thereby, interfere the interactions between tumor cells and cells of the immune system [59]. It was suggested that the negative effect of mucins on the suppression of the immune response is caused to some extent by the carbohydrate portion of the glycoprotein. It has been claimed by Hilkens and co-workers that the aberrant expression mediates the initial step in the metastatic cascade of tumor cells due to the anti-adhesive effects of MUC1 [60].

### **1.3.3 MUC1 as therapeutic agent**

Although the immune responses to MUC1 are considered to be beneficial for cancer patients, the expression of MUC1 on tumors is usually correlated with a worse prognosis. In virtually every adenocarcinoma, the level of expression of MUC1 on the cell surface is increased. Furthermore, the numerous roles of MUC1 in cellular transformation, tumor cell migration, chemoresistance, and also in immunosuppression support the increased interest in the MUC1 mucin as a “cancer-associated antigen” which may be useful in immunotherapy [57, 61].

There are multiple other reasons for considering MUC1 as a target antigen. Firstly, MUC1 may be among the first cellular structures to be encountered by the immune system as a result of its physical size. Secondly, MUC1 expression is up-regulated in malignant cells, and as a consequence of aberrant glycosylation, new epitopes are exposed on the cell surface. Thirdly, the distribution of MUC1, which is apical in normal glandular epithelia, but is being all over the surface of cancer cells, allows selectivity in any cell killing involving the whole molecule [46]. Finally, and of most importance, both cellular and humoral responses have been observed in cancer patients.

Before initiating clinical studies, preclinical testing was done using animal models. MUC1 was shown to be highly immunogenic in mouse models, thus many antibodies have been developed to the MUC1 mucin by various groups. Here, normal or malignant epithelial cells, or their membranes, were used as immunogens. Particularly, membranes of lactating mammary epithelial cells were widely used as an immunogen and it could be demonstrated that MUC1 apparently dominates the induction of an immune response [62-64]. Cytotoxic antibodies recognize membrane mucins, making the use of antigens based on MUC1 in active specific immunotherapy even more interesting [46]. Several investigations, however, showed that antibodies against MUC1 exert only a limited effect against the primary tumor, while being more effective against circulating single tumor cells. Due to their role in antibody-dependent cell-mediated cytotoxicity and complement-mediated cell lysis, anti-MUC1 may uncover cell surface receptors causing cell adhesion to be restored and tumor cells to be recognized and destroyed. It has been shown that naturally occurring anti-MUC1 in the sera of breast cancer patients favorably influenced the overall survival of these patients in stage I and stage II studies [65, 66].

Apart from being a target for the B cell immune response, MUC1 can also serve as T cell immunotarget. The first evidence for this were demonstrated by Jerome and co-workers [67]. It was shown that tumor-reactive T cells from peritumoral lymph nodes of breast cancer patients were able to destroy MUC1 positive cancer cells. The epitopes that were recognized by the T cells were localized within the tandem repeat domain of MUC1. It can

therefore be said, that a site-specific O-glycosylation has a significant impact on the antigenicity of the tandem repeat domain and also on the strength of the glycopeptide-mediated effect on human T cell proliferation. These facts have to be considered in the future designs of MUC1-based vaccines.

Several attempts have already been made to use MUC1 as therapeutic agent. MUC1 cDNA was for example used as immunogen. Unfortunately, the cDNA alone failed to give protection against MUC1-expressing tumors in MUC1 transgenic mice. However, the immunization of breast cancer patients in a small phase I/II clinical trial with a recombinant vaccinia virus expressing MUC1 and interleukin-2 showed two partial responses of the patients [57].

In other experiments, peptides were used to generate MUC1-specific immune responses. These peptides have been derived from the tandem repeat sequence of MUC1 [57, 68]. A more direct way to exploit the aberrant glycosylation of MUC1 for the use in immunotherapy is the application of tumor-associated carbohydrate antigens found on MUC1. Immunized patients pre-treated intravenously with cyclophosphamide showed strongly increased median survival than groups treated differently [46].

Recently published data of a clinical trial involves a peptide vaccine strategy for the treatment of non-small lung cancer. In this study, L-BLP25, a peptide vaccine that targets the exposed core peptide of MUC1 is used. Preclinical studies showed a cellular immune response induced by L-BLP25, which is characterized by T-cell proliferation in response to MUC1 and by the production of interferon- $\gamma$ . Updated analysis show a strong survival trend in favor of L-BLP25 [61]. This liposomal cancer vaccine also shows promise in prostate cancer in which the doubling time of prostate-specific antigens could be prolonged. [50]

Concluding, it can be said that MUC1 has many characteristics to be an interesting candidate molecule for active specific immunotherapy. This is also reflected by the number and scope of publications and early clinical studies that have been initiated.



## **CHAPTER 2**

---

AIM OF THE PROJECT



## 2 Aim of the Project

The main focus of this project is the optimization of the enzymatic cleavage of the fusion protein MUC1-IgG2a Fc to receive a potential target in immunotherapy for cancer treatment. This fusion protein is produced by recombinant Chinese Hamster Ovarian K1 cells and is composed of the extracellular part of human MUC1 and the Fc-part of immunoglobuline G, which functions as a secretion signal. Both fusion partners are linked by an enterokinase recognition site allowing an enzymatic cleavage of the fusion protein. This is necessary to receive MUC1 in its monomeric, active form for its utilization in therapeutic and immunological investigations. The currently applied process for the cleavage of MUC1-IgG2a Fc by enterokinase is highly inefficient and is causing production costs of about 100.000 € per gram MUC1, in part due to the high costs of the biocatalyst.

Therefore, the enzymatic cleavage reaction shall be characterized followed by the development of an improved process for fusion protein cleavage with emphasis on the efficient utilization of the biocatalyst.

The tasks of the project can be summarized as follows:

### PRODUCTION, ISOLATION AND PURIFICATION OF THE REACTING PROTEINS

- Optimization of the fermentation and purification procedure for enterokinase produced by recombinant *E. coli* strains to increase the yield of isolated biocatalyst;
- Optimization of the purification procedure for MUC1-IgG2a Fc produced by recombinant Chinese Hamster Ovarian K1 cells.

### INVESTIGATIONS ON THE BIOCATALYST

- Development of fluorometric and analytical methods to determine optimal reaction conditions and measure enzyme activities;
- Investigation of different carrier materials for immobilizing enterokinase; establishment of an immobilization technique to receive high remaining activities and to increase the stability of the enzyme, demonstrate the suitability of the enzyme-support preparation for fusion protein cleavage under process conditions;
- Determination of the reaction conditions for the immobilized enterokinase.

PREPARATIVE CLEAVAGE OF MUC1-IGG2A Fc

- Application of the enzyme-support preparation in appropriate reactor setups and improvement of the reactor performance by applying optimized reaction conditions;
- Comparison of the optimized process to the currently applied method;
- Development of a suitable procedure for the isolation of MUC1.



## **CHAPTER 3**

---

INVESTIGATIONS CONCERNING MUC1-IGG2A FC



### 3 Investigations concerning MUC1-IgG2a Fc

#### 3.1 Theoretical Background

The fusion protein of interest, MUC1-IgG2a Fc, consists of the human extracellular part of MUC1 and a murine IgG2a Fc (Figure 3-1). The N-terminus of MUC1 contains 16 tandem repeats, of which each has 5 potential O-glycosylation sites. The C-terminal part of the fusion protein is composed of exon 1-3 of IgG2a Fc, having a stabilizing effect on the fusion protein. Furthermore, the IgG2a Fc functions as signal peptide for the transport of MUC1-IgG2a Fc to the cell culture medium. The two proteins are linked by an enterokinase recognition site allowing the enzymatic cleavage of the fusion protein after purification to receive the final target protein MUC1 in its monomeric, active form [21].

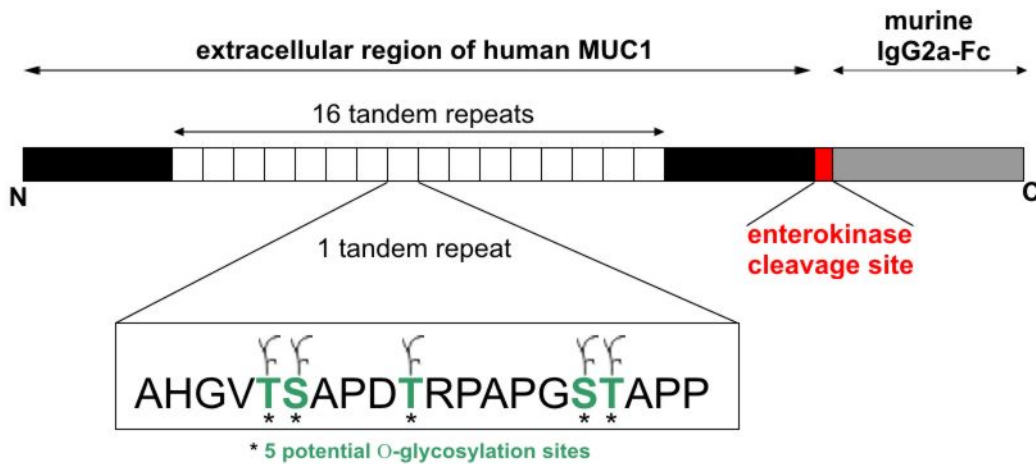


**Figure 3-1 Protein structure of the fusion protein MUC1-IgG2a Fc.**

The fusion protein has an apparent molecular weight of about 170 kDa, of which 40 % are glycans and the remaining 60 % represent the peptide part. The percentile distribution varies according to the number of glycosylation sites and the length of the glycans [69].

The cDNA encoding the fusion protein was cloned into a pcDNA3-vector und is under the control of a human cytomegalovirus promoter (CMV promoter). This vector is an expression vector with high transcription rates allowing an increased expression of the recombinant protein in mammalian cells. Therefore, Chinese Hamster Ovarian K1 (CHO K1) cells were transfected with the MUC1-IgG2A-pcDNA3-vector (Figure 10-1, Materials and Methods) for the production of the fusion protein.

### 3.2 Isolation and Purification of MUC1-IgG2a Fc

The cultivation of CHO K1 cells for the production of MUC1-IgG2a Fc was performed in cooperation with the former Cell Culture Group of the Institute of Biotechnology 2 of the Research Centre Juelich. Starting from a cryo culture of the working cell bank,  $1 \cdot 10^7$  viable cells are used as inoculum for a T75 T-flask having a final cell concentration of about  $1 \cdot 10^6$  viable cells/mL. Cultivation was performed at 37°C and 5-8 % CO<sub>2</sub>. A T-flask with  $1 \cdot 10^6$  viable cells/mL was then used for inoculation of a spinner flask, thereby entering a dynamic culture system. A spinner flask with  $1 \cdot 10^6$  viable cells/mL was then used as inoculum for a 3-5 L cultivation system. Further information is given in section 10.2.4 and 11.1.

The fusion protein MUC1-IgG2a Fc, which is secreted into the cell culture medium, has to be purified for further investigations. In the first purification step, the protein of interest is removed from the cell culture medium and, in parallel, is concentrated within the standard reaction buffer using filtration (10.2.14). Table 3-1 summarizes the concentrated MUC1-IgG2a Fc solutions received from different perfusion cultures. After the first purification step, concentrations of around 200 mg\*L<sup>-1</sup> MUC1-IgG2a Fc were obtained for each product solution.

**Table 3-1 Concentrated MUC1-IgG Fc solutions received from different perfusion cultures of CHO-K1 cells after the first purification step.**

<i>Fermentation (see appendix 11.1)</i>	<i>V<sub>cell culture medium</sub> / L</i>	<i>V<sub>concentrate</sub> / L after first purification step</i>
1) R CWPer3	8.6	0.70
2) R CWPer4	10.5	0.85
	6.0	0.60
3) RMUC1 Prot2	5.7	0.64

The received product solutions containing MUC1-IgG2a Fc were analyzed using SDS-PAGE. A protein band with the expected molecular size of about 170 kDa was detected and was specifically identified as the desired fusion protein MUC1-IgG2a Fc using specific antibodies in Western Blot analysis (Figure 3-2). As it can be seen on SDS-PAGE, there are still impurities in the protein solution that may disturb within the cleavage reaction using immobilized enterokinase as well as in analytical investigations. Therefore, further purification of the fusion protein was required.

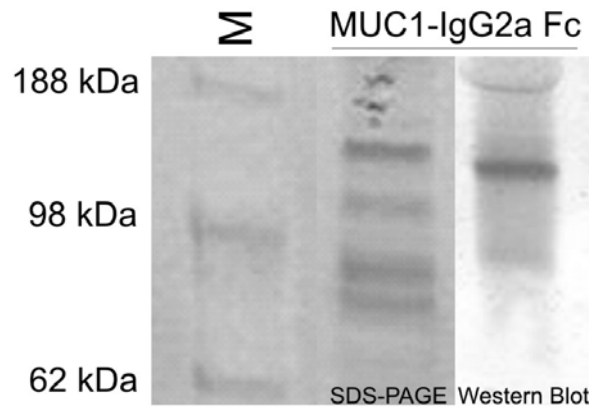


**Figure 3-2 Detectable MUC1-IgG2a Fc after the first purification step using filtration.**

To receive a sufficient purity of the fusion protein, ion exchange chromatography was applied for removing undesired proteins. Each protein possesses a specific isoelectric point, which is the pH value at which the overall net charge of the protein is zero. By changing the pH in the surrounding medium, the charge of the protein can be changed accordingly. Therefore, the proteins will bind more or less specific to the ion exchange material and can be eluted using a salt gradient.

Ion exchange chromatography has been applied before for the separation of MUC1 from the reaction mixture [21], which has similar properties as the fusion protein MUC1-IgG2a Fc. Thus, for the preparative purification of MUC1-IgG2a Fc, ion exchange chromatography seemed applicable.

Two slightly different ion exchange materials have been investigated, which differ mainly in the size of the agarose beads and thus in the overall loading capacity: 1) HiTrap QHP – Q Sepharose™ High Performance and 2) HiPrep QFF – Q Sepharose™ Fast Flow. By varying the salt gradient and regulating the flow rate, MUC1-IgG2a Fc could be further purified using the strong anion exchange material HiPrep QFF. A reference gel and the applied gradient with the resulting chromatogram are demonstrated in Figure 3-3.

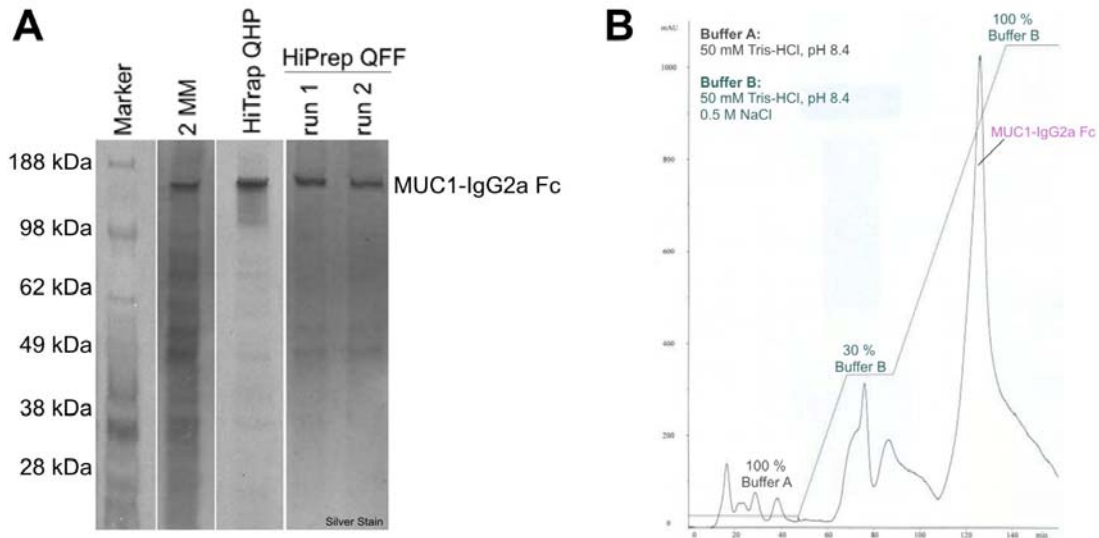


**Figure 3-3 Second purification step for MUC1-IgG2a Fc using ion exchange chromatography.**  
**A)** SDS-PAGE of the two purification steps and the comparison of the two different ion exchange materials (2MM – 2 membrane module);  
**B)** representative chromatogram received for MUC1-IgG2a Fc after ion exchange chromatography.

Using anion exchange chromatography as a second purification step, undesired proteins were removed (Figure 3-3A) by applying a specific salt gradient (Figure 3-3B). The purity of the received fusion protein was now sufficient for further experiments involving the cleavage reaction with immobilized enterokinase and analytical investigations. The batches of MUC1-IgG2a Fc were obtained having different purity degrees ranging from 27 % to more than 94 % (Figure 3-4).

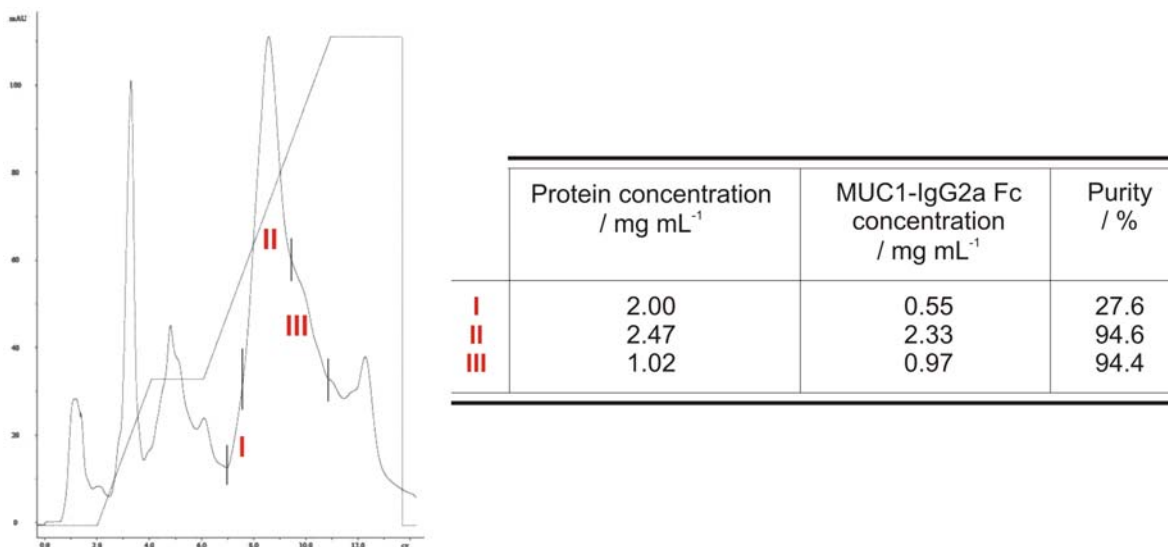


**Figure 3-4 Received fractions of MUC1-IgG2a Fc with the corresponding chromatogram (left) and the specific purity after IEC (right).**

### 3.3 Stability of MUC1-IgG2a Fc

As observed by various research groups and as described in chapter “*Enzyme characterization*”, enterokinase activity can be observed at temperatures between 25 °C and 40 °C and in a pH range between 6 to 9 [7, 70]. Due to the broad range of possible reaction conditions, it is of importance to investigate the stability of the substrate protein MUC1-IgG2a Fc at those reaction conditions.

Figure 3-5 shows a representative SDS-PAGE with samples of MUC1-IgG2a Fc taken after specific time intervals when being incubated under sterile conditions at 25 °C and 37 °C at pH 8. According to the intensities of the protein bands (analysis done as described in section 10.2.19), a degradation of the fusion protein under the investigated conditions did not occur. Same results were received for 30 °C, 35 °C and 40 °C at pH 8 and for 25 °C to 40 °C at pH 9. Thus, MUC1-IgG2a Fc seems to be stable for at least 14 days under sterile conditions at temperatures between 25 °C to 40 °C and at pH 8 and 9.

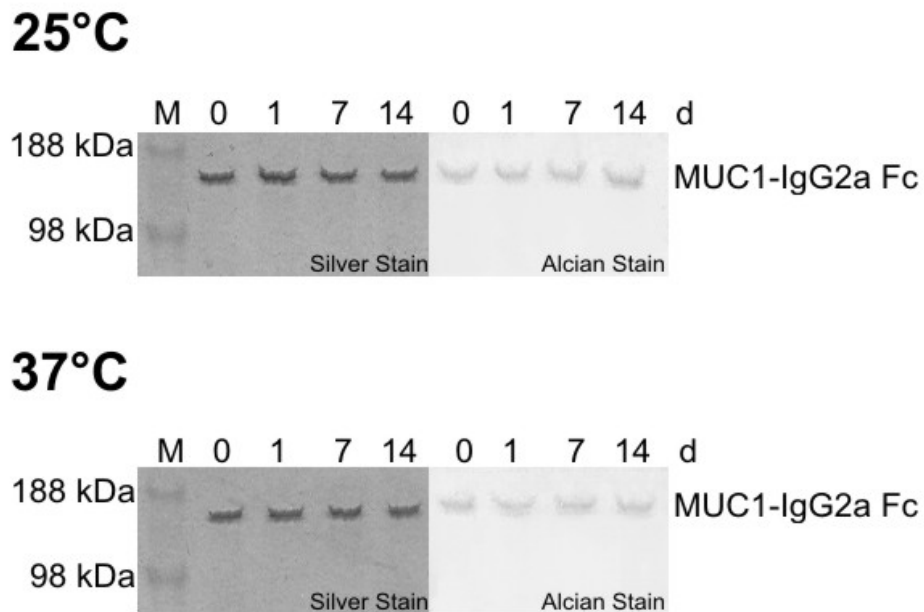


Figure 3-5 Stability of MUC1-IgG2a Fc at pH 8 (representative SDS-PAGE).

### 3.4 Summary: MUC1-IgG2a Fc

The results of this chapter can be summarized as follows:

- ❖ The fusion protein MUC1-IgG2a Fc, produced by CHO K1 cells, is transported into the cell culture medium. Using a two-membrane module, the protein was separated from the remaining medium components and concentrated within the standard reaction buffer.
- ❖ With an additional purification step undesired proteins were removed to receive MUC1-IgG2a Fc with high purities sufficient for analytical investigations and for the analysis of the cleavage reaction.
- ❖ In total, 30.8 L of cell culture medium from three different perfusion cultures containing MUC1-IgG2a Fc were purified using the 2-membrane module receiving 2.8 L concentrated MUC1-IgG2a Fc solution with a concentration of 200 mg\*L<sup>-1</sup>.
- ❖ The received MUC1-IgG2a Fc solution was applied to ion exchange chromatography for further purification. The different fractions were collected and concentrated using filtration to obtain the following batches:

<i>batch</i>	<i>MUC1-IgG2a Fc concentration</i>	<i>Purity</i>
I	0.55 mg*mL <sup>-1</sup>	27.6 %
II	2.33 mg*mL <sup>-1</sup>	94.6 %
III	0.97 mg*mL <sup>-1</sup>	94.4 %

- ❖ MUC1-IgG2a Fc was stable under sterile and protease-free conditions at pH 8 and pH 9 within a temperature range of 25 °C to 40 °C allowing a wide range of applicable reaction conditions.



## **CHAPTER 4**

---

ENTEROKINASE PRODUCTION



## 4 Enterokinase production<sup>1</sup>

### 4.1 Theoretical Background

#### 4.1.1 Metabolism of *Escherichia coli*

The microorganism *Escherichia coli* is one of the most investigated and abundantly used microorganism in the scientific world. Due to the innumerable information about *Escherichia coli*, this gram-negative bacterium became a versatile tool in the production of recombinant proteins and fine chemicals in industrial processes.

In large scale fermentation, it is of importance to supply the microorganism with sufficient amounts of carbon and nitrogen, which are not only required for microbial growth but also for the production of heterologous proteins [71]. During microbial growth, the generation of undesired by-products, such as acetate may occur, which have a negative influence on the production of recombinant proteins. Acetate formation may take place under aerobic and anaerobic conditions. Thus, a sufficient supply with oxygen has to be guaranteed to avoid an anaerobic environment, and thus decreased microbial growth, increased acetate formation, and decreased production of the target protein.

Nevertheless, at high growth rates and high glucose concentrations, the supplied carbon source may be converted into biomass and energy too slowly leading to the accumulation of acetate. This phenomenon is also called the bacterial “Crabtree-effect” [72-74]. Depending on the bacterial strain the formation of acetate above a certain concentration ( $5-10 \text{ g}_{\text{acetate}} \cdot \text{L}^{-1}$ ) [75, 76] may negatively influence growth behavior as well as the formation of heterologous proteins [73, 77].

There are several techniques to avoid the accumulation of acetate and therefore the reduction in product formation:

- 1) *Limitation of the carbon source* → controlled feed reduces growth rate and the formation of undesired by-products;
- 2) *Variation of carbon source* → glycerine is taken up slower than glucose [78];
- 3) *Cultivation in a “Dialysis” reactor* → acetate is continuously removed from the medium [79-81];
- 4) *Alternative E. coli strains* → strains that are either resistant against high acetate concentrations or generate only low amounts of acetate at high glucose concentrations [74, 82-84].

---

<sup>1</sup> In this project the light chain of enterokinase, which is catalytically active, is used. The sequence originates from bovine enterokinase.

### 4.1.2 Fermentative process engineering

For the production of enterokinase using recombinant *E. coli*, the fermentation can be divided into two different phases; a batch phase and a fed-batch phase. The growth during the batch phase can be calculated according to the following equations:

CALCULATION OF BIOMASS CHANGE OVER TIME

$$\frac{dx}{dt} = \mu_{\max} x$$

$\mu_{\max}$  : maximum specific growth rate / h<sup>-1</sup>  
 $x$  : biomass concentration / g\*L<sup>-1</sup>  
 $t$  : time / h

CALCULATION OF GROWTH RATE DEPENDENT ON SUBSTRATE CONCENTRATION  
 (MONOD-EQUATION)

$$\mu = \mu_{\max} \frac{S_l}{S_l + K_s}$$

$\mu_{\max}$  : maximum specific growth rate / h<sup>-1</sup>  
 $\mu$  : specific growth rate / h<sup>-1</sup>  
 $S_l$  : concentration of the limiting substrate / g\*L<sup>-1</sup>  
 $K_s$  : saturation constant of the limiting substrate / g\*L<sup>-1</sup>

The theoretical growth of the microorganism during batch fermentation can be divided into 6 stages: a lag phase, an acceleration phase, an exponential growth phase, a delay phase, a stationary phase and a dying phase (Figure 4-1).

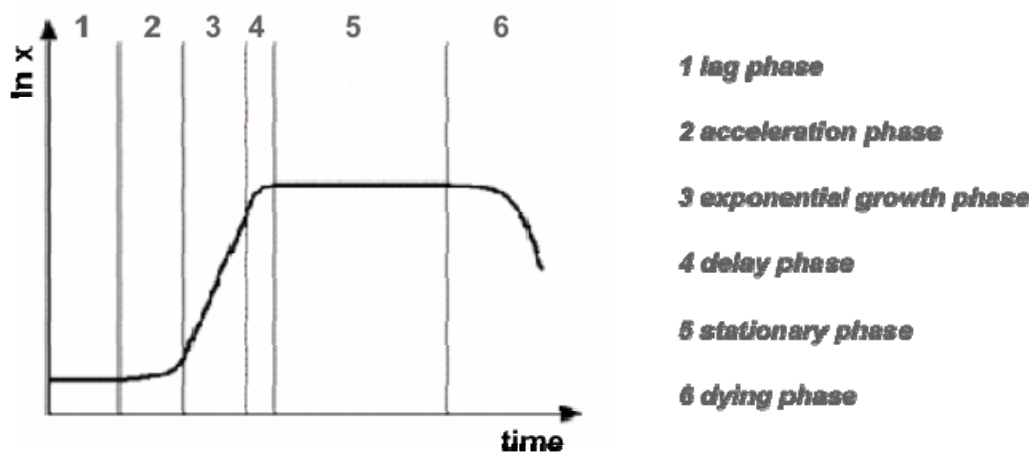


Figure 4-1 Schematic drawing of the growth behavior of microorganisms in a batch fermentation.

A batch fermentation is a so called “closed” system, in which a defined medium without a controlled substrate feed (neglecting the oxygen supply) is used. Growth rate and product

formation is mainly spontaneous and cannot be controlled. In contrast to this, a fed-batch fermentation, a “semi-open” system, cannot be divided into specific growth phases. In this case, a continuous feed of a certain substrate, for example glucose, is initiated, by which the growth behavior and product formation can be controlled. With this fermentation technique, possible limitations can be avoided allowing longer process times and a maximum utilization of the biosynthetic capability of the biomass [85]. The main differences between batch and fed-batch fermentation with regard to the change in reactor volume over time are summarized in Figure 4-2.

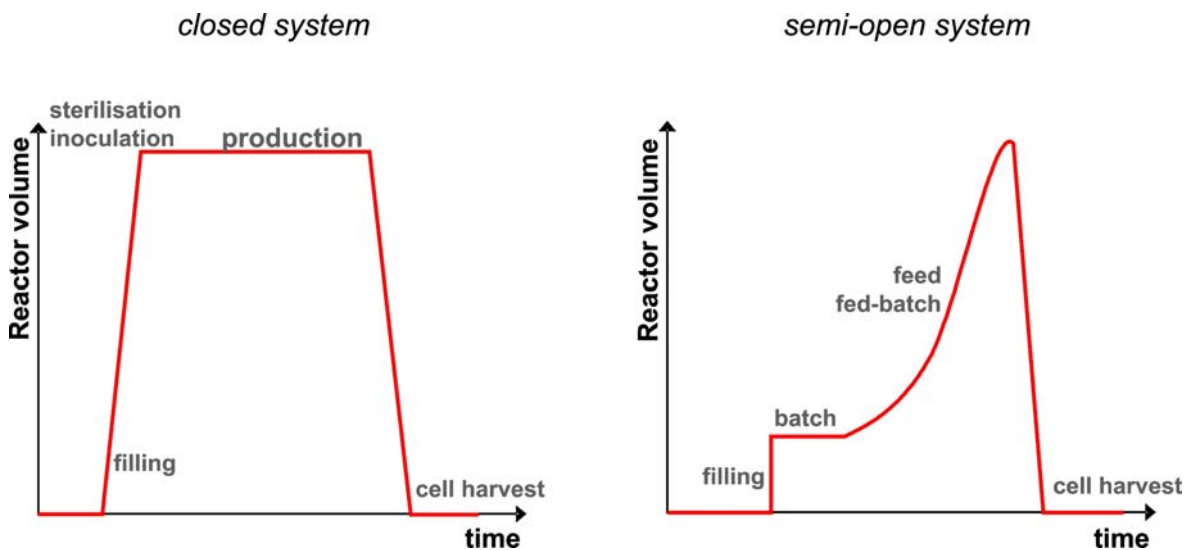


Figure 4-2 Fermentation strategies: batch fermentation (left) and fed-batch fermentation (right) [85].

### 4.1.3 Product isolation and purification

Recombinant microorganisms are widely used for the production of heterologous proteins. Besides optimizing the fermentation process itself, product isolation is the most important part in the production process.

The method of choice for product isolation depends greatly on the location of product accumulation; whether it is formed intracellularly, stored in inclusion bodies or secreted into the medium. Furthermore, the concentration and the physical and chemical properties of the target protein also influence the method applied for product isolation. The final application, either as a chemical precursor or as a pure supplement in the pharmaceutical industry, must be considered for the development of an appropriate downstream process with the necessary purity of the final product [86].

In case of intracellular product formation, microbial cells need to be lysed to gain the desired protein. Methods for cell disruption and thereby for product recovery are summarized in Table 4-1. Regardless of the isolation method, the target protein will be received in either a protein suspension containing all the proteins of the lysed cells or in

the culture broth together with the supplements. One of the most widely used technique for isolating and purifying proteins from suspension is affinity chromatography.

**Table 4-1 Selected methods for cell disruption.**

<i>Physical &amp; mechanical methods</i>	<i>Chemical methods</i>
freeze and thaw	detergents
ultrasonication	osmosis
French press	acid-base treatment
high pressure homogenisator	enzymatic cell lysis

Affinity chromatography involves the specific binding of proteins to metal ions, which have been immobilized to a stationary phase. Amines, amino acids or nucleotides, which are present in the mobile phase bind to the metal ions and can then be eluted specifically. The most abundantly method used involves immobilized nickel ions to which the amino acid histidine binds with a very high affinity. On a genetic level, the so called *His-Tag*, a sequence of at least six histidines, can be linked to the protein. Thereby, the affinity of the target protein for nickel ions is increased compared to naturally occurring proteins, which allows a simplified isolation and purification from protein suspensions and culture broths.

## **4.2 Fermentation of *Escherichia coli*<sup>2</sup>**

For the determination of the best expression host for enterokinase production, both strains, *E. coli* K12 G1968 and *E. coli* BL 21 DE3\*, have been compared with regard to growth behavior, glucose consumption and acetate formation. Furthermore, product formation was also analyzed and compared to the different fermentation parameters.

For a better understanding three representative fermentations will be discussed in the following sections.

### **4.2.1 Growth of expression hosts**

To compare the growth of both strains in the pre-culture, minimal medium was inoculated with cryo-cultures having similar optical densities. However, as it can be seen in Figure 4-3 *E. coli* K12 reaches an optical density of about 3.5 after ~10 h, whereas *E. coli* BL21 requires ~18 h. A prolonged incubation of the pre-cultures was avoided due to possible limitations. The differences in growth behavior might be explained by differing biomass concentrations within the cryo-cultures, taking living and dead cells into account.

<sup>2</sup> The results in this section were generated by Daniel Minör for his diploma thesis.

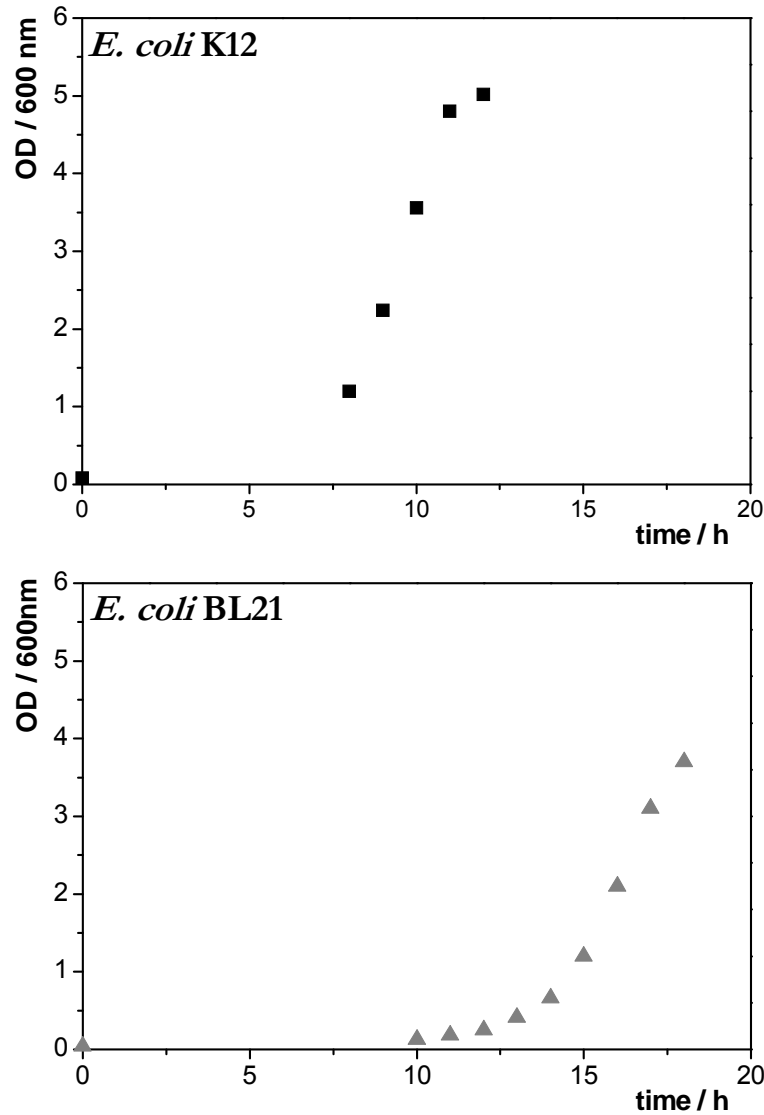


**Figure 4-3 Growth behavior of the expression strains *E. coli* K12 and *E. coli* BL21 in the pre-culture.**

The cultures with a starting optical density (OD<sub>600</sub>) of 0.08 were incubated at 37 °C and 150 rpm in minimal medium M9.

The main culture, carried out in a 30 L bioreactor, was inoculated with pre-cultures having similar optical densities to be able to compare the different fermentations. The growth of the microorganisms was quantified by determining the optical density and the cell dry weight (CDW).

The cultivation of the microorganisms can be divided into two phases, a batch phase for biomass production and a fed-batch phase with reduced temperature for product formation. During the fed-batch phase, glucose was added to avoid reduced microbial growth due to substrate limitation. Furthermore, a reduction in growth temperature results in deceleration of the metabolism of the microorganisms and thereby in the inhibition of inclusion body formation.

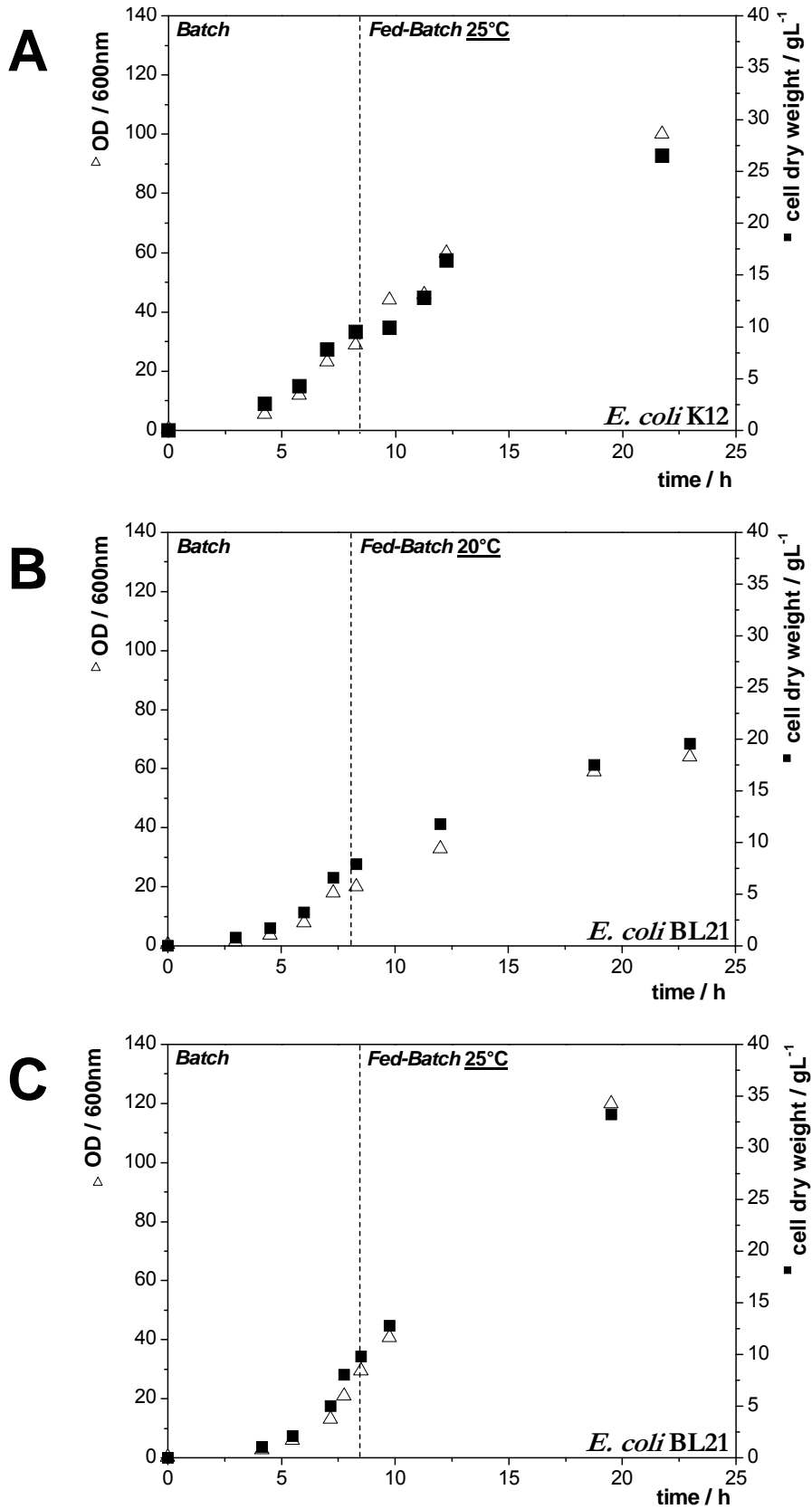


**Figure 4-4** Growth behavior of the expression strains *E. coli* K12 and *E. coli* BL21 in the main culture.

Microbial fermentation was performed using minimal medium M9 and 37 °C in the batch phase. With initiation of the glucose feed, the temperature was reduced as stated: **A)** *E. coli* K12 at 25 °C; **B)** *E. coli* BL21 at 20 °C, **C)** *E. coli* BL21 at 25 °C.



After inoculation, the cultivation of the microorganisms was carried out in a batch mode to generate biomass for product formation. During that phase the growth parameters were identical for all fermentations. Figure 4-4 shows the growth curves received for the main culture separated into batch and fed-batch phase for the two expression hosts.

Despite having the same fermentation parameters, there were differences in growth for *E. coli* K12 and *E. coli* BL21. *E. coli* K12 possessed a very short lag phase of about 2 h entering a negligible acceleration phase which was followed by exponential growth (Figure 4-4A). During fermentation, *E. coli* K12 reached a growth rate ( $\mu$ ) during the batch mode of  $0.47 \text{ h}^{-1}$ . In comparison, the lag phase of *E. coli* BL21 took 3 to 4 h (Figure 4-4B & C). Nevertheless, this strain reached higher growth rates of  $0.53 \text{ h}^{-1}$  and  $0.79 \text{ h}^{-1}$ . The higher growth rates for *E. coli* BL21 compensated for the longer lag phase, resulting in similar cultivation times during the batch phase of about 7 h (*E. coli* K12) to 7.5 h (*E. coli* BL21) for both production strains. The growth rates for the investigated strains are summarized in Table 4-2.

**Table 4-2 Growth rates  $\mu$  of the expression hosts reached during batch phase.**

<i>Strain</i>	<i>Temperature during batch (fed-batch) / °C</i>	<i>Specific growth rate (<math>\mu</math>) during batch phase / <math>\text{h}^{-1}</math></i>
<i>E. coli</i> K12	37 °C (25 °C)	0.47
<i>E. coli</i> BL21	37 °C (20 °C)	0.53
	37 °C (25 °C)	0.79

After the batch phase, a fed-batch mode was applied in which the temperature was decreased to avoid the formation of inclusion bodies and to increase accessible product formation. Furthermore, glucose was continuously added to supply the culture with a carbon source and to further increase biomass concentration.

As it can be seen in Figure 4-4, exponential growth was replaced by linear or stagnated growth after the temperature has been reduced from 37 °C to 20 °C or 25 °C. Linear growth with slight stagnation could be observed for *E. coli* K12, which has to adjust to the reduced temperature of 25 °C (Figure 4-4A). A final optical density of 100 and a CDW of  $26.48 \text{ g} \cdot \text{L}^{-1}$  were achieved after approximately 22 h (Table 4-3). In case of *E. coli* BL21, this could not be observed under the same conditions. Instead, exponential growth changed into a linear behavior when reducing growth temperature to 20 °C, whereas at 25 °C a strong linear growth was observed (Figure 4-4B&C). Optical densities and cell dry weights for *E. coli* BL21 varied depending on the temperature applied during the fed-batch

phase (Table 4-3). When grown at 20 °C, the optical density and the cell dry weight received were below the values for *E. coli* K12. In comparison, an improvement in cell growth was achieved at 25 °C, at which the optical density and the cell dry weight were increased.

**Table 4-3 Final values for OD and CDW received in the main culture.**

<i>Strain</i>	<i>Temperature during fed-batch / °C</i>	<i>Duration of fermentation / h</i>	<i>Final OD<sub>600</sub></i>	<i>Final CDW / g*L<sup>-1</sup></i>
<i>E. coli</i> K12	25	21.75	100	26.48
<i>E. coli</i> BL21	20	23.00	64	19.15
	25	19.50	120	33.24

According to the final values summarized in Table 4-3, *E. coli* BL21 cultivated at 25 °C during fed-batch phase, reached the highest biomass concentration in a short fermentation time. In contrast, *E. coli* BL21 cultivated at 20 °C reached only 57 % of the CDW after 23 h fermentation time, which emphasized the suboptimal growth conditions at this temperature. After approximately 22 h of fermentation, *E. coli* K12 measured about 80 % of CDW.

The given biomass yield in relation to the starting glucose concentration (Table 4-4) shows that the glucose was more efficiently converted into biomass by *E. coli* BL21 (20 °C:  $Y_S = 0.30$ , 25 °C:  $Y_S = 0.34$ ) than by *E. coli* K12 (25 °C:  $Y_S = 0.22$ ). This might be caused by a surplus of glucose in the metabolism, causing the glucose taken up not to be converted completely. In case of *E. coli* K12, the starting glucose concentration might have been too high resulting in a bacterial *Crabtree*-effect [74, 83, 84, 87]. Taking the resulting space-time yield into account emphasizes the high productivity of biomass over the duration of the fermentation for *E. coli* BL21 grown at 25 °C, which was  $1.7 \text{ g*L}^{-1}\text{*h}^{-1}$  (Table 4-4). For *E. coli* K12 and *E. coli* BL21 grown at 20 °C the space-time yield was either  $1.21 \text{ g*L}^{-1}\text{*h}^{-1}$  or  $0.85 \text{ g L}^{-1}\text{*h}^{-1}$ , being lower than for *E. coli* BL21 at 25 °C.

In case of biomass production at the given fermentation parameters, *E. coli* BL21 with a reduced fed-batch temperature of 25 °C seems to be the better candidate for the production process of enterokinase. Nevertheless, other factors have to be taken into account before choosing the final production strain, such as glucose consumption, acetate formation and most important product formation.

**Table 4-4 Biomass yield in correlation with the utilized glucose and resulting biomass production rate.**

<i>Strain</i>	<i>Temperature during fed-batch / °C</i>	<i>Duration of fermentation / h</i>	<i>Specific biomass yield in relation to substrate <math>Y_S</math></i>	<i>Biomass production rate / <math>g \cdot L^{-1} \cdot h^{-1}</math></i>
<i>E. coli</i> K12	25	21.75	0.22	1.21
<i>E. coli</i> BL21	20	23.00	0.30	0.85
	25	19.5	0.34	1.70

#### 4.2.2 Glucose consumption

Glucose was used as carbon source throughout the fermentation. Since the culture medium of the main culture was sterilized *in situ* causing slight variations in the starting concentration of the substrate which should be  $30 \text{ g} \cdot \text{L}^{-1}$ . The utilization of glucose during the three different fermentation processes is visualized in Figure 4-5.

The decrease of the glucose concentration correlates to the exponential growth of the microorganisms. As stated before, the growth behavior of the used strains differs in the batch phase causing different concentrations of glucose before going into the fed-batch mode. The glucose feed was adjusted according to the rate of glucose consumption at the end of the batch phase, which is stated in Table 4-5. The glucose concentration before starting the glucose feed varied from  $4.95 \text{ g} \cdot \text{L}^{-1}$  for *E. coli* K12 to  $12.5 \text{ g} \cdot \text{L}^{-1}$  for *E. coli* BL21. Thus, *E. coli* K12 has the highest rate of glucose consumption with  $2.77 \text{ g} \cdot \text{L}^{-1} \cdot \text{h}^{-1}$  compared to *E. coli* BL21 grown at  $20 \text{ }^\circ\text{C}$  with  $2.06 \text{ g} \cdot \text{L}^{-1} \cdot \text{h}^{-1}$  and  $2.28 \text{ g} \cdot \text{L}^{-1} \cdot \text{h}^{-1}$  when decreasing the temperature to  $25 \text{ }^\circ\text{C}$ .

**Table 4-5 Rate of glucose consumption during batch fermentation.**

<i>Strain</i>	<i>Temperature during fed-batch / °C</i>	<i>Rate of glucose consumption / <math>g \cdot L^{-1} \cdot h^{-1}</math></i>
<i>E. coli</i> K12	25	2.77
<i>E. coli</i> BL21	20	2.06
	25	2.28

The concentration of the glucose feed was set to  $500 \text{ g} \cdot \text{L}^{-1}$ . To define an appropriate feed rate, a limiting glucose concentration of  $0.1 \text{ g} \cdot \text{L}^{-1}$  was defined. At this substrate

concentration and a  $K_S$  value of  $0.001 \text{ g}\cdot\text{L}^{-1}$ , *E. coli* is still able to grow with 99 % of the maximum growth rate possible [88].

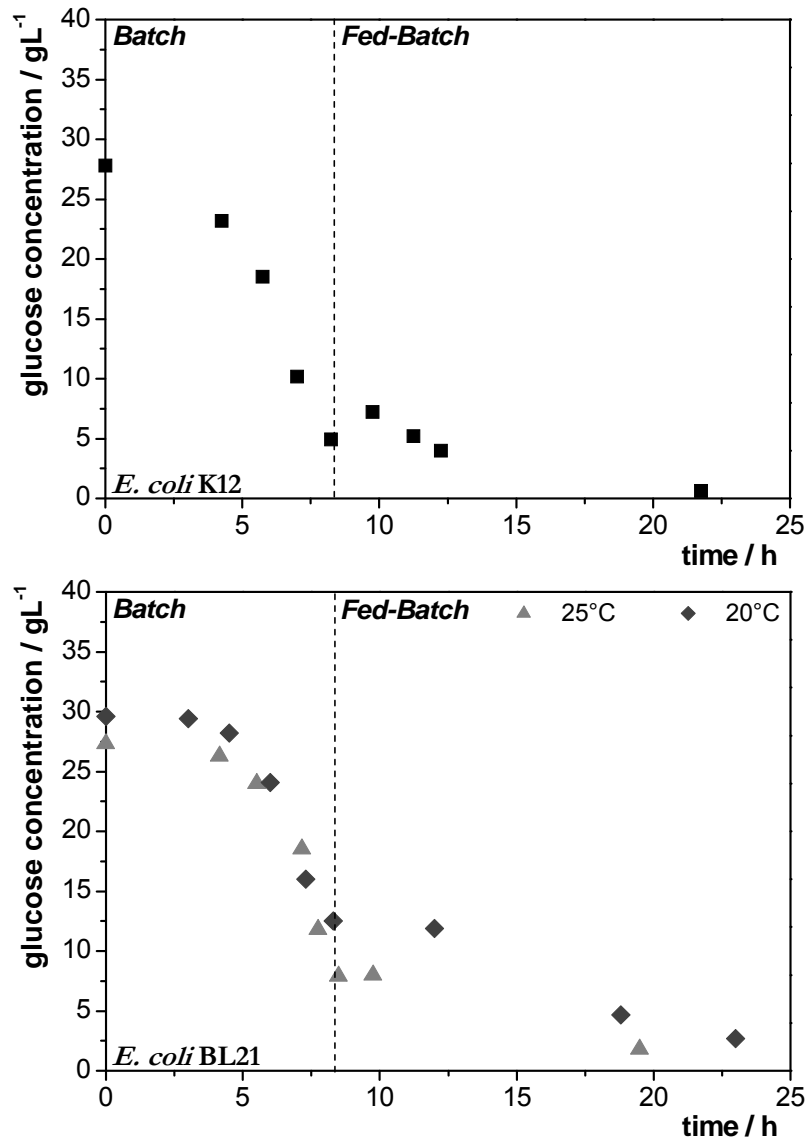


**Figure 4-5** Glucose concentration during the fermentation process.

The feed rate was adjusted according to the calculated consumption rates of glucose. When decreasing the temperature to 25 °C within the fed-batch phase, a feed rate of  $250 \text{ mL}\cdot\text{h}^{-1}$  for the glucose supply was sufficient to avoid substrate limitation in the stated fermentations for *E. coli* K12 and *E. coli* BL21 (Figure 4-5). An even lower feed rate of  $100 \text{ mL}\cdot\text{h}^{-1}$  was applied in case of *E. coli* BL21 with 20 °C as cultivation temperature. The differences in glucose consumption and feed rate adjustment can be explained by the change in metabolism influenced by the growth temperature.

**Table 4-6 Rate of glucose consumption during fed-batch phase.**

<i>Strain</i>	<i>Temperature during fed-batch / °C</i>	<i>Rate of glucose consumption / g*L<sup>-1</sup>*h<sup>-1</sup></i>
<i>E. coli</i> K12	25	6.57
<i>E. coli</i> BL21	20	3.34
	25	6.80

According to the rates of glucose consumption during the fed-batch phase (Table 4-6) glucose was taken up in similar concentrations by both *E. coli* strains when being grown at 25 °C. The utilization of substrate for *E. coli* K12 was 6.57 g\*L<sup>-1</sup>\*h<sup>-1</sup>, only slightly lower than for *E. coli* BL21, which measured 6.80 g\*L<sup>-1</sup>\*h<sup>-1</sup>. Nevertheless, it has been described before that the conversion of glucose to biomass is much more efficient for *E. coli* BL21 than for *E. coli* K12. As it was expected, the consumption of glucose for *E. coli* BL21 at 20 °C was much lower, measuring only 3.34 g\*L<sup>-1</sup>\*h<sup>-1</sup>. In all cases, a limitation of glucose could be avoided throughout the entire fermentation processes.

### 4.2.3 Acetate formation

When using glucose as carbon source for the fermentation of microorganisms, the formation of undesired by-products, such as acetate, may occur. The development of acetate is not only dependent on anaerobic conditions during fermentation, it can also take place under aerobic conditions [74, 83, 84, 87]. To avoid the formation of acetate, a sufficient supply of oxygen has to be guaranteed. High growth rates and high glucose concentrations, however, may lead to acetate accumulation due to an excess of the carbon source which cannot be converted into biomass fast enough.

Since the accumulation of acetate negatively influences the formation of heterologous proteins, a continuous control of acetate formation is necessary throughout fermentation. For the selection of the most effective production strain, it is of importance to have as low acetate formation as possible to ensure the utilization of glucose for biomass production and product development. In Figure 4-6, the formation of acetate during the course of the fermentation is visualized. In general it can be said that *E. coli* K12 produced much more acetate than *E. coli* BL21. The final acetate concentrations, summarized in Table 4-7, measured less than 1 g\*L<sup>-1</sup> for *E. coli* BL21 and more than 5 g\*L<sup>-1</sup> for *E. coli* K12.

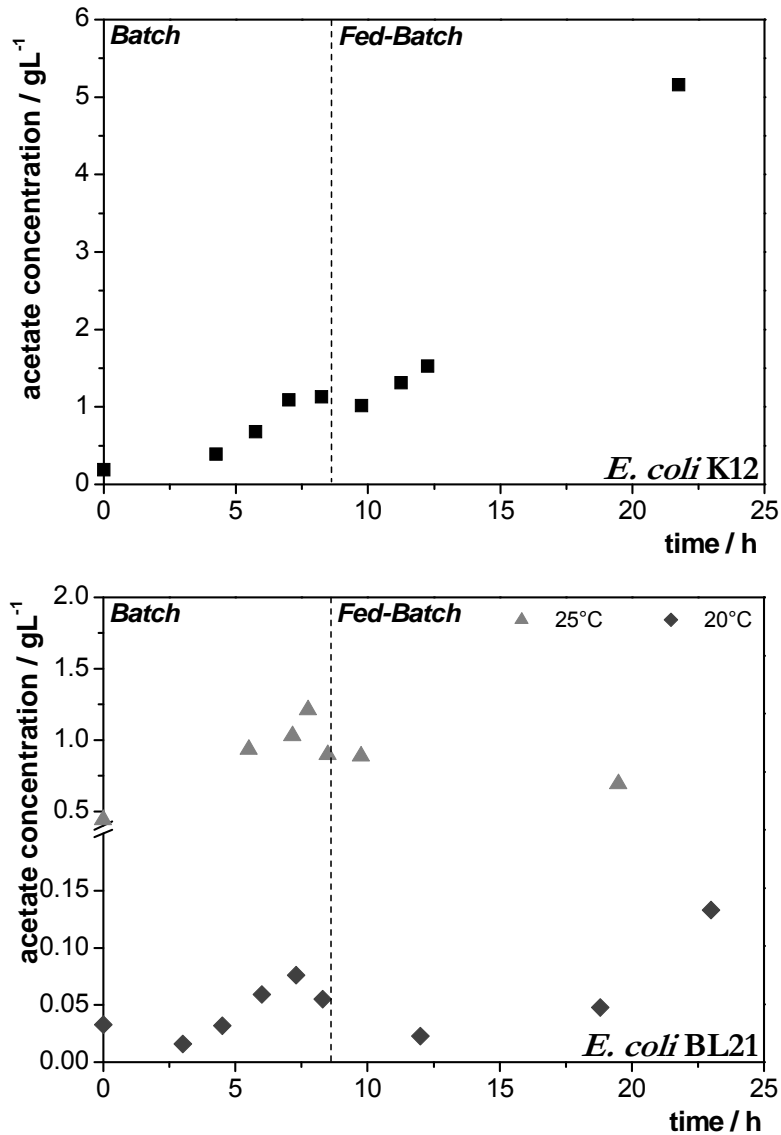


**Figure 4-6 Acetate formation of the expression hosts during fermentation.**

Expecting similar results for the acetate formation in case of all *E. coli* strains, independent of the temperature during the fed-batch phase, significant variations could be observed. During the batch phase, a maximum in acetate concentration occurred within the exponential growth, reaching its highest value of 1.21 g\*L<sup>-1</sup> for *E. coli* BL21 (25 °C). In all three cases, the acetate concentration slightly decreased again, before going into the fed-batch mode. Here, the differences in acetate formation are even more significant. *E. coli* K12 seemed to accumulate acetate in high quantities reaching a final concentration of 5.16 g\*L<sup>-1</sup>, whereas for *E. coli* BL21 (25 °C) acetate concentration further decreased to 0.69 g\*L<sup>-1</sup>. A negligible increase to 0.13 g\*L<sup>-1</sup> was observed for *E. coli* BL21 grown at 20 °C during fed-batch.

**Table 4-7 Final acetate concentrations measured during large scale fermentation.**

<i>Strain</i>	<i>Temperature during fed-batch / °C</i>	<i>Acetate concentration / g*L<sup>-1</sup></i>
<i>E. coli</i> K12	25	5.16
<i>E. coli</i> BL21	20	0.13
	25	0.69

The measured values for final acetate concentrations do not correlate with values described in the literature for *E. coli* K12 of 14 g\*L<sup>-1</sup> and 2 g\*L<sup>-1</sup> for *E. coli* BL21 [74, 83]. This could be explained with the reduction in growth temperature to 20 °C and 25 °C, which is below the optimal growth temperature for this microorganism. Nevertheless, *E. coli* K12 accumulates acetate in higher quantities than *E. coli* BL21, which demonstrates the same tendency as described by other researchers.

The high amount of acetate found in the culture medium may have caused the stagnated growth for *E. coli* K12 in the fed-batch phase. Furthermore, the low biomass yield ( $Y_s = 0.22$ ) can also be explained with the high acetate concentration, since the majority of glucose was used for the formation of acetate instead of biomass formation.

#### **4.2.4 Summary of fermentation**

According to the received results of the fermentation concerning glucose consumption, utilization of glucose to biomass, acetate formation and received optical densities and cell dry weights, the favored expression host was selected. It was shown, that *E. coli* BL21, cultivated at 25 °C in the fed-batch phase has several advantages compared to the other expression host, *E. coli* K12. It reached the highest growth rate with an optical density of 120 and a cell dry weight of 33.2 g\*L<sup>-1</sup>. Furthermore, the glucose consumption was moderate with high conversion into biomass and a very low acetate formation. By choosing *E. coli* strain BL21 as expression host, the production of recombinant enterokinase occurs constitutively.

### 4.3 Product isolation and purification<sup>3</sup>

#### 4.3.1 Enterokinase isolation with IMAC

The received biomass, after fermentation, was constantly cooled to reduce the action of proteases and a resulting loss of the produced enterokinase fusion protein. For cell disruption, the cell mass was applied to ultrasonication in a constant flow. Different times of sonication have been investigated to guarantee complete cell disruption. Prior to applying the protein solution to affinity chromatography, the lysed cells were separated from the solution by centrifugation. The recombinant protein DsbA/EK<sub>L</sub> (50 kDa) consists of two fusion partners which are linked by an enterokinase cleavage site and an adjacent His-Tag (Figure 4-7). This allows the purification of the desired protein by ion metal affinity chromatography (IMAC).

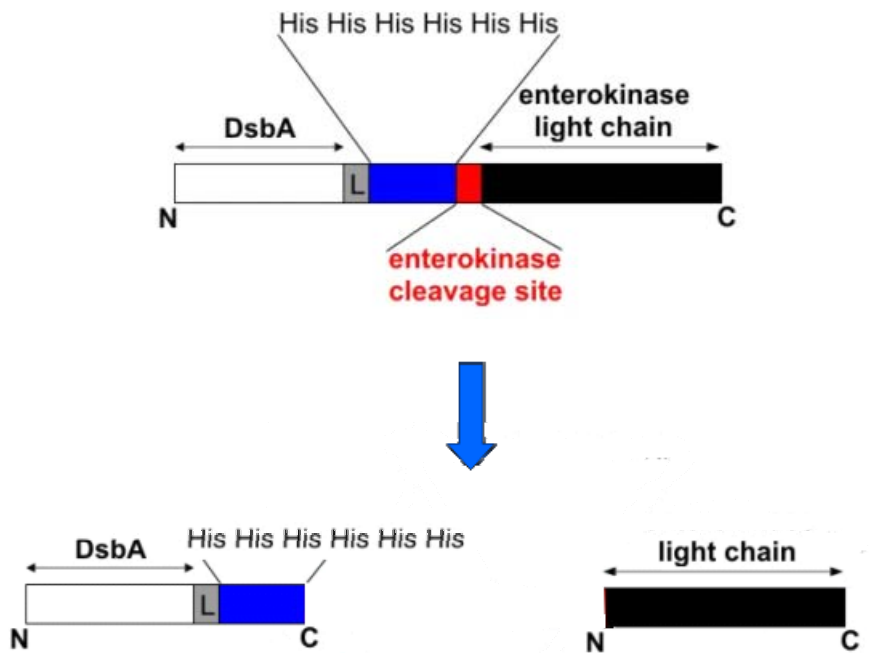


**Figure 4-7 Structure of the fusion protein DsbA/EK<sub>L</sub> for the production of the catalytic subunit of enterokinase.**

After cleavage of the fusion protein by enterokinase at the specific cleavage site, two product proteins develop: the fusion partner with the His-Tag and the desired enzyme without a purification Tag.

The general technical set-up involves the use of columns packed with sepharose onto which nickel ions have been immobilized. Purification using column affinity chromatography has some experimental limitations for the purification of large amounts of biomass, such as 1) application of protein solutions with low concentration to ensure the complete utilization of the entire binding capacity, which in part depends on the column

<sup>3</sup> The results in this section were generated by Daniel Minör for his diploma thesis.



size and the applied flow rate, 2) pressure limit and possible clogging of the material, and most important 3) long process times. The latter point is the most critical step in case of enterokinase purification using this specific expression system. Long purification procedures enhance spontaneously occurring autocatalysis of the desired fusion protein and thus, the loss of active enterokinase, since the protein lacks the important His-Tag for binding to the purification material.

To circumvent these difficulties, we established a new approach – a batch binding chamber, in which the sepharose is hold back by a nylon net (Figure 4-8). In both cases, the target protein was bound to the sepharose, non-specifically bound proteins were washed off and elution was initiated by increasing the imidazole concentration. The eluted fractions were pooled and analyzed using SDS-PAGE (Figure 4-9).

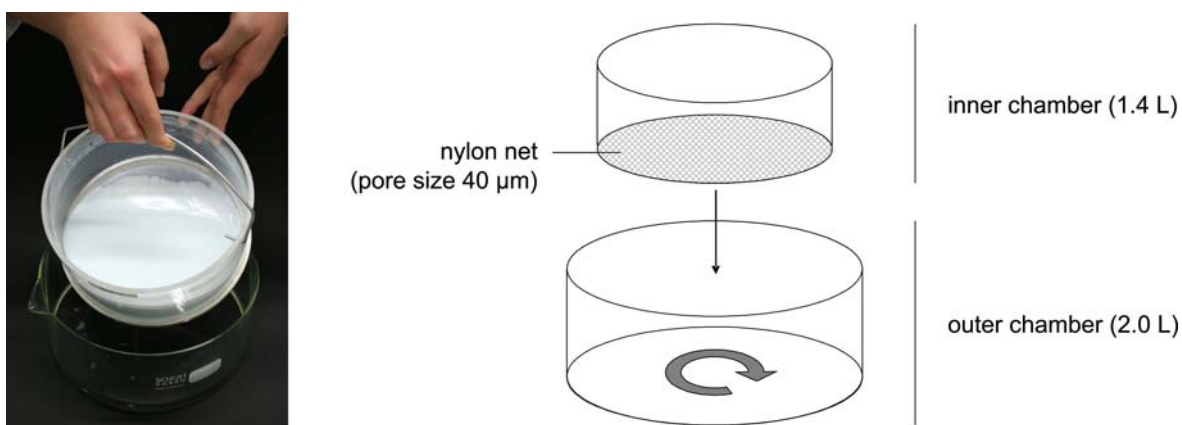


**Figure 4-8** Batch binding chamber used for the isolation of enterokinase by affinity chromatography.

In case of the column set-up, autocatalysis seems to occur during the long purification process, causing the undesired fusion partner to remain bound to the sepharose, while the target protein enterokinase flows through the column and is lost. This correlates with the protein bands found in SDS-PAGE, in which the fusion partner DsbA-linker-His (23.7 kDa) was found in much larger quantity than enterokinase (Figure 4-9A). Furthermore, enzyme activity could not be found in the eluted fractions, independent of the *E. coli* strain used. To allow autocatalysis of the possibly remaining fusion protein to occur, the protein solution was incubated at 4 °C before a concentration of the eluate was carried out. As it can be seen in Figure 4-9A, the incubation of the eluted fraction at 4 °C showed no difference to the non-incubated sample indicating that no further autocatalysis occurred. Therefore, the measured activities are due to the concentration of the eluate.

In case of *E. coli* K12, an enzyme activity of  $0.07 \text{ U} \cdot \text{g}_{\text{wCW}}^{-1}$  could be measured, which corresponds to  $2.16 \text{ } \mu\text{g}_{\text{EK}} \cdot \text{g}_{\text{wCW}}^{-1}$ . For *E. coli* BL21, enterokinase activity measured  $0.005 \text{ U} \cdot \text{g}_{\text{wCW}}^{-1}$  ( $= 0.152 \text{ } \mu\text{g}_{\text{EK}} \cdot \text{g}_{\text{wCW}}^{-1}$ ) produced (Table 4-8). Compared to the enterokinase

yields of about  $8 \mu\text{g}_{\text{EK}} \cdot \text{g}_{\text{wcv}}^{-1}$  received by Collins-Racie [7], our application proves that large quantities of active enterokinase get lost during purification using the common column chromatography, which is verified by the large quantities of fusion partner purified (Figure 4-9A).

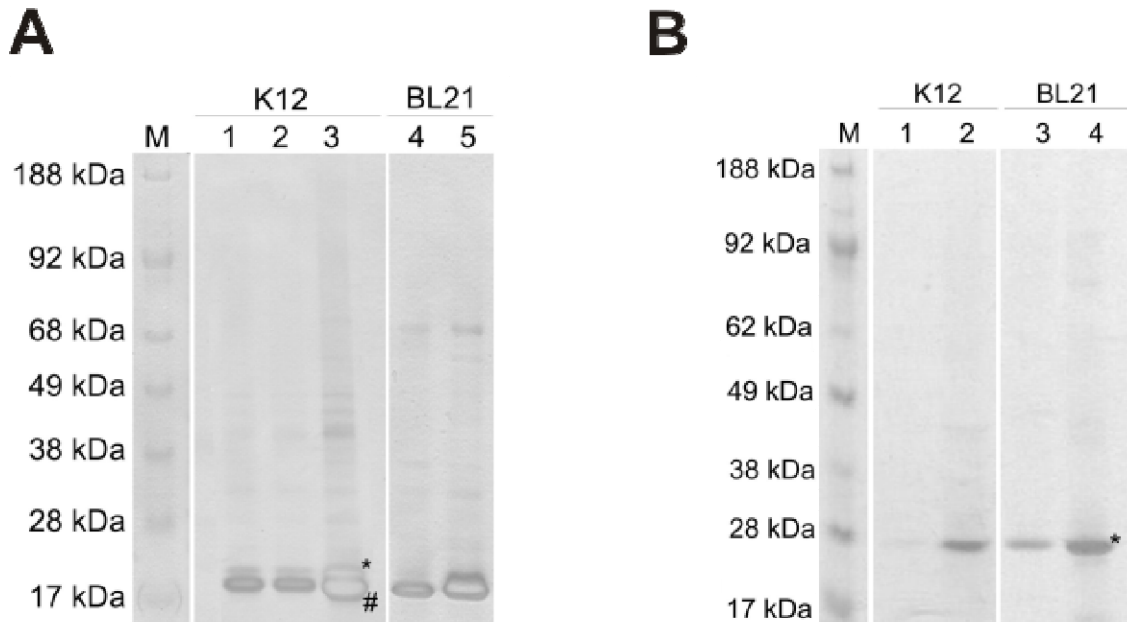


**Figure 4-9 SDS-PAGE of isolated enterokinase using different technical setups.**

(\* enterokinase with 26.3 kDa, # DsbA-Linker-*His* with 23.7 kDa)

**A) column affinity chromatography :** M – size marker, 1-3 *E. coli* K12 (1 – eluted fraction, 2 – eluted fraction after incubation at 4°C for 12 h, 3 – concentrated enterokinase), 4 & 5 *E. coli* BL21 (4 – eluted fraction, 5 – concentrated enterokinase);

**B) batch binding chamber:** M – size marker, 1 & 2 *E. coli* K12 (1 – eluted fraction 1:10, 2 – concentrated enterokinase 1:30), 3 & 4 *E. coli* BL21 (3 – eluted fraction 1:10, 4 – concentrated enterokinase 1:30).

Due to very high amounts of biomass received after 20 L fermentations and the need of a fast and simple downstream process for enterokinase production, a more efficient purification method was developed. By using a batch binding chamber (Figure 4-8), pressure limitations could be avoided and the process time was reduced by at least half, compared to Collins-Racie. Furthermore, the entire purification process is much more simplified allowing fast buffer changes without any loss of eluted protein. Loss of enterokinase due to autocatalysis could also be avoided due to the shortened process time. Spontaneous autocatalysis is assumed to start when the protein solution reaches a concentration of at least  $1 \text{ mg} \cdot \text{mL}^{-1}$ , which was achieved by ultrafiltration. The velocity of fusion protein cleavage rises with increasing protein concentration in the eluate. During the purification process, the fusion partner DsbA-Linker-*His* is lost, since it could not be detected on SDS-PAGE (Figure 4-9B). After concentration, activity of the isolated enterokinase was determined, measuring  $2.05 \text{ U} \cdot \text{g}_{\text{wcv}}^{-1}$  for *E. coli* K12 and  $3.61 \text{ U} \cdot \text{g}_{\text{wcv}}^{-1}$

for *E. coli* BL21 (Table 4-8). Thus, the isolated enterokinase using the batch binding chamber was calculated to be 63.29  $\mu\text{g}_{\text{EK}} \cdot \text{g}_{\text{wCW}}^{-1}$  in case of *E. coli* K12 and 111.5  $\mu\text{g}_{\text{EK}} \cdot \text{g}_{\text{wCW}}^{-1}$  for *E. coli* BL21 (Table 4-8). With the original method developed by Collins-Racie 8  $\mu\text{g}_{\text{EK}} \cdot \text{g}_{\text{wCW}}^{-1}$  could be isolated. Using the same expression system, *E. coli* K12, and applying our newly developed purification procedure, the enzyme yield was increased by a factor of 8. Taking into account that with *E. coli* BL21 protein yields should be increase due to constitutive production, the total yield of enzyme isolated was improved by a factor of 14 (Figure 4-10).

**Table 4-8 Activity and amount of isolated enterokinase produced by different expression hosts using varying purification procedures.**

<i>Method</i>	<i>Column</i>		<i>Batch</i>	
<i>E. coli</i>	K12	BL12	K12	BL21
Activity / $\text{U} \cdot \text{g}_{\text{wCW}}^{-1}$	0.07	0.005	2.05	3.61
Yield / $\mu\text{g}_{\text{EK}} \cdot \text{g}_{\text{wCW}}^{-1}$	2.16	0.152	63.29	111.50

In addition to increasing the amount of active enterokinase isolated, the required time for purification was significantly decreased by half, making the entire downstream process more efficient. Furthermore, the procedure can be carried out with only minimum effort resulting in large quantities of pure, active enterokinase.

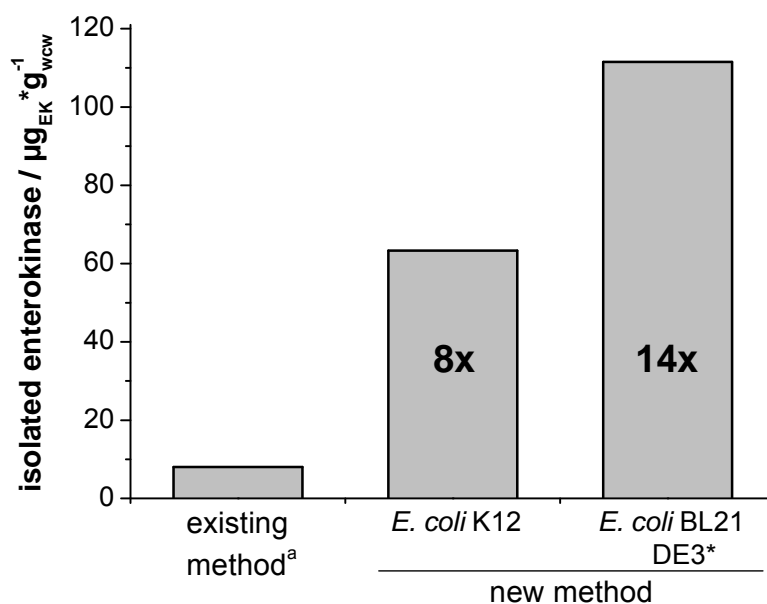


**Figure 4-10 Enterokinase yields received by using an improved downstream process involving the use of a batch binding chamber for enzyme isolation (<sup>a</sup> [7]).**

Enterokinase production using different yeast strains reaches a volumetric productivity of  $31.5 \mu\text{g}_{\text{EK}} \cdot \text{L}^{-1} \cdot \text{h}^{-1}$  to  $182 \mu\text{g}_{\text{EK}} \cdot \text{L}^{-1} \cdot \text{h}^{-1}$  [89, 90]. With our isolation and purification approach a formulation rate of  $214 \mu\text{g}_{\text{EK}} \cdot \text{L}^{-1} \cdot \text{h}^{-1}$  could be achieved, which means a maximum increase by a factor of 7.

#### 4.3.2 Enterokinase purification with anion exchange chromatography

The main goal was to develop a fast and efficient purification procedure for enterokinase, making it an attractive tool for the cleavage of pharmacologically important fusion proteins. By introducing an additional purification step using ion exchange chromatography the purity of the isolated enterokinase could be improved further. This is of great importance when using enterokinase for more complex applications, such as immobilization, in which undesired proteins can disturb the coupling reaction and can influence the remaining activity of the immobilized enzyme.

By using a strong anion exchanger, proteins can be eluted using a specific salt gradient according to their isoelectric point (Figure 4-11). As a result, remaining impurities were removed as it can be seen on the corresponding SDS-PAGE (Figure 4-11A). In Figure 4-11B, a representative chromatogram with the applied salt gradient is shown. The additional purification step using ion exchange chromatography was performed without any loss in activity of the biocatalyst (Figure 4-11C).

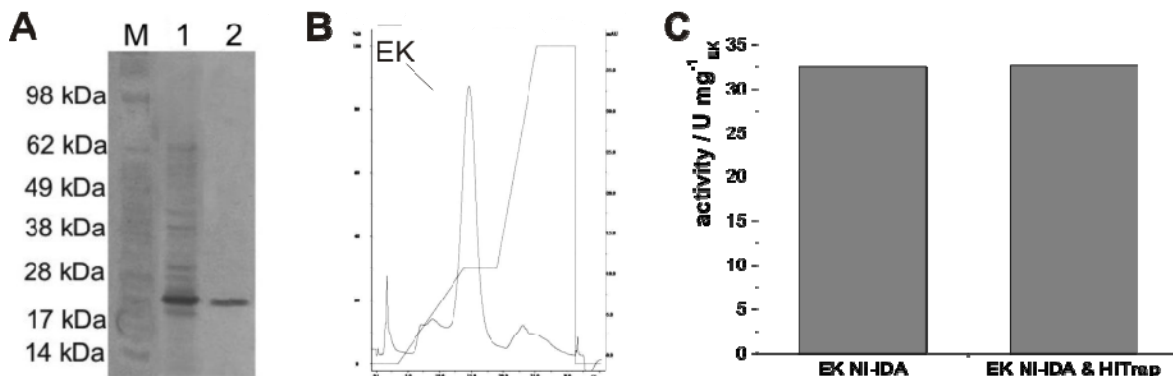


**Figure 4-11 Purification of isolated enterokinase using ion exchange chromatography.**  
**A)** SDS-PAGE: M – size marker, 1 – enterokinase after Ni-IDA sepharose, 2 – enterokinase after IEC;  
**B)** corresponding chromatogram received for IEC;  
**C)** activity of purified enterokinase.

In conclusion, enterokinase can be produced in sufficient quantities without losing activity during the purification process. Furthermore, enterokinase can be applied to immobilization without the coupling reaction or enzyme activity being influenced by protein impurities.

### 4.4 New Expression plasmid

As it has been emphasized before, the purification process of enterokinase with the existing expression plasmid has one particular disadvantage: during a long downstream process spontaneous autocatalysis occurs cleaving off the fusion partner with the significant His-Tag required for purification. Thus, the desired protein, the enzyme enterokinase, cannot actively be bound and purified. Instead, the fusion partner DsbA-linker-His binds to the nickel ions and is eluted during the purification process, whereas the enterokinase is eliminated from the system (Figure 4-12 left).

By changing the technical set-up of the purification procedure the time required for the downstream process was drastically decreased resulting in a significant increase in the enzyme yield. However, by introducing a change at the genetic level, the loss of the purification Tag could be avoided completely. Therefore, a new expression plasmid for enterokinase production was constructed, in which the His-Tag was shifted from the N-terminal side of the enterokinase to the C-terminal side. If autocatalysis occurs spontaneously, the fusion partner will be cleaved off with the His-Tag still being linked to enterokinase, which could now be purified (Figure 4-12 right). According to literature research, the activity of enterokinase should not be affected by aligning additional amino acids to the C-terminal side of the protein structure, whereas any N-terminal extensions may block enzyme activity [89, 91].

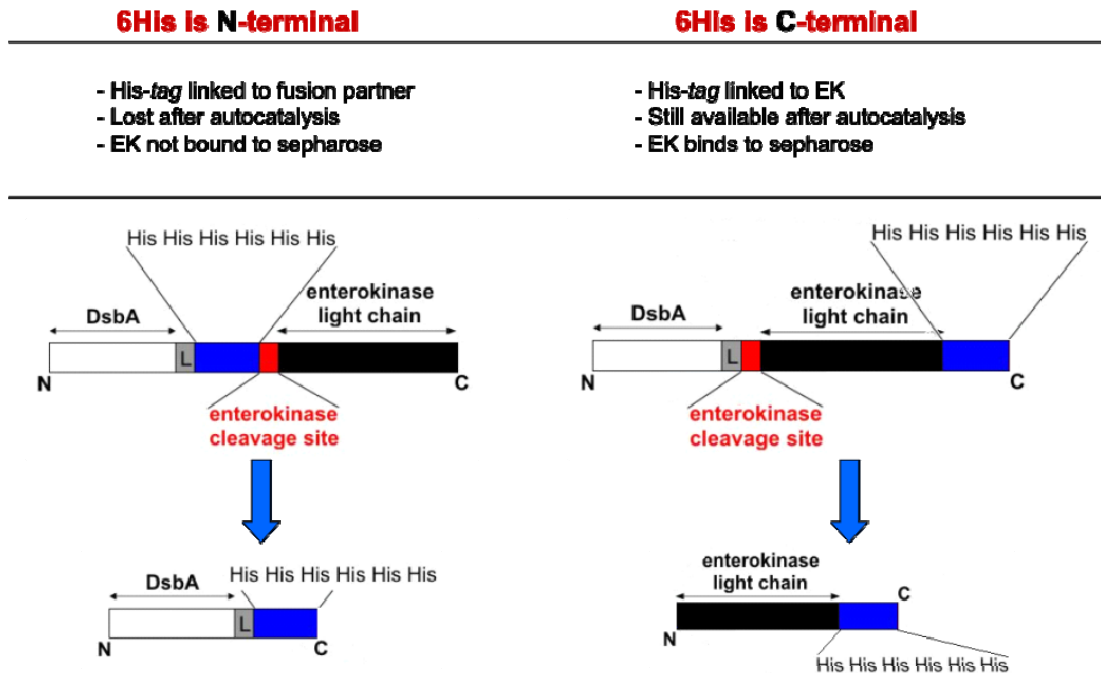


**Figure 4-12 Comparison of the two expression systems for the production of enterokinase.**  
**Left:** existing system with the His-Tag being N-terminal to the enterokinase cleavage site;  
**Right:** new system with the His-Tag being at the C-terminal side of the enterokinase.

The expression host *E. coli* B21 DE3\* was transformed with the new expression plasmid, which is under the control of the T5 promoter. Therefore, the induction of the promoter was necessary to initiate expression.

Fermentation of the new expression host was carried out with the previously described method with an additional induction step. The fusion protein DsbA-linker-EK-*His* was isolated and purified with the optimized downstream process, which has been described in previous sections of this chapter. As it can be seen in Figure 4-13 (left), a protein with the appropriate size of about 50 kDa could be isolated and purified representing the desired fusion protein. Furthermore, a 26 kDa protein, possibly enterokinase, was also isolated. Unexpectedly, when analyzing the received protein solution, no enzyme activity could be detected. Several explanations for the loss of enzyme activity are summarized in Figure 4-13 (right). However, changes in the purification procedure to circumvent any negative influences on enzyme activity did not result in enzyme activity in the eluted protein solution.

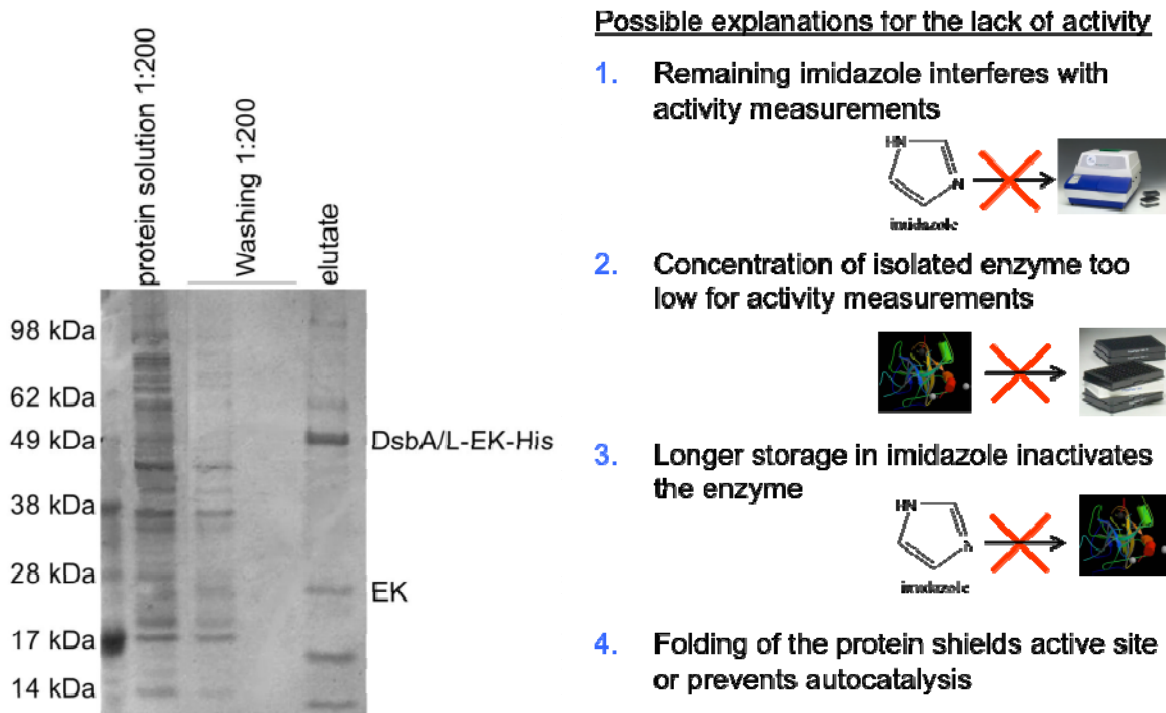


**Figure 4-13 Results for isolation and purification of enterokinase using the new expression system.**

**Left:** representing SDS-PAGE showing distinct protein bands at 26 kDa (EK) and 50 kDa (DsbA/L-EK-*His*);

**Right:** explanations for the lack in enzyme activity in eluted fraction.

The downstream process has been varied as described below to eliminate any influential factors:

- to 1) Extensive washing with standard reaction buffer to ensure complete removal of imidazole from the solution;
- to 2) Significantly increasing biomass for enzyme isolation to receive higher protein concentration in eluate;
- to 3) Decreasing the exposure time to imidazole by reducing process times.

Early investigations on the development of expression systems for the production of enterokinase showed, that N-terminal extensions negatively influence enterokinase activity, whereas alignments at the C-terminus of the protein still result in full enzymatic activity [7, 89, 91]. Despite this, the translocation of the His-Tag to the C-terminal side may have changed the folding of the protein causing the active site to be shielded or not sufficiently accessible for autocatalysis to occur.

#### 4.5 Summary: Enterokinase production

The results received for the production of the enzyme enterokinase can be summarized as follows:

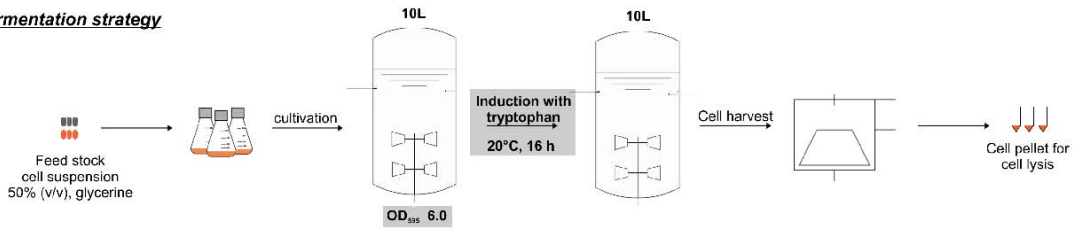
- ❖ The light chain of enterokinase produced as fusion protein DsbA/EK<sub>L</sub> is expressed by the recombinant *E. coli* strains K12 and BL21. The fermentation procedure has been optimized with regard to glucose consumption, acetate, biomass, and product formation.
- ❖ Investigations proved *E. coli* BL21 cultured at 25 °C to be the best suited expression host for the production of enterokinase receiving the highest biomass yield of 33.2 g\*L<sup>-1</sup> with a very low acetate formation of 0.69 g\*L<sup>-1</sup> and a moderate glucose consumption of 6.8 g\*L<sup>-1</sup>\*h<sup>-1</sup>.
- ❖ A newly developed, simpler downstream process (Figure 4-14) using a batch binding chamber for affinity chromatography circumvented the loss of enterokinase due to autocatalysis and reduced the process time by half.
- ❖ The enterokinase yield was increased 8-fold for the induced expression system *E. coli* K12 from 8 µg<sub>EK</sub>\*g<sub>wcw</sub><sup>-1</sup> to 63.3 µg<sub>EK</sub>\*g<sub>wcw</sub><sup>-1</sup>, and a 14-fold increase was achieved using a constitutive expression system with *E. coli* BL21 receiving 111.5 µg<sub>EK</sub>\*g<sub>wcw</sub><sup>-1</sup>.
- ❖ In comparison with yeast expression systems, a 7-fold increase in the formulation rate from 31.5 g\*L<sup>-1</sup>\*h<sup>-1</sup> to 214 g\*L<sup>-1</sup>\*h<sup>-1</sup> was achieved.
- ❖ A new expression system, in which the His-Tag is linked to enterokinase instead of to the fusion partner, could not further simplify the downstream process. The eluted protein showed no enzymatic activity.

The final fermentation and purification strategies are summarized and compared in Figure 4-14.

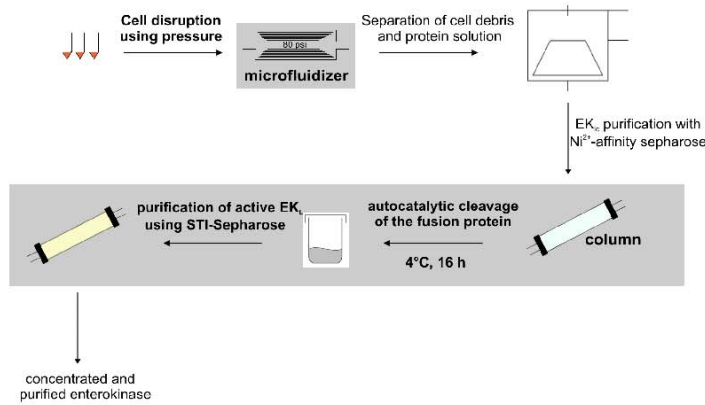


***E. coli* K 12**  
**original method**

**Fermentation strategy**

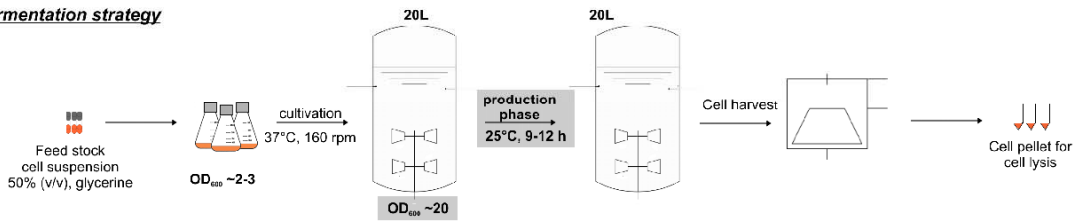


**Purification strategy**



***E. coli* BL21 DE3\***  
**new method**

**Fermentation strategy**



**Purification strategy**

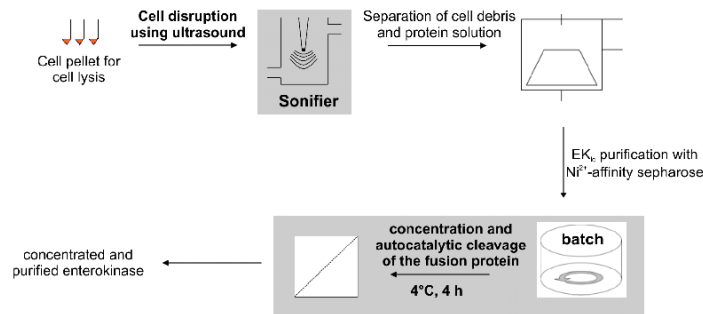


Figure 4-14 Comparison of the final production processes for enterokinase.



## **CHAPTER 5**

---

ENZYME CHARACTERIZATION



## 5 Enzyme characterization

### 5.1 Theoretical Background

Within an organism, the catalytic activity of various enzymes has to be regulated to coordinate numerous metabolic processes successfully. Nevertheless, each enzyme represents a highly specific catalyst for single reactions. Enzymes at large, however, become so diverse, as it is required by the organism. The velocity of an enzyme-catalyzed reaction is not just dependent on the thermodynamic factors of the reaction itself, but also by the catalytic properties of the enzyme. Parameters such as temperature, pH, and the ionic strength of the reaction medium can influence enzyme properties. Apart from this, the velocity of the enzymatic reaction is also determined by the substrate concentration [S]. In general, reaction velocity increases with rising substrate concentration until a steady state is reached, representing the maximum reaction velocity ( $V_{\max}$ ). The simplest case, in which only one substrate is converted, can be described with the Michaelis-Menten equation:

$$V_0 = \frac{V_{\max} \cdot [S]}{K_M + [S]}$$

[S]	substrate concentration at the beginning of the reaction / $\mu\text{M}$
$V_0$	starting reaction velocity at a specific substrate concentration / $\text{U} \cdot \text{mg}_{\text{EK}}^{-1}$
$V_{\max}$	maximum velocity of the reaction achieved with this substrate concentration / $\text{U} \cdot \text{mg}_{\text{EK}}^{-1}$
$K_M$	Michaelis constant; reaction takes place with half the maximum reaction velocity at this substrate concentration; represents the degree of affinity of the enzyme towards the substrate / $\mu\text{M}$

Enzymes contain a large number of acid and base groups, which are mainly located on their surface. As it is known from general chemistry, the charges of these groups vary according to the pH of the reaction medium. This, of course, influences the total net charge of the molecule, the distribution of charges on the outer surface of the enzyme and in consequence the reactivity of the catalytically active groups. Considering these facts, the pH of the reaction medium affects the activity, the structural stability and solubility of the enzyme.

The ionic strength of the solution is an important factor affecting enzyme activity in catalytic reactions which depend on the movement of charged molecules relative to each

other. Thus, it is of importance to choose the most effective buffer system for a specific enzymatic reaction. Considering the effect of the temperature on the activity of enzymes, reaction rates will rise with increasing temperature in accordance with the Arrhenius equation:

$$k = Ae^{-E_A / RT}$$

k	kinetic rate constant for the reaction / -
A	Arrhenius constant (frequency factor) / -
E <sub>A</sub>	standard free energy of activation / J*mol <sup>-1</sup>
R	gas law constant / J*mol <sup>-1</sup> *K <sup>-1</sup>
T	absolute temperature / K

Generally, using enzymes at high temperatures would have some advantages such as exploitation of the increasing reaction rates and the cumulative protection against microbial contamination. However, enzymes as proteins undergo essentially irreversible denaturation entailing a significant loss in catalytic activity at temperatures above those to which they are ordinarily exposed in their natural environment. Thus, enzyme activity with regard to enzyme stability at certain temperatures has to be considered to determine specific reaction parameters.

For the characterization of enterokinase light chain two different substrates were used: a synthetic substrate composed of the enterokinase recognition sequence linked via an amide bond to the fluorophore 2-naphthylamide (2NA) and the recombinant fusion protein with the enterokinase cleavage site as linker. To find the optimal reaction parameters for both substrates, investigations on the activity influenced by temperature, pH, substrate concentration, and buffer composition have been carried out for both substrates.

## **5.2 Synthetic substrate GD<sub>4</sub>K-2NA<sup>4</sup>**

The use of the synthetic substrate GD<sub>4</sub>K-2NA was first introduced by Antonowicz in 1980 [92]. Since that time, this substrate is widely used for fluorometric and colorimetric assays utilized for enterokinase investigations. As it can be seen in Figure 5-1 enterokinase activity and half-life time has been determined in dependency of pH, temperature, substrate concentration, and buffer composition.

---

<sup>4</sup> All results presented in this section were obtained using EKMax™ (Invitrogen, Carlsbad, USA).

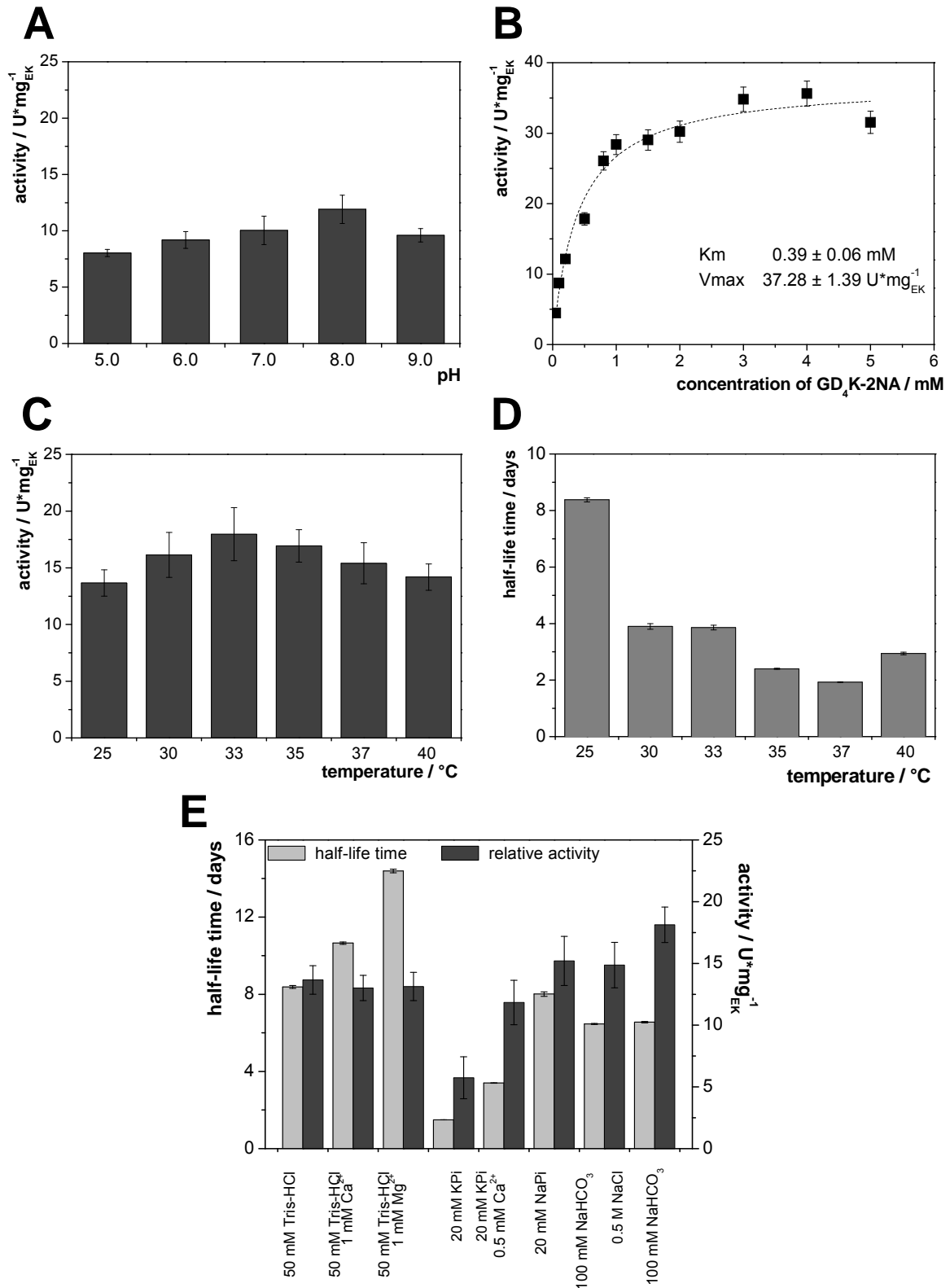


**Figure 5-1 Determination of reaction parameters for the synthetic substrate GD<sub>4</sub>K-2NA.** All measurements were performed in 50 mM Tris-HCl, pH 8.0 using 0.1 mM GD<sub>4</sub>K-2NA, if not stated otherwise. **A)** pH dependency of enterokinase activity measured at 25 °C, **B)** substrate dependency of enterokinase activity measured at 33 °C, **C)** temperature dependency of enterokinase activity, **D)** half-life time of enterokinase at different temperatures, **E)** activity and half-life time at 33 °C of enterokinase using different buffer compositions.

Using the synthetic substrate GD<sub>4</sub>K-2NA, a pH optimum of 8.0 (Figure 5-1A) as well as a  $K_M$  of 0.39 mM and a  $V_{max}$  of 37.3 U\*mg<sub>EK</sub><sup>-1</sup> (Figure 5-1B) were determined. Enterokinase purified from rat small intestine was shown to have a pH optimum at 8.2 and a  $K_M$  of 0.17 mM [92]. For human enterokinase produced in recombinant *E. coli*, the  $K_M$  value was calculated to be 0.16 mM with a pH optimum at 7.5 [93]. The variation for the given values may be the result of different buffer compositions used in activity measurements. Furthermore, variable excitation filters (337 nm or 350 nm) and emission wavelengths (420 nm or 460 nm) were applied, which may have also contributed to the slight variations in the measured values.

When investigating the activity at different reaction temperatures, enterokinase shows highest activity at 33 °C with 18.0 ± 2.3 U\*mg<sub>EK</sub><sup>-1</sup> and measuring less than 80 % at 25 °C and 40 °C (Figure 5-1C). However, at temperatures different from their natural environment, enzymes may undergo irreversible denaturation which can result in a significant loss of biological activity. Therefore, the half-life at various temperatures was also determined, measuring about 8.38 ± 0.07 days at 25 °C. With increasing temperature, the storage stability decreased more than 50 % for 30 °C and 33 °C. A half-life time of about 1.9 ± 0.1 days was determined for 37 °C (Figure 5-1D). Although having highest activity at 33 °C, optimal reaction conditions include a temperature of 25 °C due to a maximum half-life of 8 days.

Considering a wide variety of buffer compositions, enterokinase activity and half-life time were determined to find optimal reaction solutions for fusion protein cleavage and immobilization of enterokinase. Buffers with higher ionic strength, such as sodium carbonate buffer, are preferred for the immobilization of enterokinase, but also sodium phosphate buffer was recommended by the vendor of the carrier material investigated (see chapter 6). Although activity was highest for sodium carbonate buffer with 18.1 ± 1.4 U\*mg<sub>EK</sub><sup>-1</sup>, the half-life time was less than 7 days. For sodium phosphate buffer an activity of 15.2 ± 2.0 U\*mg<sub>EK</sub><sup>-1</sup> was determined with a half-life time of 8.61 ± 0.01 days (Figure 5-1E). Taking into account that during the coupling of enterokinase to a carrier material the activity of the biocatalyst is of minor interest, the half-life time of the enzyme in that buffer system, however, is much more important considering the time required for the coupling reaction. Thus, sodium phosphate buffer was used for immobilization. Finding the most suited buffer for the cleavage reaction, the activity in combination to the half-life time had to be considered. When comparing the different buffer variations using Tris-HCl either supplemented with Mg<sup>2+</sup> or Ca<sup>2+</sup>, similar activities of approximately 13 U\*mg<sub>EK</sub><sup>-1</sup> were found. Mikhailova and co-workers already investigated the effect of calcium ions on the hydrolysis of low molecular weight substrates catalyzed by different forms of enterokinase [94]. They found a 3-fold activation in hydrolysis of the synthetic



substrate GD<sub>4</sub>K-2NA by the natural full-length enterokinase. In case of enterokinase light chain, an activation effect using different concentrations of Ca<sup>2+</sup> was not detected by Mikhailova. This correlates with our findings, in which the activity of enterokinase could not be increase by adding metal ions. The enzyme stability, however, seems to be greatly influenced by the addition of metal ions. The half-life time of 8.38 ± 0.07 days could be increased adding Ca<sup>2+</sup> to 10.65 ± 0.06 days and even to 14.59 ± 0.09 days when using Mg<sup>2+</sup> as supplement (Figure 5-1E).

### **5.3 MUC1-IgG2a Fc as substrate<sup>5</sup>**

As mentioned before, enzyme activity is influenced by a variety of parameters. Therefore, reaction parameters had to be determined when changing the substrate to MUC1-IgG2a Fc. While it is unlikely to receive significant changes in temperature and pH dependency, a difference in the measured activity and substrate affinity of enterokinase was expected.

As before, using the synthetic substrate, enterokinase shows highest activity (11.9 ± 1.3 U\*mg<sub>EK</sub><sup>-1</sup>) at pH 8.0, reaching about 70 % at pH 7.0 and approximately 35 % at pH 9.5. As mentioned before, the charge of acid and base groups within a protein changes with varying pH influencing the activity, the structural stability and also the solubility of proteins. Nevertheless, it could be shown in Chapter 3 that the fusion protein MUC1-IgG2a Fc is stable at pH 8 and 9 in a temperature range between 25 °C and 40 °C.

Considering the findings for enterokinase activity with the synthetic substrate, the enzyme exhibits its highest half-life time (8.38 ± 0.07 days) at 25 °C. Increasing temperatures result in loss of activity over time. Thus, even when measuring highest activity of 7.2 ± 0.4 U\*mg<sub>EK</sub><sup>-1</sup> at 40 °C / 45 °C in fusion protein cleavage, it can be assumed that degradation of both proteins at such high temperatures occur. Furthermore, performing the cleavage reaction at temperatures above 25 °C drastically reduces the half-life time of the biocatalyst.

In contrast to the synthetic substrate GD<sub>4</sub>K-2NA, an increase of fusion protein concentration in the reaction solution above 5 µM (0.8 mg\*mL<sup>-1</sup>) causes a drastic reduction in enzyme activity. Highest activities of 26.2 ± 1.3 U\*mg<sub>EK</sub><sup>-1</sup> were measured at a concentration range between 2.7 µM and 4.5 µM of MUC1-IgG2a Fc. A drastic decrease of about 80 % was observed at substrate concentrations of 9 µM to 10 µM measuring 5.5 ± 0.3 U\*mg<sub>EK</sub><sup>-1</sup>. The inhibitory effect of MUC1-IgG2a Fc suggests a substrate surplus

---

<sup>5</sup> All results presented in this section were obtained using isolated EK produced by the expression host *E. coli* BL21.

inhibition, but might in parallel be caused by additional side reactions, such as a possible product inhibition of either MUC1 or IgG2a Fc.

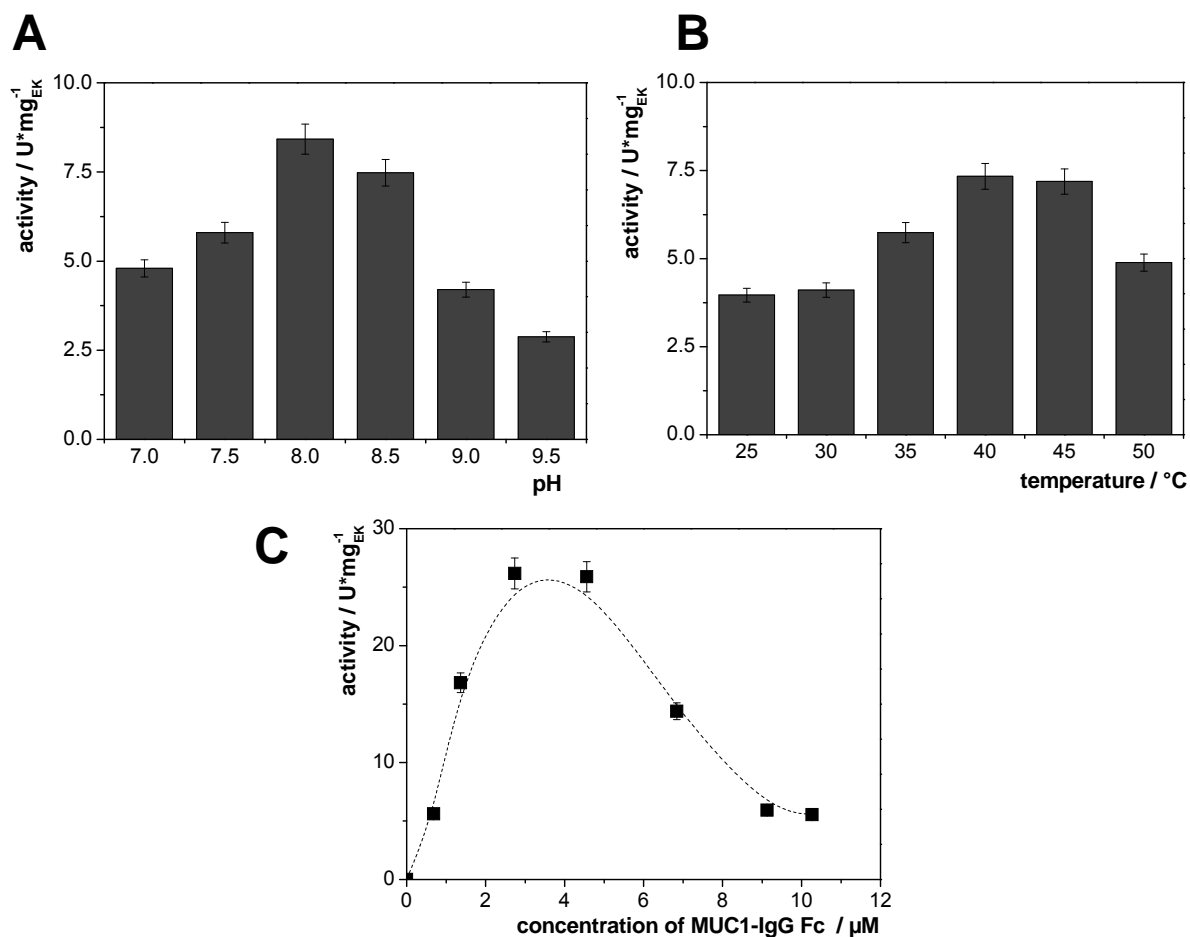


**Figure 5-2 Determination of reaction parameters for MUC1-IgG2a Fc as substrate.** All investigations were performed in 50 mM Tris-HCl, pH 8.0 using 0.233 mg\*mL<sup>-1</sup> MUC1-IgG2a Fc at 33 °C, if not stated otherwise. **A)** pH dependency of enterokinase activity, **B)** enterokinase activity dependent on different temperatures, **C)** activity influenced by different substrate concentrations.

Comparing the activity of enterokinase for the synthetic substrate GD<sub>4</sub>K-2NA and for the fusion protein MUC1-IgG2a Fc, a slight reduction in specific activity of enterokinase for the different substrates was determined. The affinity of enterokinase for the substrate MUC1-IgG2a Fc differs compared to the synthetic substrate GD<sub>4</sub>K-2NA, which might be caused by the different sizes of the substrates as well as the accessibility of the enterokinase cleavage site within the substrate molecule. A  $K_M$  of  $0.39 \pm 0.06$  mM could be determined for GD<sub>4</sub>K-2NA, whereas the  $K_M$  for the fusion protein lies in the μM range.

## 5.4 Summary: Enzyme Characterization

The findings of the chapter “*Enzyme Characterization*” can be concluded as follows:

### SYNTHETIC SUBSTRATE GD<sub>4</sub>K-2NA

- ❖ The optimal reaction parameters for the hydrolysis of GD<sub>4</sub>K-2NA were determined fluorometrically. Enterokinase shows highest enzymatic activity at pH 8.0 and 25 °C. Under those reaction conditions, enterokinase possesses a half-life time of  $8.38 \pm 0.07$  days. The influence of substrate concentration can be described by Michaelis-Menten kinetics yielding a  $K_M$  of  $0.39 \pm 0.06$  mM and a  $V_{Max}$  of  $37.3 \pm 1.4$  U\*mg<sub>EK</sub><sup>-1</sup>.
- ❖ Investigating buffer compositions, 50 mM Tris-HCl, pH 8.0, proved to be the most suited reaction buffer, whereas 20 mM NaPi, pH 8.0, is preferably used for immobilizing enterokinase. Measured activity and reached half-life time are comparable for both buffer systems.

### MUC1-IgG2A Fc

- ❖ The reaction parameters for the cleavage of MUC1-IgG2a Fc have not changed significantly with regard to the influence of temperature or pH of the reaction medium compared to the values determined for GD<sub>4</sub>K-2NA. Enterokinase shows highest enzymatic activity at pH 8.0 and 25 °C.
- ❖ With concentrations above 5 μM MUC1-IgG2a Fc, inhibitory effects negatively influence enzyme activity.
- ❖ Enterokinase shows a lower specific activity for MUC1-IgG2a Fc compared to the synthetic substrate. This is supported by the fact, that substrate affinity of enterokinase to the fusion protein MUC1-IgG2a Fc is lower with a  $K_M$  in the μM range.



## **CHAPTER 6**

---

IMMOBILIZATION OF ENTEROKINASE



## 6 Immobilization of enterokinase<sup>6,7</sup>

### 6.1 Theoretical Background

In general, enzymes are used as catalysts that are not recovered from the reaction. In this case, they are added to the substrate solution, incubated at certain reaction conditions and subsequently destroyed. Such processes involve mainly bulk enzymes such as amylase and dehydrogenases. In case of more expensive enzymes, the reaction setup needs to be changed with regard to efficient utilization of the biocatalyst. This can either be achieved by holding back the enzyme by a membrane using for example an enzyme-membrane reactor [95] or by immobilizing the biocatalyst on or in a carrier material [96]. In both cases, several advantages can be achieved:

- the stabilization of the biocatalyst,
- the recovery and re-use of enzymes, for example in batch reactors,
- the development of continuously operated enzyme reactors,
- the possibility of multi-enzyme systems, and
- the easy removal of the biocatalyst from the reaction mixture and thus, simplified product purification.

It has to be considered, however, that apart from the named advantages the enzyme also loses activity, which results in higher enzyme amounts required. Furthermore, the process may become technically more complex, but may also be simplified with regard to product purification.

Different immobilization techniques have been developed including covalent coupling [97, 98], enzyme cross-linking molecules (cross-linked enzyme aggregates) [99-101], adsorption on a carrier [102], ionic interactions [103] and the encapsulation in polymeric gels or membranes [104-106]. A summary of possible immobilization techniques is given in Figure 6-1.

In the last decades, only a few attempts have been made to immobilize enterokinase for different purposes involving the enclosure into synthetic phospholipid-vesicles [107] or

---

<sup>6</sup> The results of this chapter have been published: Kubitzki T, Noll T, Lütz S (2008) Immobilization of bovine enterokinase and application of the immobilized enzyme in fusion protein cleavage. *Bioprocess Biosystems Engineering* **31**:173-182

<sup>7</sup> All investigations involved the use of EKMax™ (Invitrogen, Carlsbad, USA).

reconstituted soybean phospholipid-vesicles [108]. Other groups covalently immobilized enterokinase followed by solid-phase refolding of the enzyme [109].

## Immobilization techniques

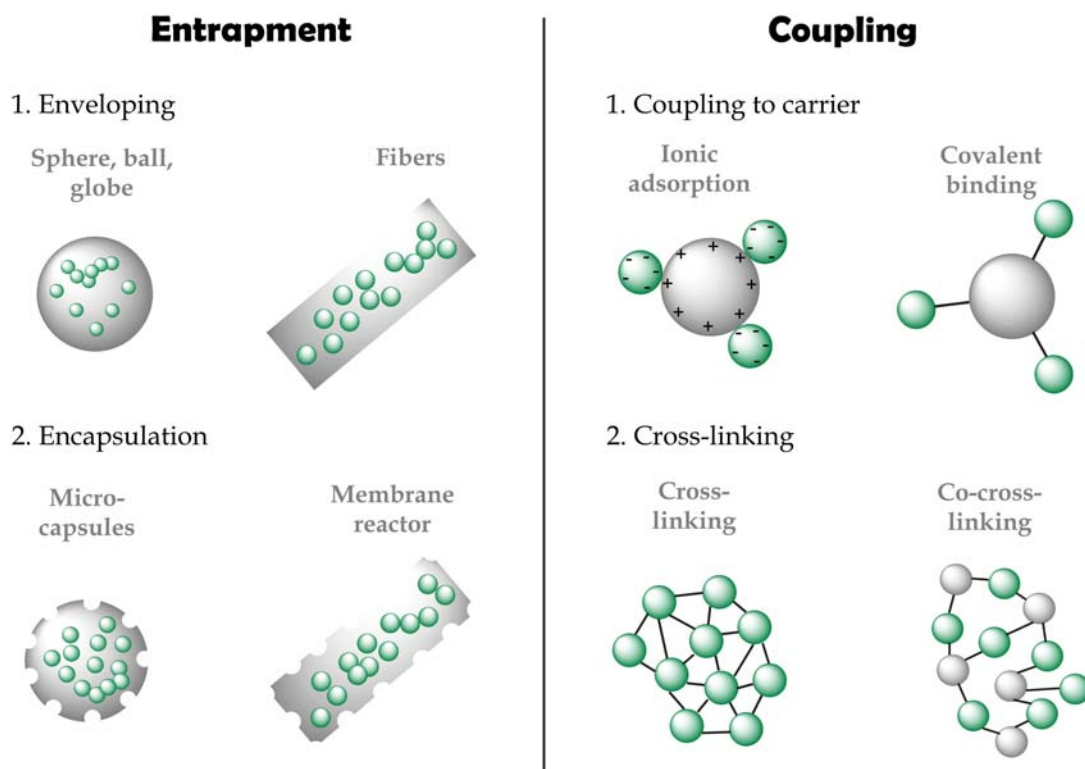


**Figure 6-1** Immobilization techniques.

For the immobilization of enterokinase several different porous or non-porous carrier materials have been investigated differing in their properties, such as:

- particle size,
- density of functional groups,
- the degree of porosity,
- pore sizes and lengths of spacer.

In the following section only the most promising carrier materials, Sepabeads® EC-HA203 and Estapor paramagnetic microspheres M2, will be described in more detail.



## 6.2 Immobilization on porous beads

Prior to detailed investigations on the immobilization technique, the loading capacity of the carrier material was analyzed using either enterokinase or the fusion protein MUC1-IgG2a Fc as offered protein. The received results are presented in Figure 6-2. Varying amounts of protein were offered to the same amount of carrier material. By determining the protein bound to the carrier material, the loading capacity of the support can be determined. To investigate whether there is an influence of the protein load on enzyme activity; the biocatalyst and the substrate MUC1-IgG2a Fc have been analyzed separately.

Independent of the protein applied to the carrier, a linear correlation was determined between the offered protein and the protein adsorbed to the porous support. A maximum of  $0.04 \text{ mg}_{\text{MUC1-IgG2a Fc}}$  was adsorbed on one mg carrier.

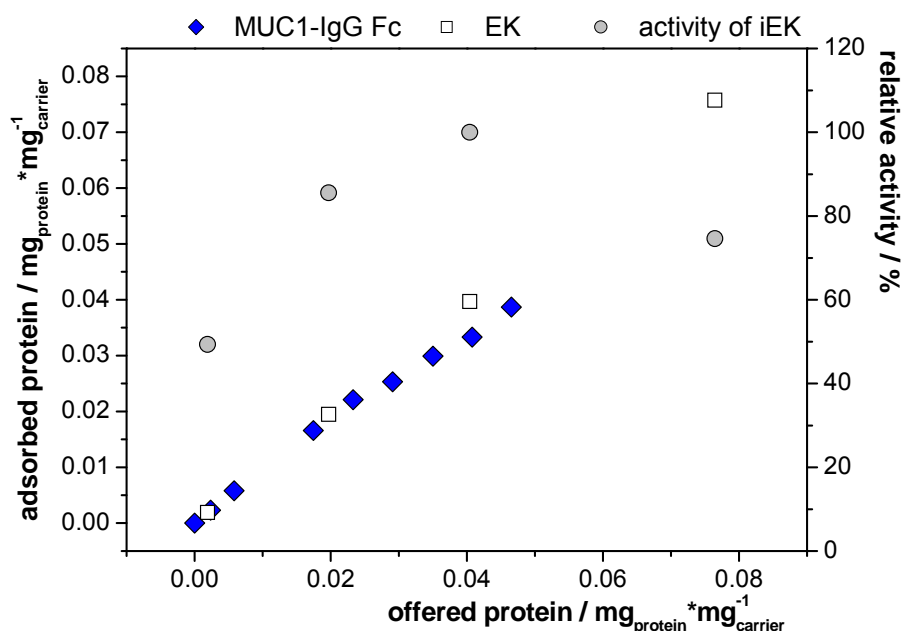


**Figure 6-2 Loading capacity of activated Sepabeads® EC-HA203.**

In case of the biocatalyst, equal amounts of protein adsorbed to the carrier material. The remaining activity, however, is mainly influenced by the loading capacity of the enzyme-support preparation. It has to be emphasized that by immobilizing enzymes, a reduction in catalytic activity can occur. This can be caused by possible changes in the protein structure or by a reduced accessibility of the active site for the substrate. This, however, can be compensated by loading high amounts of biocatalyst on the carrier. Nevertheless, increasing the amount of enzyme bound to the carrier, may in turn lead to steric hindrance resulting in a further decrease of enzyme activity.

With increasing amount of enterokinase offered to the porous support, enzyme activity also increased, reaching its maximum with  $0.04 \text{ mg}_{\text{protein}} \cdot \text{mg}_{\text{carrier}}^{-1}$ . A further increase in loaded biocatalyst caused a drop in relative activity to approximately 75 % (Figure 6-2).

As it was expected, enzymatic activity decreased after a maximum of adsorbed protein was reached (Figure 6-2). This leads to the conclusion that only a limited number of functional groups can be occupied by enterokinase before steric hindrance causes the active site to be blocked. Figure 6-3A shows the binding of small amounts of enzyme to the carrier support with sufficient accessibility of the active site allowing easy binding of the substrate. In contrast to this, if more biocatalyst is present in the solution, the binding behavior may change to allow every enzyme molecule to couple to a single functional group of the carrier material. Thereby, the structure of the protein may change resulting in the shielding and a reduced accessibility of the active site. Thus, substrate molecules can not reach the enzyme molecule leading to a decrease in measurable enzyme activity (Figure 6-3B).

This phenomenon was only observed when using enterokinase as offered protein. When blocking remaining functional groups with glycine, 2-mercaptoethanol or even the fusion protein MUC1-IgG2a Fc, a decrease in remaining activity could not be observed. This further contributes to the assumption that surrounding enzyme molecules may compete for the accessibility of the active site.



**Figure 6-3** Influence of bound enzyme to enzyme activity.

- A)** Enzyme bound to the carrier still allows substrate to reach the active site of enzyme molecule;
- B)** Increased enzyme load causes enzyme molecules to bind in a different conformation to the carrier decreasing the accessibility of the active site and leading to lower remaining activity of the immobilized enzyme.

For the immobilization of enterokinase on hexamethylamino Sepabeads, a low ionic strength buffer was used to ensure fast binding of the protein to the carrier [110]. Prior to coupling, a pre-activation of the functional groups of the carrier with glutardialdehyde (GDA) is necessary to allow covalent binding of the enzyme to the carrier material via nucleophilic groups. Investigations, however, showed that increasing concentrations of

glutaraldehyde resulted in decreased remaining activities of the enzyme-support preparation (Figure 6-4).

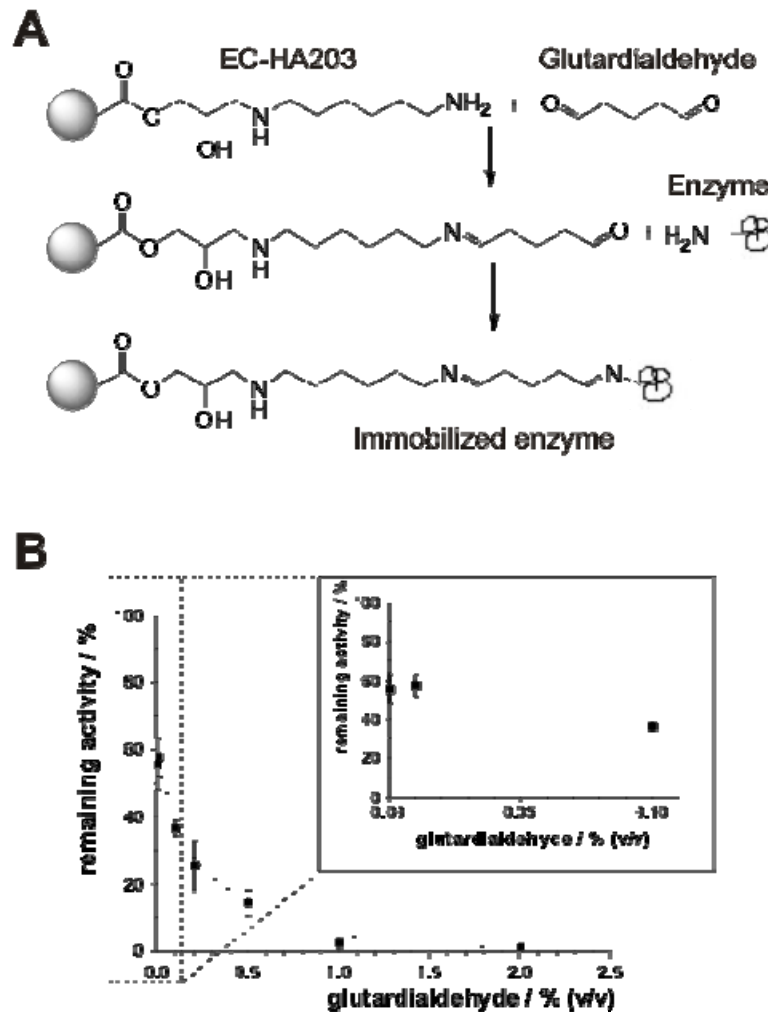


**Figure 6-4** Immobilization of enterokinase on activated porous material.

The carrier material Sepabeads® EC-HA203 was activated with 0.02 % glutaraldehyde prior to the coupling reaction.

- A)** Activation reaction using glutaraldehyde followed by the coupling of the enzyme,  
**B)** Remaining activity of the enzyme-support preparation reaching a maximum of about 60 % and decreasing with increasing glutaraldehyde concentration.

A low ionic strength buffer with a glutaraldehyde concentration of 2 % (v/v) yielded a remaining activity of the enzyme-support preparation of only 1 %. A reduction of glutaraldehyde concentration to 0.5 % (v/v) resulted in a fourteen-fold increase and a further decrease of glutaraldehyde to 0.01 % (v/v) gave a remaining activity of about 60 %, which is comparable with the immobilization to a non-activated carrier material (Figure 6-4). Passive adsorption rather than covalent coupling will predominantly occur when activation takes place with low glutaraldehyde concentrations.

Confirming that the enterokinase is stably bound to the support material is crucial for continuous applications. To determine whether the immobilization procedure has a

stabilizing effect on the enzyme, the storage stabilities of the different enzyme-support preparations were analyzed at 23 °C and 4 °C (Figure 6-5). At 23 °C, a half-life time of  $8.4 \pm 0.1$  days was determined for the free enzyme. The enzyme-support preparation produced by passive adsorption showed a half-life time of  $29 \pm 4$  days at the same storage temperature. Inducing covalent binding with 0.1 % glutardialdehyde, the immobilized enzyme showed a 4.3-fold increase in stability ( $36 \pm 5$  days). A further increase in glutardialdehyde concentration causes a decrease in stability to  $16 \pm 4$  days, still meaning 2-fold increase compared to the free enzyme at 23 °C.

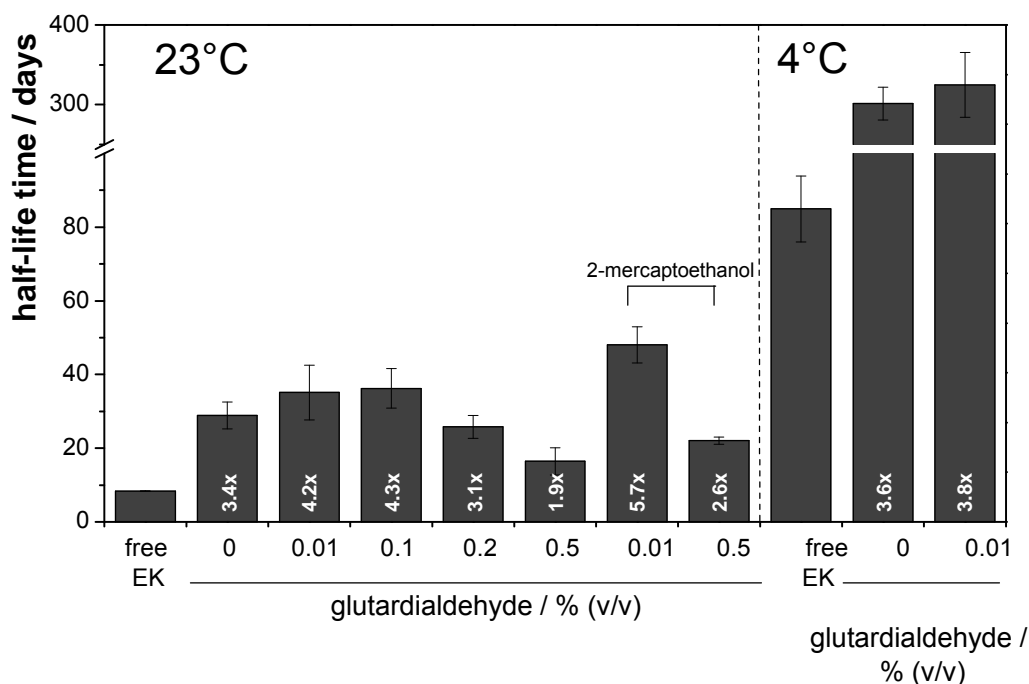


**Figure 6-5 Storage stability of enterokinase immobilized on Sepabeads® EC-HA203.**

It has been reported that the post-treatment with 2-mercaptoethanol is a convenient method for blocking remaining aldehyde groups of the carrier. 2-mercaptoethanol reacts with the free aldehyde groups resulting in an O,S-acetal formation. For the immobilization of an alcohol dehydrogenase, 2-mercaptoethanol has been used as a blocking agent having no significant influence on the remaining activity, but showing a strong effect on stabilizing the enzyme-support preparation [98]. Investigations have demonstrated that a post-treatment with 1 % 2-mercaptoethanol had no significant effect on the remaining activity of 60 % when activating the carrier with 0.01 % glutardialdehyde (Figure 6-4). Furthermore, treating the remaining functional groups with 2-mercaptoethanol further stabilizes the immobilized enzyme reaching a half-life time of  $48 \pm 5$  days (Figure 6-5).

When storing the enzyme-support preparation at 4 °C, the half-life time increases by a factor of 3.6-3.8 (more than 10 months) compared to the free enzyme stored at the same temperature ( $84.9 \pm 8.9$  days). This allows long-time storage and a large scale

immobilization of enterokinase without significant loss in activity over time. Under the storage conditions mentioned above, the enzyme is not washed off the carrier between the activity measurements indicating a stable coupling of the enzyme to the support material with covalent and adsorptive interactions and a sufficient stabilizing effect (Figure 6-5).

### 6.3 Immobilization on magnetic particles

There are several advantages to use magnetic particles for the immobilization of the enzyme enterokinase, such as

- i) the higher specific surface area per reactor volume compared to the Sepabeads<sup>®</sup>,
- ii) lower mass transfer limitations due to the absence of pores, and
- iii) fast and facile separation of the immobilized enzyme from the reaction mixture by applying a magnetic field [111].

Many techniques for activating magnetic particles have been reported. For the immobilization of enterokinase on paramagnetic microspheres, functional groups were activated with either glutardialdehyde (GDA) or N-(3-dimethylaminopropyl)-N-ethylcarbodiimide (EDCA). Taking into account the influence of glutardialdehyde on the activity of enterokinase for the immobilization on Sepabeads<sup>®</sup>, glutardialdehyde concentrations below 1 % (v/v) were used for the activation of the paramagnetic microspheres. With this approach remaining activities of approximately 20 %, regardless of the glutardialdehyde concentration (Figure 6-6) could be achieved.

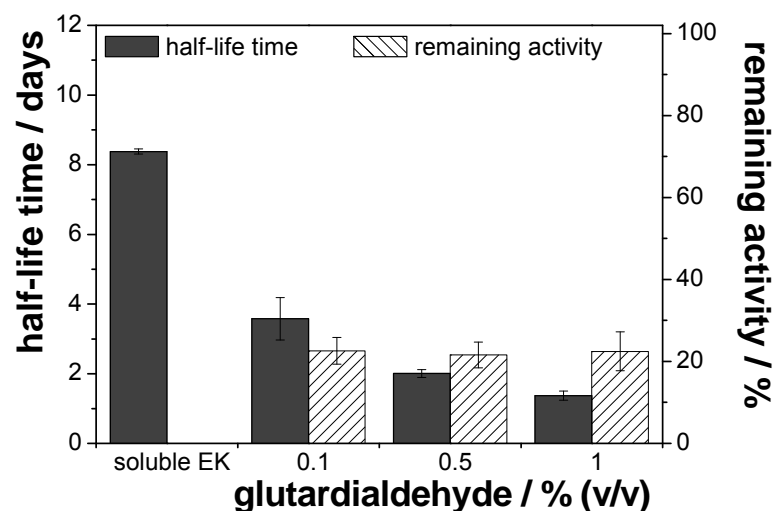


Figure 6-6 Half-life time and remaining activity of enterokinase immobilized on magnetic microspheres activated with glutardialdehyde.

By immobilizing enterokinase on Sepabeads® EC-HA203, a stabilizing effect of the biocatalyst could be observed, which was also expected for the immobilization on paramagnetic microspheres. Unfortunately, the half-life time of the enzyme-support preparation drops to  $3.6 \pm 0.6$  days when activating with 0.1 % (v/v) glutardialdehyde. With higher glutardialdehyde concentration the stability decreased even more (Figure 6-6).

The second approach for the activation of the magnetic microspheres involves EDCA, which has also been applied for immobilization of alcohol dehydrogenase on this carrier [111]. After activating the functional groups, enterokinase was successfully immobilized receiving remaining activities of 60 % without blocking free functional groups.

For blocking the non-occupied functional groups, two different compounds were investigated. 2-mercaptoethanol as blocking agent yielded a remaining activity of approximately 40 %. When using glycine the activity of the enzyme-support preparations varied depending on the incubation time between 50 % and 64 % (Figure 6-7A). Furthermore, the treatment with sodium borohydride reduces the Schiff bases making the binding of the enzyme to the support more stable. The treatment with sodium borohydride, however, decreases the remaining activity of the immobilized enzyme (data not shown).

Different immobilization procedures have been described for magnetic particles, in which the coupling reaction to  $\text{NH}_2$ -modified magnetic particles was performed at pH 6.0 (according to vendor's recommendations). This however, is in contrast to the pH dependency determined for enterokinase activity, at which enterokinase shows highest activity at pH 8.0 [17]. Therefore, storage stability of enterokinase immobilized on magnetic particles was also investigated at pH 8.0. Interestingly, the half-life time is influenced by the pH as well as the blocking agent used. When blocking with 2-mercaptoethanol, higher stability of  $7.5 \pm 2$  days was obtained when stored at pH 8.0 than at pH 6.0 ( $t_{1/2} = 3.8 \pm 1$  days, Figure 6-7B). In case of glycine as a blocking agent, it is *vice versa*. Here, the half-life time is increased at pH 6.0 ( $11.9 \pm 1$  days) compared to pH 8.0 ( $5.7 \pm 1$  days). However, the stability of the free enzyme of  $8 \pm 0.1$  days was only slightly increased by immobilization on magnetic particles (Figure 6-7B).

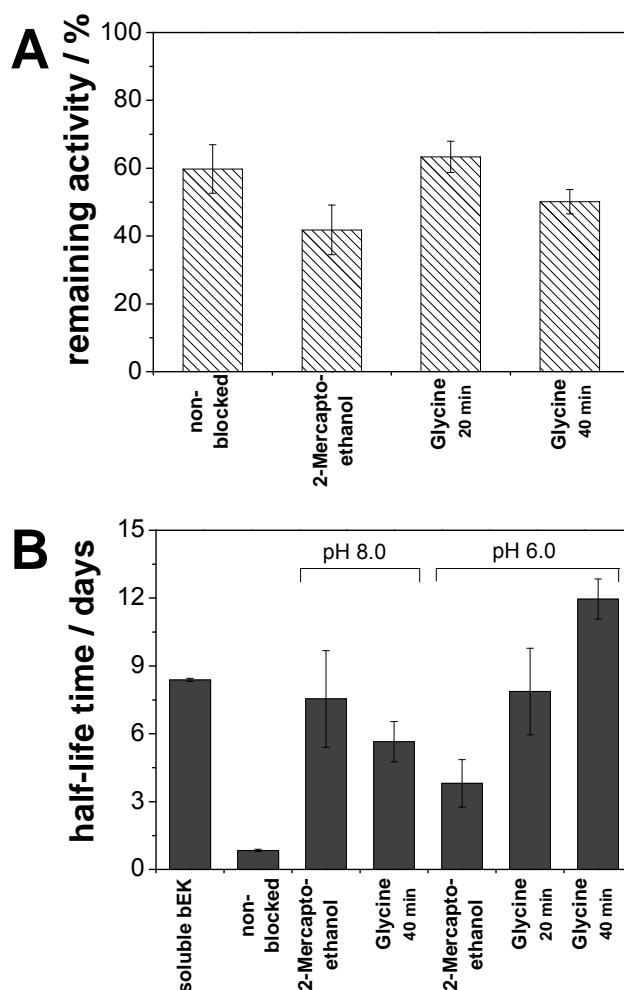


**Figure 6-7 Remaining activity (A) and half-life time (B) of enterokinase immobilized on paramagnetic microspheres activated with EDCA.**

A major aim in industrial application of enzymes is to recover the biocatalyst from the reaction mixture and to receive a stabilizing effect for example by immobilization, but there is no guaranteeing that immobilization stabilizes the enzyme structure. It has been stated that only a multipoint covalent attachment may improve stability by conserving the original enzyme structure [112]. Although having high remaining activities after immobilizing EK on paramagnetic microspheres, we observed a decrease in half-life time, which might be caused by structural changes occurring during storage. This indicates that the enzyme is bound by single-point rather than a multipoint covalent attachment. In this case, there are two possible explanations for the missing stabilizing effect: 1) being bound at a single point to the carrier allows protein refolding changing the structure of the active site or shielding it from the reaction mixture, or 2) surrounding functional groups, either blocked or non-blocked, react with the protein inducing a structural change. In both cases, activity of the enzyme is diminished which is reflected by lower half-life times.

## 6.4 Reaction parameters of immobilized enterokinase

Enzyme immobilization can cause changes in the tertiary structure of the protein. This in turn may influence the activity at specific reaction conditions. Therefore, it was investigated how the activity of immobilized enterokinase either on magnetic microspheres or on Sepabeads® EC-HA203 is influenced by temperature or pH. These results were generated using the synthetic substrate GD<sub>4</sub>K-2NA and were compared to the free enzyme (Figure 6-8). Free enterokinase displays highest activity at pH 8.0 and 33 °C. Nevertheless, it has been stated before that enterokinase possesses a higher stability at 25 °C, thus being the reaction temperature of choice.

After immobilization, those parameters may change depending on the carrier material used for immobilization. In case of Sepabeads® EC-HA203, highest activity of the immobilized enzyme was measured at pH 9.0 and 25 °C (Figure 6-8 A & B). Enterokinase immobilized on magnetic microspheres (activated with EDCA) showed highest activity at pH 6.0 and 25 °C (Figure 6-8 C & D). Despite this, soluble enterokinase as well as both immobilized forms has lowest activity at pH 5. Thus, when applying the enzyme-support preparation to the cleavage reaction of fusion proteins, the reaction parameters have to be adjusted accordingly depending on the immobilization technique employed.

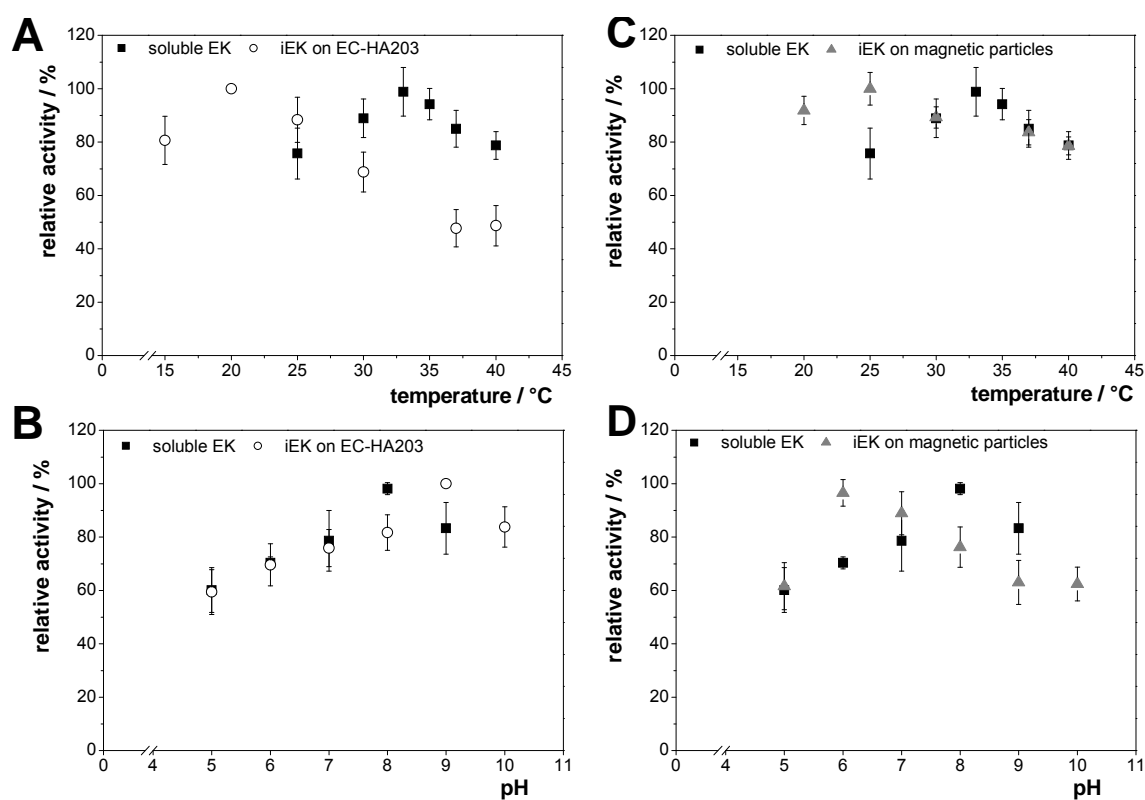


**Figure 6-8** Reaction parameters of immobilized enterokinase compared to the free enzyme.

Activities of the enzyme-support preparations (iEK) using either Sepabeads® EC-HA203 (A & B) or paramagnetic microspheres (C & D) dependent on temperature and pH.



## 6.5 Fusion protein cleavage by immobilized enterokinase

The aim of immobilization was the repeated application of enterokinase in fusion protein cleavage. The substrate protein MUC1-IgG2a Fc has to be cleaved by enterokinase to gain the biologically active form of MUC1. The specific glycosylation pattern of MUC1 is used to develop MUC1-based immunogens in cancer therapy [21, 49, 113].

The samples, taken at specific time points, were analyzed by SDS-PAGE and Western Blot, which specifically visualize proteins possessing IgG Fc. Thus, only the fusion protein MUC1-IgG2a Fc and the cleaved signal peptide IgG Fc can be detected. Besides Western Blot analysis, proteins were also visualized using Alcian blue, which specifically stains glycoproteins, such as MUC1-IgG2a Fc and MUC1. All results presented in this section have been generated using Alcian Blue. However, MUC1 and IgG Fc are generated in equimolar amounts, making the confirmation of only one product sufficient for the verification of the applicability of enterokinase immobilized onto a certain support material.

It was shown by other research groups that free enterokinase can be used to cleave the fusion protein MUC1-IgG2a Fc gaining the desired product MUC1, which could also be affirmed (Figure 6-9) [21]. To investigate whether the immobilized enterokinase can still be used for the cleavage reaction of the fusion protein, the developed enzyme-support preparations have been applied to the cleavage reaction.

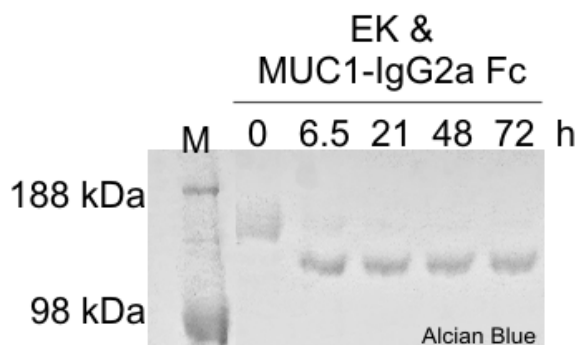


**Figure 6-9 Cleavage of MUC1-IgG2a Fc by free enterokinase.**

The control cleavage reaction was performed in 50 mM Tris-HCl, pH 8.0 at 37 °C according to Bäckström *et al.* [21].

Prior to the cleavage reaction, however, the fusion protein was incubated in the presence of the different carrier without enzyme for detection of any side reactions. A degradation of the fusion protein caused by the carrier could not be observed for both materials, Estapor paramagnetic microspheres M2 and Sepabeads® EC-HA203 (Figure 6-10). This suggests that no undesired side reactions occurred, which is verified by the lack of additional protein bands resulting from degradation. This was additionally confirmed by Silver Stain, which is a more sensitive staining procedure.

The cleavage of the fusion protein with immobilized enterokinase was induced by adding MUC1-IgG2a Fc to the enzyme-support preparation and the reaction proceeded under shaking conditions. After 72 h the entire reaction mixture was removed from the immobilized biocatalyst.

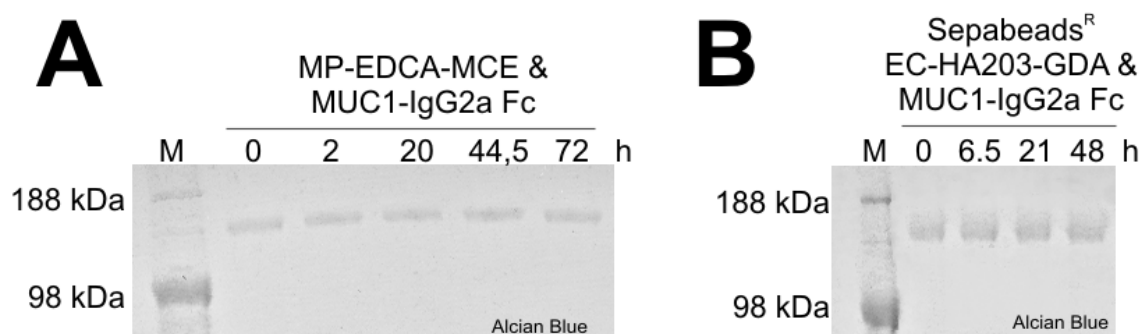


**Figure 6-10 Incubation of MUC1-IgG2a Fc in presence of the carrier material.**  
 0.233 mg·mL<sup>-1</sup> MUC1-IgG2a Fc were incubated at 25 °C in the presence of 50 mg carrier material in 50 mM Tris-HCl, pH 8.0 and 1400 rpm.  
**A)** Magnetic particles (MP) activated with EDCA and blocked with 2-mercaptoethanol (MCE);  
**B)** Sepabeads® EC-HA203 activated with glutardialdehyde (GDA).

Figure 6-11A summarizes the results for the cleavage of MUC1-IgG2a Fc with enterokinase immobilized on Estapor magnetic microspheres at the stated reaction conditions (pH 6.0, 25 °C). As can be seen on the gel, MUC1-IgG2a Fc is present throughout the cleavage reaction without significant decrease in band intensity up to 72 h. Additionally, MUC1, the desired target protein, could not be detected using Alcian stain. Investigating the samples using Silver Stain or, more specifically, Western Blot, did also not reveal the development of IgG Fc which should be cleaved off during the reaction. Thus, the fusion protein MUC1-IgG2a Fc could not be cleaved by enterokinase immobilized on Estapor magnetic microspheres, a non-porous carrier material. The reason might be the very small size of the magnetic particles (particle diameter: 1.0-2.0 µm) with the functional groups on the outer surface. Since all functional groups of the support material were occupied either by the bound enterokinase or by 2-mercaptoethanol, steric hindrance between the neighboring groups might prevent the large fusion protein to reach the active site of the small enterokinase. Consequently, MUC1-IgG2a Fc was not cleaved into the desired products MUC1 and IgG Fc. Thus, Estapor magnetic particles seemed not to be suitable for immobilizing small enzymes, which are used for the cleavage of large fusion proteins.

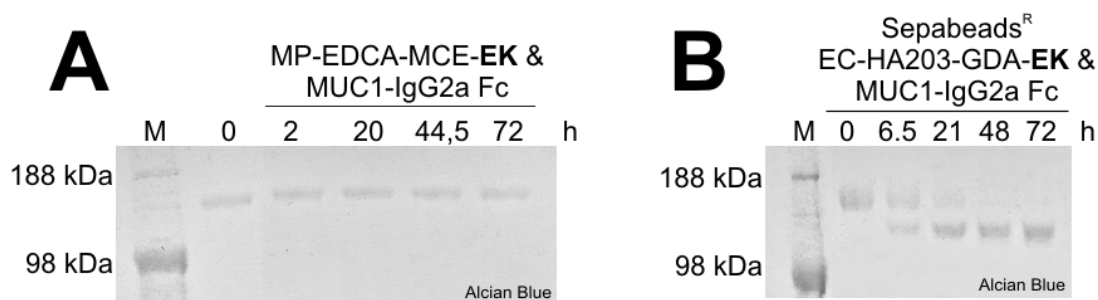


**Figure 6-11 Cleavage reactions of MUC1-IgG2a Fc using enterokinase immobilized on different carrier.**

The cleavage reaction was performed by applying  $1.16 \text{ mg} \cdot \text{mL}^{-1}$  MUC1-IgG2a Fc in 50 mM Tris-HCl to 100 mg immobilized enzyme.

- A)** magnetic particles (MP) activated with EDCA and blocked with MCE, cleavage reaction occurred at pH 6 and  $25 \text{ }^\circ\text{C}$ ;  
**B)** Sepabeads<sup>®</sup> EC-HA203 activated with GDA, cleavage reaction occurred at pH 9.0 and  $25 \text{ }^\circ\text{C}$ .

Another immobilization technique for enterokinase involved the activated porous carrier Sepabeads<sup>®</sup> EC-HA203. The received results are demonstrated in Figure 6-11B. Using a specific antibody in Western Blot analysis, IgG2a Fc could already be detected after 6.5 hours (data not shown). With Alcian stain, MUC1 could also be found after 6.5 hours increasing with proceeding reaction time. Furthermore, the amount of MUC1-IgG2a Fc decreases, whereas MUC1 increased indicating complete fusion protein cleavage after 72 h. Same results were received for IgG2a Fc using different analytical methods.

This data reveals that enterokinase immobilized on the porous carrier material Sepabeads<sup>®</sup> EC-HA203 was successfully applied to the cleavage of the fusion protein MUC1-IgG2a Fc leading to complete fusion protein cleavage and the generation of the desired target protein MUC1. For efficient utilization of the biocatalyst, the enzyme-support preparation has to be applied to several repeated cleavage reactions, on the one side to prove its process stability, and on the other side to justify the additional immobilization procedure in the reaction process.

## **6.6 Reaction kinetics for MUC1-IgG2a Fc cleavage by immobilized enterokinase**

Due to the previous findings that reaction parameters might slightly vary depending on the use of soluble or immobilized enterokinase in the hydrolysis of the synthetic substrate GD<sub>4</sub>K-2NA (see section 6.4), the activity of enterokinase immobilized on Sepabeads<sup>®</sup> EC-HA203 has been determined also using the fusion protein MUC1-IgG2a Fc as substrate. The received results are summarized in Figure 6-12.

As determined before for the soluble enterokinase, highest activity is found at pH 8 and 25 °C for the hydrolysis of the synthetic substrate GD<sub>4</sub>K-2NA (Figure 5-1A & C) and also for the cleavage of MUC1-IgG2a Fc (Figure 5-2A & B). At these reaction conditions, enterokinase possesses the highest half-life time of  $8.38 \pm 0.07$  days (Figure 5-1D). Using the immobilized biocatalyst for the determination of the reaction parameters, similar results were obtained. Enterokinase immobilized on Sepabeads<sup>®</sup> EC-HA203 exhibits highest activity of  $3.7 \pm 0.2$  U\*mg<sub>iEK</sub><sup>-1</sup> at pH 8.0. The activity at this pH is more pronounced compared to the results received for the free enterokinase, observing a more distinct decrease in remaining activity to  $0.6 \pm 0.03$  U\*mg<sub>iEK</sub><sup>-1</sup> at pH 7.0 and  $1.1 \pm 0.05$  U\*mg<sub>iEK</sub><sup>-1</sup> at pH 9.0. Due to immobilization, the structure of the protein molecule might have changed exposing different amino acids to the reaction mixture. By changing the pH in the surrounding medium, the side chains of specific amino acids become charged, which might influence the enzymatic activity of the biocatalyst as well as the binding behavior of the substrate molecule.

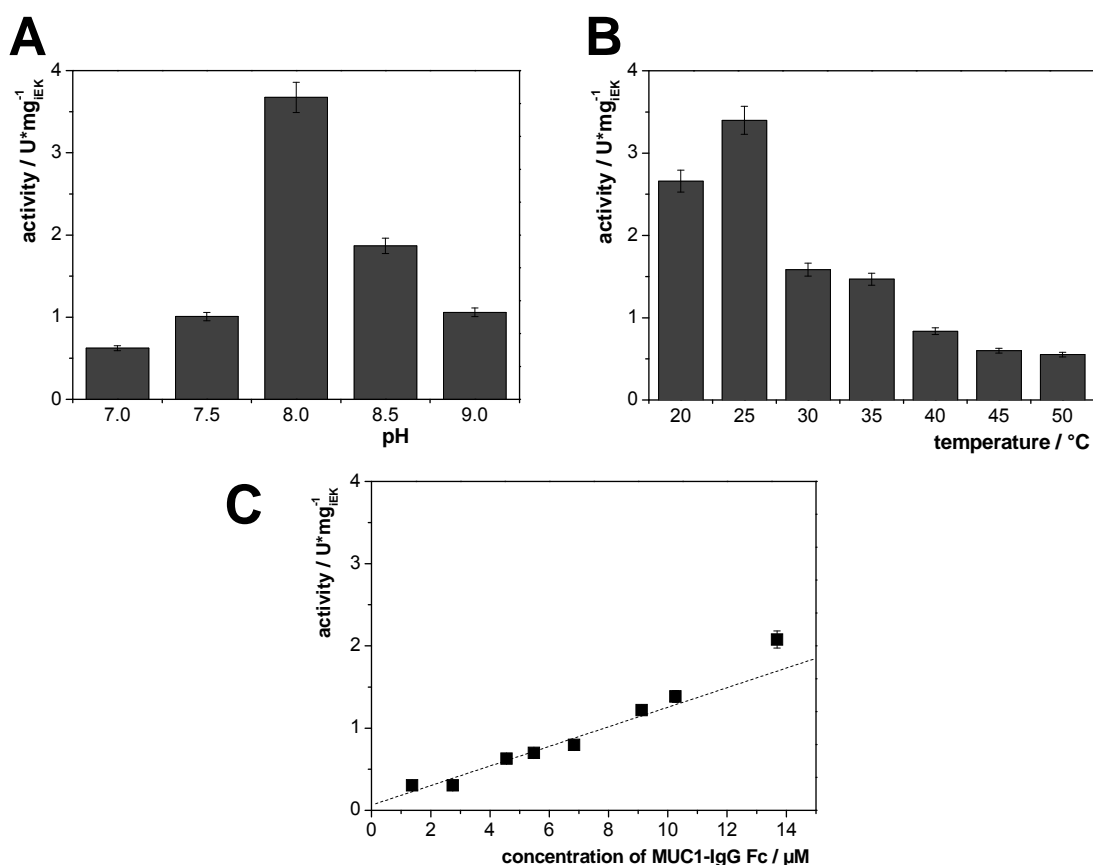


**Figure 6-12** Reaction parameters for the cleavage of MUC1-IgG2a Fc by immobilized enterokinase (iEK).

All measurements were performed in 50 mM Tris-HCl, pH 8.0 at 25 °C and 1400 rpm using  $1.16 \text{ mg} \cdot \text{mL}^{-1}$  MUC1-IgG2a Fc.

**A)** influence of pH on activity of immobilized enterokinase; **B)** influence of temperature on activity of enterokinase immobilized on porous material; **C)** activity of the enzyme-support preparation dependent on substrate concentration showing a linear correlation.

The optimum temperature for highest enzymatic activity was determined in correlation with the stability of the biocatalyst. Using the synthetic substrate GD<sub>4</sub>K-2NA, highest activity was measured at 33 °C, but enterokinase possess only a half-life time of  $30.2 \pm 5.9$  days. Considering the stability, working temperature was set to 25 °C, at which enterokinase has a half-life of  $65.5 \pm 5.2$  days (Figure 5-1C & D). Using MUC1-IgG2a Fc as substrate, soluble enterokinase seems to be most active at temperatures as high as 40 to 45 °C. This, however, might be caused by partial degradation of the substrate molecule as well as the biocatalyst. The enzyme-support preparation possesses the highest activity of  $3.4 \pm 0.2 \text{ U} \cdot \text{mg}_{\text{IEK}}^{-1}$  at 25 °C, which correlates with the determined half-life time for the enzyme. As it was expected, enzyme activity decreases with rising reaction temperature.

As stated before, an inhibition at MUC1-IgG2a Fc concentrations higher than 5 μM were observed for soluble enterokinase. In case of the enzyme-support preparation this effect could not be observed. Instead, a linear correlation between the applied substrate concentration and the measured enzyme activity could be found. In chapter 6.2 the loading capacity of porous material was investigated showing that 0.04 mg MUC1-IgG2a Fc can adsorb to one mg support material even if the carrier was not activated with glutardialdehyde prior to incubation.

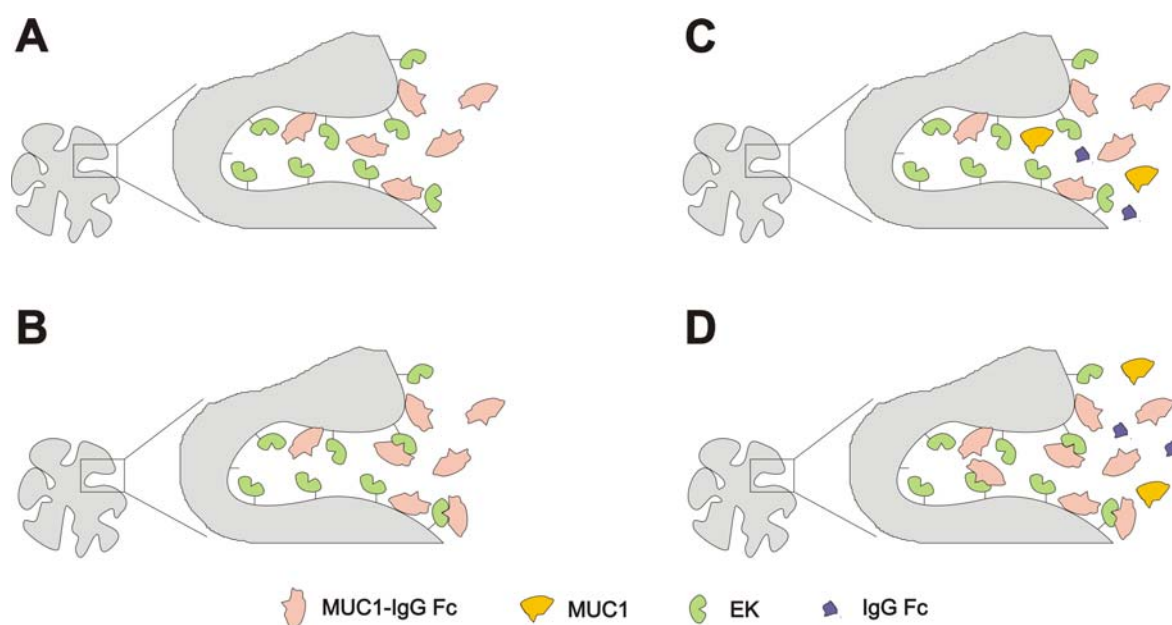


**Figure 6-13 Influence of immobilization on substrate surplus inhibition.**

The presence of porous support material causes unspecific adsorption of MUC1-IgG2a Fc reducing the concentration in the reaction solution (A), remaining MUC1-IgG2a Fc binds to the active site of EK (B) and is cleaved into MUC1 and IgG2a Fc (C). Uncleaved MUC1-IgG2a Fc in the solution binds to the enzyme or adsorbs to carrier material (D).

By immobilizing enterokinase on a porous support, substrate surplus inhibition seems to be circumvented (Figure 6-13). Due to an adsorptive effect, MUC1-IgG2a Fc present in the reaction solution unspecifically binds to the carrier material, mimicking a lower concentration in the reaction mixture (Figure 6-13A). Substrate concentration in the solution further decreases due to additional binding of MUC1-IgG2a Fc to immobilized enzyme (Figure 6-13B). At the same time, cleavage of the fusion protein takes place generating the product proteins MUC1 and IgG2a Fc and making immobilized enterokinase again available for substrate binding and cleavage (Figure 6-13C). Thus, new MUC1-IgG2a Fc either being released by desorption from the carrier material due to a concentration gradient or being present as free molecules in the reaction medium binds to the immobilized biocatalyst for further cleavage (Figure 6-13D). If desorption of the fusion protein from the support material occurs, other protein molecules may at the same time adsorb to the carrier, thus reducing substrate concentration in the reaction mixture and avoiding the inhibition of the immobilized enzyme by MUC1-IgG2a Fc.

Taking these findings into account, an additional saturation step of the carrier material had to be implemented, prior to initiating the actual cleavage reaction. For saturation, MUC1-IgG2a Fc should preferably be used, to avoid the introduction of other possible reactants, such as chemicals or even proteins. These components may interfere with the cleavage reaction and need to be removed from the reaction mixture making the purification process of the final product more complicated. Furthermore, MUC1-IgG2a Fc used for saturation of the support is still available for the cleavage reaction due to desorption of the substrate proteins from the carrier, which was described in Figure 6-13.

## 6.7 Summary: Immobilization

The results of immobilizing enterokinase can be summarized as follows:

- ❖ Enterokinase can be immobilized on either non-porous (Estapor magnetic microspheres) or porous material (hexamethylamino Sepabeads®) receiving remaining activities of up to 60 %.
- ❖ Such high remaining activities are yet unreported compared to the few attempts yielding only 30 % by coupling the enzyme to glyoxyl agarose beads [19, 109].
- ❖ The immobilization of enterokinase on Estapor paramagnetic microspheres did not stabilize the biocatalyst. The produced enzyme-support preparation was not able to cleave the fusion protein MUC1-IgG2a Fc.
- ❖ A stabilizing effect was only observed with hexamethylamino Sepabeads® increasing half-life time at 25 °C to approximately 50 days. An additional treatment with 2-mercaptoethanol resulted in a significant 6-fold increase in half-life time compared to the free enzyme without influencing enzyme activity.
- ❖ When stored at 4 °C, a supreme stabilizing effect, displayed by a half-life time greater than 330 days was achieved. This allows large-scale immobilization set-ups and long-time storage of the enzyme-support preparation.
- ❖ Enzyme immobilized on hexamethylamino Sepabeads® could successfully be applied to fusion protein cleavage producing the target protein MUC1.
- ❖ Reaction parameters have been determined showing similar results as received for the free enzyme: pH 8.0 and 25 °C are used for further investigations.
- ❖ By using porous carrier material, substrate surplus inhibition observed for the soluble enzyme can be overcome, showing a linear correlation between the activity of the enzyme-support preparation and the applied substrate concentration.
- ❖ The immobilized enzyme can easily be removed from the reaction system and the re-use of the biocatalyst is now possible.





## **CHAPTER 7**

---

APPLICATION OF IMMOBILIZED ENTEROKINASE IN  
FUSION PROTEIN CLEAVAGE



## 7 Application of the immobilized enterokinase in fusion protein cleavage<sup>8</sup>

### 7.1 Theoretical Background

For applying the enzyme-support preparation in a preparative cleavage of the fusion protein MUC1-IgG2a Fc, a suitable reactor set-up needs to be found. Generally, there are three types of an ideal reactor:

- 1) Discontinuously operated stirred batch reactor,
- 2) Continuously operated stirred tank reactor, and
- 3) Plug flow reactor.

The cleavage reaction with immobilized enterokinase was carried out either in a continuously operated stirred tank reactor (CSTR) or in repetitive batch reactors. Therefore, only these two ideal reactor types will be describes in more detail.

In case of a CSTR, the reaction will be performed continuously making a constant supply with substrate solution and a permanent product removal necessary (Figure 7-1A). Thus, it is an open reaction system. At steady-state, equilibrium develops between the flow rate into and the mass flow rate out of the reactor. The reaction proceeds at the reaction rate associated with the final (output) concentration. Such a reactor system is well suited for reactions that are influenced by substrate surplus inhibitions, because of the low substrate concentrations that can be applied [85].

In contrast to this, the batch reactor is characterized as a closed reaction system, since a supply with substrate or the removal of product does not occur (Figure 7-1B). In the beginning of the reaction, the reaction vessel is filled with all required substances before the catalyst – the enzyme – is added to start the reaction. As soon as the desired conversion is achieved, the reaction is stopped by either inactivating or removing the biocatalyst. Figure 7-1B shows the change of reaction conditions over time. The reaction starts with high substrate and low product concentrations, which is *vice versa* at the end of the reaction [85].

---

<sup>8</sup> All results presented in this section were received using isolated EK produced by the expression host *E. coli* BL21.

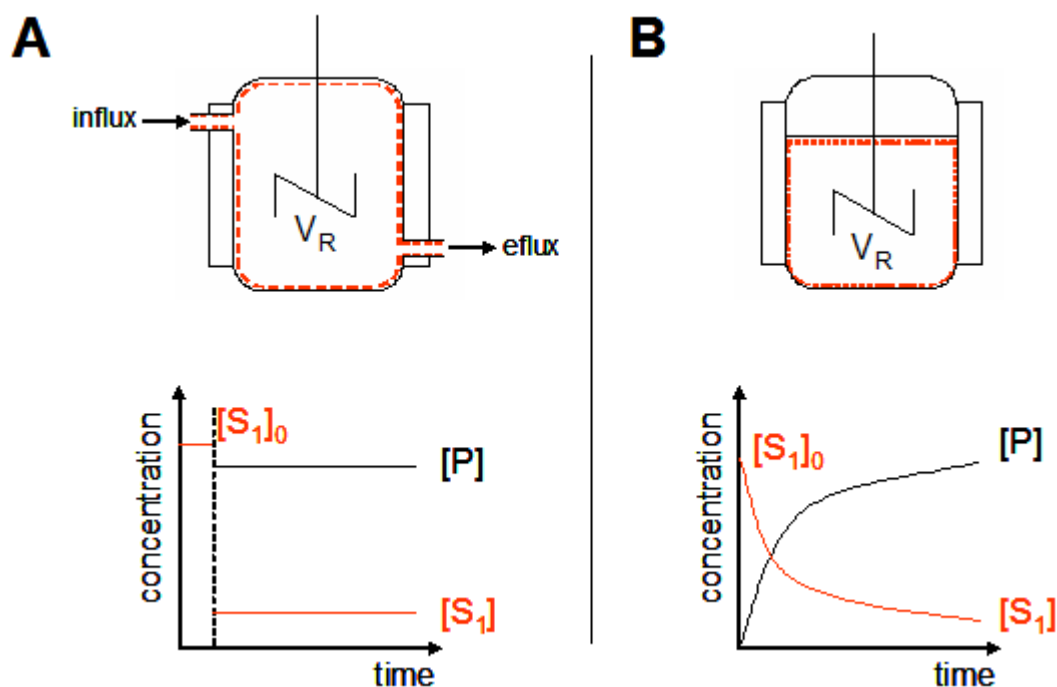


**Figure 7-1 Comparison of CSTR and batch reactor.**  
 A) Scheme of a CSTR;  
 B) Scheme of a batch reactor with the change in concentration over time.

## 7.2 Continuous process

As it could be shown in the previous chapter, enterokinase immobilized on Sepabeads® EC-HA203 was successfully applied in fusion protein cleavage. The re-utilization as well as the stability of the enzyme-support preparation has to be investigated under process conditions. Therefore, the biocatalyst was applied in a continuous reaction process (Figure 7-2, scheme in section 10.2.20), which was performed under sterile and protease-free conditions to avoid the degradation of MUC1-IgG2a Fc or the product MUC1.

It was mentioned before that a saturation of the carrier material is necessary. Therefore, fusion protein was added to the enzyme-support preparation to allow a cleavage reaction to occur in a batch mode. To guarantee complete saturation, this batch reaction was repeated under the same conditions (Figure 7-2 I). A conversion of approximately 80 % could be achieved for the two batch reactions. Afterwards, a flow rate of  $1.7 \text{ mL} \cdot \text{h}^{-1}$  was applied to initiate a continuous reaction mode. Regularly withdrawn samples showed a constant cleavage of the fusion protein receiving about 60 % conversion. The CSTR shows a stable production of MUC1 for  $\sim 1.5$  residence times followed by a drastic drop in conversion to 40 % (Figure 7-2). To increase conversion and to analyze the activity of the immobilized enterokinase, the continuous process was stopped going back into a batch reaction. This, however, could not increase conversion, which further decreased to less than 20 % (Figure 7-2 II).

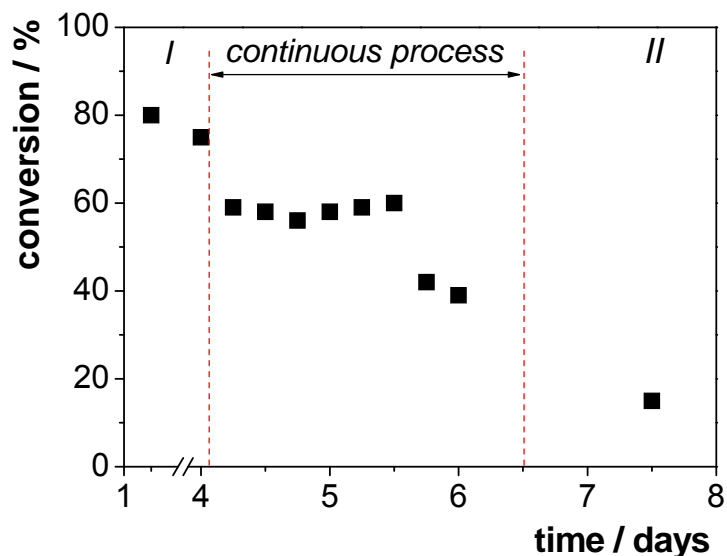


**Figure 7-2** Continuous reactor setup for the cleavage of MUC1-IgG2a Fc by immobilized enterokinase.

The set reaction conditions involved  $2.32 \text{ mg}\cdot\text{ml}^{-1}$  MUC1-IgG2a Fc in standard reaction buffer incubated with  $2.2 \text{ U}\cdot\text{g}_{\text{Sepabeads}}^{-1}$  (determined with GD<sub>4</sub>K-2NA) immobilized enterokinase in a reaction volume of 40 mL at pH 8.0, 25 °C and stirring with 700 rpm. A flow rate of  $1.7 \text{ mL}\cdot\text{h}^{-1}$  was applied. Section I & II represent cleavage reactions by the enzyme-support preparations under batch conditions.

The continuous cleavage reaction under the given reaction conditions yielded a space-time yield of  $1.34 \text{ g}\cdot(\text{L}\cdot\text{d})^{-1}$  and a total turnover number of 6000. The enzyme-support preparation was used for a total of 3 batch reactions and a continuous reaction mode of 1.5 residence times, which added to a total process time of 7.5 days.

Within the described process, the conversion decreased from 80 % to 60 % after going into a continuous process, and further to 40 % after 1.5 residence times. Generally, 5 residence times are required to either reach a steady-state in conversion or to recognize desorption of the biocatalyst from the support material. In the collected fractions, however, no enterokinase activity could be measured verifying that no biocatalyst was washed off the carrier. Furthermore, the enzyme-support preparation showed also no enzymatic activity at the end of the process suggesting a possible inactivation of the biocatalyst. This might be caused by the physical stress induced by the constant stirring of the reaction solution and the developing shear forces. The high substrate concentrations applied and the long reaction times might have also contributed to enzyme inactivation.

Apart from this, sample evaluation further complicated the course of the continuous process. The collected fractions were analyzed with the method described in section 10.2.19 using SDS-PAGE and a staining technique specific for glycoproteins. Due to the long time required for sample evaluation, an *online*-monitoring of the continuous process could not take place. Thus, it was not possible to respond to changes within the process in

a fast manner to prevent the conversion from decreasing by e.g. increasing the residence time or increasing the mixing rate to reduce film diffusion.

Due to insufficient conversion and the difficulties in monitoring the reaction, the cleavage reaction of MUC1-IgG2a Fc in a continuous process was not further investigated. Instead, the enzyme-support preparation was used repeatedly for fusion protein cleavage.

### 7.3 Repetitive batch experiments

In repetitive batch experiments, MUC1-IgG2a Fc was added to the enzyme-support preparation initiating the cleavage reaction. After 24 hours the reaction was stopped and new substrate solution was again mixed with the same immobilized enzyme. Instead of stirring, the reaction mixture was mixed by constant shaking to reduce shear forces and thereby possible inactivation of the biocatalyst. For each batch experiment, enzyme activity was determined. The results of the repeated utilization of immobilized enterokinase are summarized in Figure 7-3.

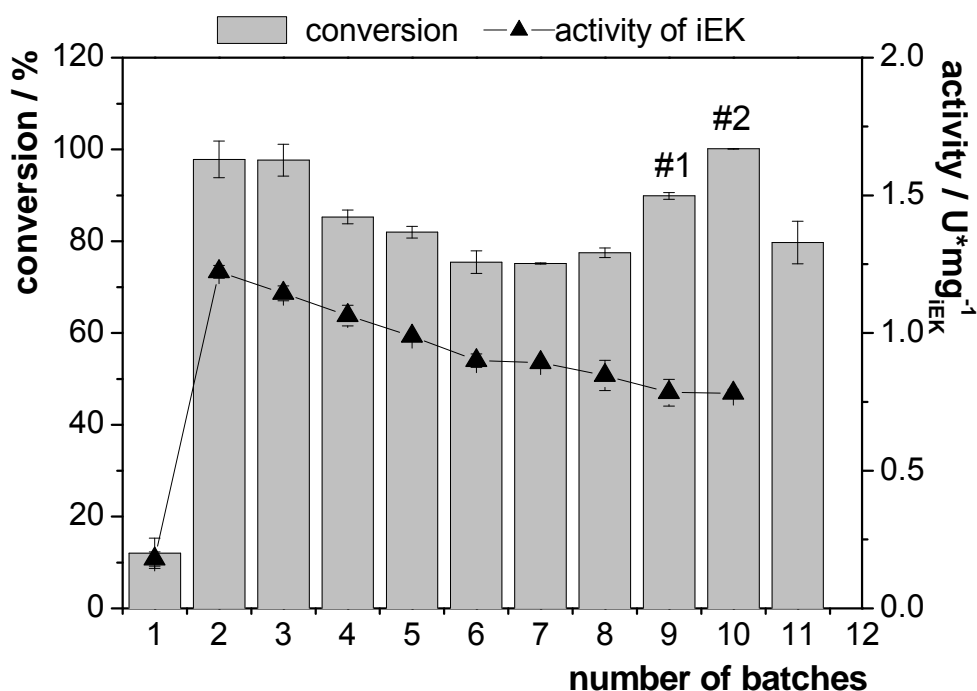


**Figure 7-3 Application of immobilized enterokinase (iEK) in repetitive fusion protein cleavage.**

The experiment was performed in duplicates. The reaction solution was removed after 24 h (increased process time: #1 – 27 h, #2 – 33 h) and new substrate solution was added to the enzyme-support preparation starting a new cleavage reaction. The set reaction conditions involved  $1.16 \text{ mg} \cdot \text{mL}^{-1}$  MUC1-IgG2a Fc in standard reaction buffer incubated with  $1.1 \text{ U} \cdot \text{g}_{\text{Sepabeads}}^{-1}$  (determined with GD<sub>4</sub>K-2NA) immobilized enterokinase in a reaction volume of 1 mL at pH 8.0, 25 °C and under shaking conditions.

The first batch reaction was required to saturate the carrier material, which is accompanied by a low conversion of  $12.0 \pm 3.3 \%$  and an enzyme activity of  $0.18 \pm 0.03 \text{ U} \cdot \text{mg}_{\text{IEK}}^{-1}$ . Enzyme activity is determined by the amount of product, which is produced over a specific time. Since the majority of the fusion protein adsorbed to the support material, only a small amount could be cleaved by immobilized enterokinase resulting in a low enzyme activity. This, however, does not reflect the actual activity of the enzyme-support preparation, as can be seen in the second batch. Here, the measured enzyme activity measured  $1.22 \pm 0.02 \text{ U} \cdot \text{mg}_{\text{IEK}}^{-1}$ . A conversion of  $97.8 \pm 3.9 \%$  was achieved after a reaction time of 24 h. A similar result was received for the third batch reaction with a slight decrease in enzymatic activity. In the following cleavage reactions re-using the immobilized enterokinase, a further decrease in enzyme activity was observed, subsequently leading to a decrease in conversion. Due to the reduction in the activity of the enzyme-support preparation, less MUC1-IgG2a Fc is cleaved in the same reaction time. Thereby, a conversion of  $77.5 \pm 1.1 \%$  with a remaining activity for enterokinase of  $0.85 \pm 0.05 \text{ U} \cdot \text{mg}_{\text{IEK}}^{-1}$  were received. To determine whether 100 % conversion can still be achieved using the enzyme-support preparation, the process time of the cleavage reaction was prolonged. As it can be seen with the results for the batch reactions 9 and 10, conversion of MUC1-IgG2a Fc could be increased by a longer process time, reaching 100 % conversion after 33 h in batch 10. Activity of the enzyme-support preparation of this batch reaction measured  $0.78 \pm 0.01 \text{ U} \cdot \text{mg}_{\text{IEK}}^{-1}$ .

Thus, immobilized enterokinase was successfully applied in repeated cleavage reactions, in which 100 % conversion can be achieved taking the decrease in enzyme activity into account and increasing the process time accordingly. Table 7-1 summarizes the process results achieved with this reaction concept. For the determination of the half-life time, the highest activity measured was considered as starting activity and adding the days of the already proceeded reaction.

**Table 7-1 Process parameters for the repeated utilization of immobilized enterokinase.**

$t_{1/2}$ of enzyme-support preparation	$15.40 \pm 0.99$ days
space-time yield	$0.92 \text{ g} \cdot (\text{L} \cdot \text{d})^{-1}$
<i>ttn</i>	33500

Since the application of the enzyme-support preparation in repetitive cleavage reactions was successful, slight changes in process conditions have been introduced to improve the half-life of the immobilized enzyme:

- 1) reduction of MUC1-IgG2a Fc concentration to reduce the stress on the enzyme;
- 2) addition of metal ions to the reaction mixture.

The addition of magnesium to the standard reaction buffer caused a significant increase in the half-life by almost 50 % measuring  $14.59 \pm 0.09$  days for the free enzyme (Figure 5-1D). Thus, it can be assumed that by adding magnesium to the reaction mixture, the stability of the immobilized enterokinase might also be increased. In case of the free enterokinase, magnesium may stabilize the protein structure preventing conformational changes of the protein during incubation. By immobilization, the enzyme stability could already be increased (Figure 6-5), which might be further improved by using magnesium as a supplement.

To investigate the influence of magnesium and the reduced substrate concentration on the half-life time of the enzyme-support preparation, repeated fusion protein cleavages were carried out either in the presence or absence of magnesium. Prior to use, the immobilized enterokinase was stored for about 2 months at 4 °C, which should have no significant influence on the activity according to previous investigations (Figure 6-5).

**Table 7-2** Process parameters of the repeated utilization of immobilized enterokinase in the presence or absence of  $Mg^{2+}$ .

<i>process parameters</i>	<i>without <math>Mg^{2+}</math></i>	<i>with <math>Mg^{2+}</math></i>
$t_{1/2}$ of enzyme-support preparation / days	$13.70 \pm 3.47$	$11.75 \pm 1.98$
space time yield / $g^*(L*d)^{-1}$	0.33	0.32
<i>ttn</i>	22700	23500

As it is presented in Figure 7-4, the enzyme-support preparations were used in 18 cleavage reactions showing similar reaction modes independent on the presence or absence of magnesium. About four batch reactions are necessary to saturate the carrier material, which is indicated by rising conversion and enzyme activity. The fifth cleavage reaction carried out with the immobilized enzyme yielded a conversion of 96 % and a



remaining activity of  $1.44 \text{ U} \cdot \text{mg}_{\text{iEK}}^{-1}$  when  $\text{Mg}^{2+}$  was added to the reaction mixture. Without  $\text{Mg}^{2+}$ , 99 % conversion with  $1.16 \text{ U} \cdot \text{mg}_{\text{iEK}}^{-1}$  could be determined. With proceeding re-utilization, activity of the enzyme-support preparation decreased, as it could be observed before, reaching final values of  $0.36 \text{ U} \cdot \text{mg}_{\text{iEK}}^{-1}$  (with  $\text{Mg}^{2+}$ ) and  $0.39 \text{ U} \cdot \text{mg}_{\text{iEK}}^{-1}$  (without  $\text{Mg}^{2+}$ ). In both reaction setups, the conversion decreased to 50 % in batch 18. The process parameters received are summarized in Table 7-2.

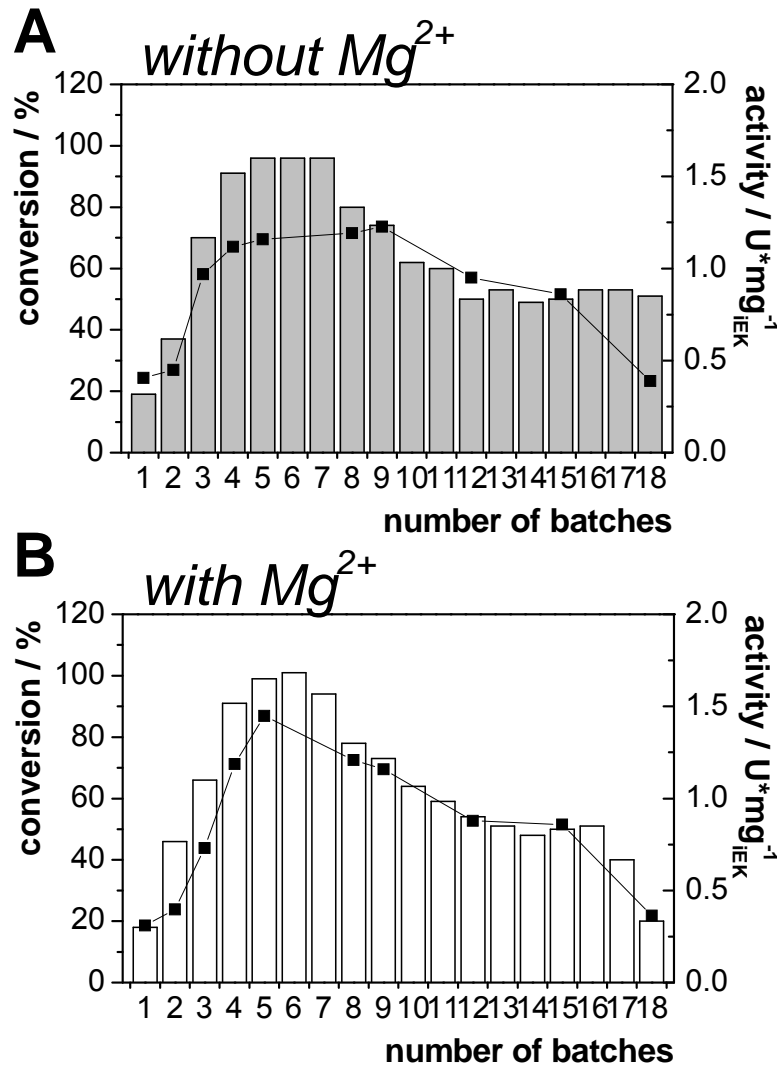


**Figure 7-4** Repeated fusion protein cleavage by immobilized enterokinase (iEK) in the absence and presence of magnesium.

The reaction solution was removed after 24 h and new substrate solution was added to the enzyme-support preparation starting a new cleavage reaction. The set reaction conditions involved  $0.63 \text{ mg} \cdot \text{mL}^{-1}$  MUC1-IgG2a Fc incubated with  $1.1 \text{ U} \cdot \text{g}_{\text{Sepabeads}}^{-1}$  (determined with GD<sub>4</sub>K-2NA) immobilized enterokinase in a reaction volume of 1 mL at pH 8.0, 25 °C and 1400 rpm. The enzyme-support preparation was stored at 4 °C for 2 months prior to use. The standard reaction buffer was supplemented with 1 mM magnesium ions.

**A)** repetitive batches in the absence of magnesium;

**B)** influence of magnesium on activity and stability of immobilized enterokinase.

According to the received results, a stabilizing effect for the enzyme-support preparation could not be observed when adding  $Mg^{2+}$  to the reaction mixture, as it was expected with regard to the data received for free enterokinase (Figure 5-1E). This suggests that  $Mg^{2+}$  has the same effect on preserving a specific protein structure as when immobilizing the biocatalyst. In both cases, a conformational change of the protein leading to decreased enzyme activity is prevented.

#### **7.4 Summary: Application of immobilized enterokinase**

The received results during the application of the enzyme-support preparation in the cleavage reaction of MUC1-IgG2a Fc can be summarized as follows:

- ❖ Of the investigated reactor systems, the repeated utilization of the immobilized enterokinase is the most suited concept in the cleavage of MUC1-IgG2a Fc with regard to conversion, enzyme stability, enzyme utilization and reaction monitoring.
- ❖ The enzyme-support preparation was re-used for a maximum of 18 batch reactions proving its process stability and significantly increasing the utilization of the biocatalyst ( $ttn = 33500$ ) and reaching a space-time yield of  $0.92 \text{ g} \cdot (\text{L} \cdot \text{d})^{-1}$ .
- ❖ 100 % conversion can be achieved with every batch reaction taking enzyme inactivation into account and increasing the process time accordingly.
- ❖ The supplementation of  $Mg^{2+}$  does not contribute to the stability of the enzyme-support preparation.

## **CHAPTER 8**

---

PRODUCT PURIFICATION



## 8 Product purification

### 8.1 Improvement of the purification procedure

After the fusion protein MUC1-IgG2a Fc is cleaved into IgG2a Fc and the target protein MUC1, it is of importance to obtain a pure product protein. Several different purification techniques have been applied including ion exchange chromatography and ultrafiltration.

In case of ion exchange chromatography, a strong anion exchange material has been used allowing the elution of the proteins with a specific salt gradient according to the isoelectric point of the different proteins. This method has already been described by Bäckström *et al* [6] for the purification of MUC1. Here, the fusion protein was incubated with soluble enterokinase until complete cleavage of the fusion protein was detected. The reaction mixture was then applied to ion exchange chromatography separating IgG2a Fc and MUC1.

Although using the same purification procedure and receiving a similar chromatogram for elution some distinct impurities at 30 kDa and 43 kDa were detected with SDS-PAGE followed by Silver staining (Figure 8-1A). This suggests that the undesired proteins possess a similar isoelectric point as the target protein MUC1 being eluted at the same salt concentration. By changing the pH of the used elution buffer the overall charge of the proteins changes resulting in a different elution pattern. Since the amino acid composition of the unwanted proteins was not known, it was investigated whether a change in pH and in the elution gradient may improve product purity. Unfortunately, this did not yield higher purity of MUC1. With this purification procedure, a product purity of approximately 60 % was achieved. For further research or a pharmaceutical application, a purity degree of more than 95 % of the product is at least necessary.

According to SDS-PAGE, the size of the unwanted proteins is smaller than 100 kDa. Therefore, ultrafiltration using a membrane with a 100 kDa cut-off was applied after ion exchange chromatography. As it can be seen on the SDS-gel (Figure 8-1B), the product solution was more concentrated rather than further purified. When comparing the solution before (B) and after (A) the filtration step, the two major impurities at 30 and 43 kDa are still present in the product solution suggesting these proteins to have sterically large structures that cannot diffuse through the pores of the membrane. This is supported by the fact that no proteins were found in the filtrate (F) solution.

Keeping in mind the size of MUC1 with 140 kDa, membranes with a cut-off higher than 100 kDa may lead to a loss of the product protein, which might diffuse through the pores

of the membrane. Nevertheless, a membrane with a molecular weight cut-off of 300 kDa (XM300) was used for ultrafiltration. After the cleavage reaction was completed, the protein solution was directly applied to ultrafiltration. To wash out the undesired proteins and to remove residual salt, the retentate was washed several times with ultra-pure water. According to Figure 8-1C, the main impurities at 30 and 43 kDa are washed out with each washing step. Comparing the product solution before (B) and after filtration (A) the amount of impurities was significantly reduced with regard to the proteins found at 30 and 43 kDa. For complete removal, the number of washing steps was increased, which resulted in the production of MUC1 with a purity of more than 90 %.

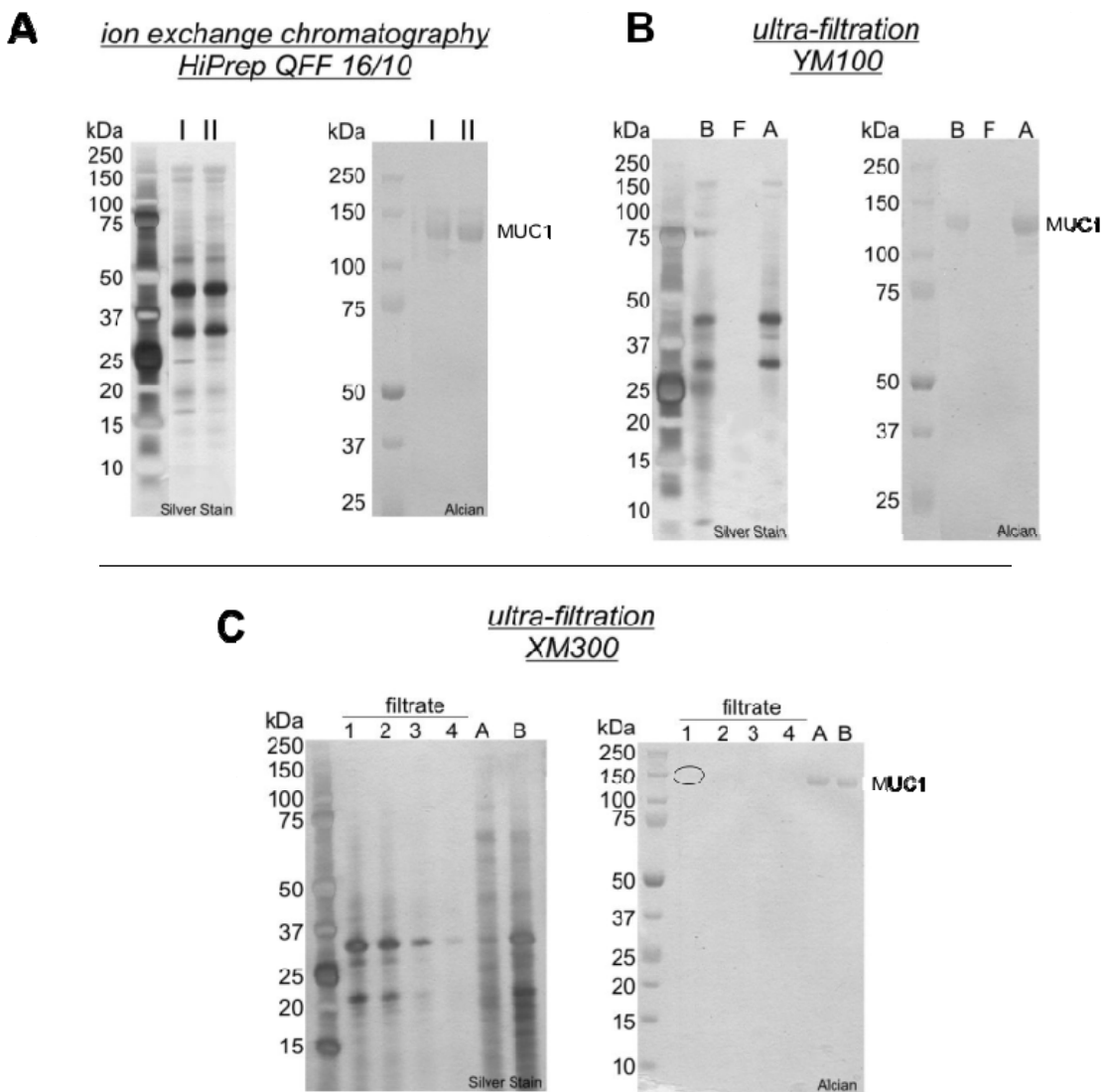


**Figure 8-1 Techniques applied for the purification of MUC1.**  
**A)** MUC1 was eluted with a gradient of NaCl in IEC: I and II represent different fractions of the eluting process;  
**B)** Solution of cleavage reaction was applied to ultra-filtration with a 100 kDa cut-off: B – before filtration, F – filtrate, A – after filtration;  
**C)** Reaction solution was applied to a membrane with a 300 kDa cut-off: B – before filtration, A – after filtration, circle – very slight MUC1 band.

With the finally used membrane having a 300 kDa cut-off, the unwanted proteins were successfully removed, with only a neglectable amount of MUC1 – less than 5 % - being lost in the first washing step.

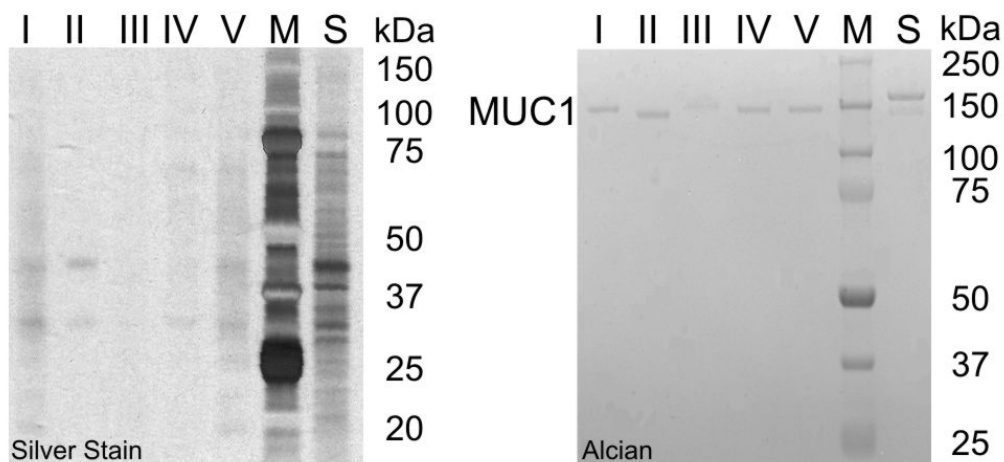


**Figure 8-2 SDS-PAGE of the obtained lyophilisates containing MUC1.**  
 I to V – different lyophilisates (1:100). M – size marker, S – first extracted standard: MUC1-IgG2a Fc (0.233 mg\*mL<sup>-1</sup>).

The reaction mixtures of the different cleavage reactions – using free enterokinase, using immobilized enterokinase, continuous cleavage, and repetitive cleavage – were purified according to the finally developed purification procedure involving the membrane XM300. The received retentates were lyophilized and analyzed for their MUC1 content using SDS-PAGE followed by Silver and Alcian staining (Figure 8-2). Afterwards, the MUC1 content was determined using the analytical method described in 10.2.19. With the received results, the purity of the lyophilisates was determined, which are summarized in Table 8-1.

**Table 8-1 MUC1 content and purity degree of the obtained lyophilisates.**

		<i>Lyophilisate / mg</i>	<i>MUC1 content / mg</i>	<i>Purity / %</i>
I	repetitive batch 1	43.0	40.9	95.1
II	repetitive batch 2 (Mg-dependency)	42.7	39.3	92.1
III	continuous cleavage	30.0	18.6	62.0
IV	analytical investigations soluble EK	12.0	11.3	94.6
V	analytical investigations immobilized EK	11.0	10.3	93.5

So far, the purification method for MUC1 involved the application of ion exchange chromatography, which is limited by the amount of protein that can be loaded onto the column and the long process time. Furthermore, a sufficient purity could not be achieved. Now, ultrafiltration using a membrane with a cut-off of 300 kDa is applied, significantly reducing process time and increasing product purity from 60 to more than 90 %. Although, this is still not sufficient for pharmaceutical applications, the approach, however, gave promising results, with still some room for improvements.

## 8.2 Summary: Product purification

The findings of this chapter can be summarized as follows:

- The application of ion exchange chromatography results in a purity of MUC1 of 60 %, not sufficient for further investigations or pharmaceutical applications.
- The purity of MUC1 can be improved by using ultrafiltration. Here, a membrane with a molecular weight cut-off of 300 kDa was most suited increasing the purity of MUC1 to more than 90 % and significantly reducing process time. The entire purification procedure was more simplified.
- Finally, 100 mg lyophilized MUC1 with a purity of 94 % could be produced (Figure 8-3).

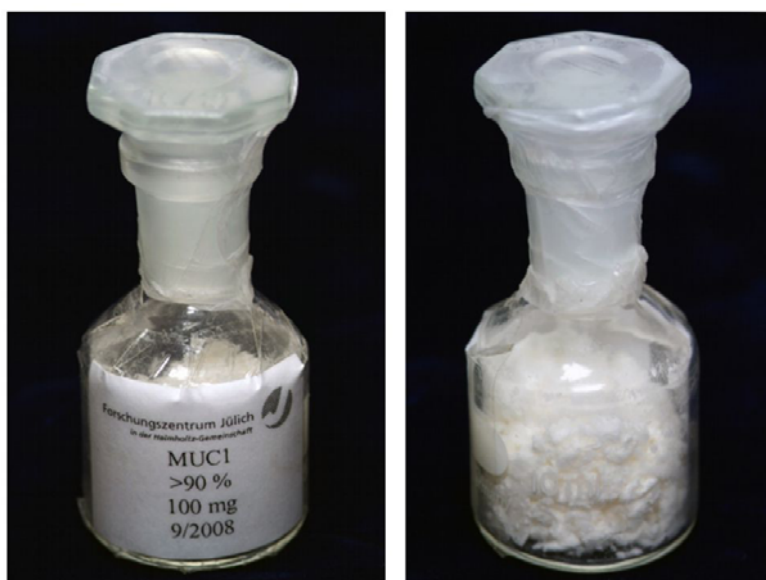


Figure 8-3 Lyophilized MUC1 with a purity of 94 %.



## **CHAPTER 9**

---

CONCLUSION AND OUTLOOK



## 9 Conclusion and Outlook

The aim of the project was to characterize the cleavage reaction of the fusion protein MUC1-IgG2a Fc by the enzyme enterokinase finding the optimal reaction parameters. With the received results an improved process for fusion protein cleavage had to be developed with emphasis on the efficient utilization of the biocatalyst.

### 9.1 Supply of the reacting proteins

Prior to process optimization, the availability of the reacting proteins had to be guaranteed making the optimization of the fermentation and purification procedure for MUC1-IgG2a Fc necessary. In a corporative research project between the Goteborg University, Sweden and the Research Centre Juelich, Germany, the production and purification of the fusion protein by recombinant CHO K1 cells has been investigated improving the productivity of the expression host and the amount of isolated fusion protein [21]. Thus, the substrate protein could be supplied sufficiently.

Apart from this, the supply of the biocatalyst was of more importance. Although, enterokinase is commercially available, the high purchasing costs, however, do not contribute to making enterokinase an attractive tool in fusion protein cleavage. Therefore, it was necessary to establish an improved and very efficient production and purification procedure receiving high amounts of pure and active biocatalyst. Collins-Racie *et. al* [7] developed a very suitable expression host; enterokinase light chain could be produced as a fusion protein by recombinant *E. coli* K12. The fusion protein contains an enterokinase recognition site and a His-Tag, allowing the purification of the protein using column affinity chromatography followed by autocatalysis to receive active enterokinase light chain in its monomeric form. Using this process, Collins-Racie and co-workers were able to produce  $8 \mu\text{g}_{\text{EK}} \cdot \text{g}_{\text{wcv}}^{-1}$  [7].

Within this project, the production procedure was further optimized with regard to fermentation conditions and the applied downstream process, when using *E. coli* K12 as well as *E. coli* BL21 as production hosts. The fermentation procedure was optimized with regard to glucose consumption, acetate, biomass, and product formation. When comparing the two different expression strains, *E. coli* BL21 seemed to be more suited due to higher optical densities and cell dry weights reached. Furthermore, moderate glucose consumption with high conversion into biomass accompanied by very low acetate formation was observed. After fermentation, the downstream process needed to be improved. By introducing a new technical setup for affinity chromatography – a batch binding chamber – the purification process was significantly simplified and the process

time was reduced by half. Using *E. coli* K12, an inducible expression system, for enterokinase production under optimized fermentation conditions and applying the improved purification procedure, the yield of biocatalyst was increased 8-fold, measuring  $63.3 \mu\text{g}_{\text{EK}} \cdot \text{g}_{\text{wCW}}^{-1}$ . In comparison to this, *E. coli* BL21 represents constitutive protein expression expecting higher enzyme yields, subsequently. With this expression host, an increase in isolated enterokinase by a factor of 14 ( $111.5 \mu\text{g}_{\text{EK}} \cdot \text{g}_{\text{wCW}}^{-1}$ ) was achieved. Apart from using recombinant *E. coli* for enterokinase production, the utilization of different yeast strains has also been described. In these cases, volumetric productivities of  $31.5 \mu\text{g}_{\text{EK}} \cdot \text{L}^{-1} \cdot \text{h}^{-1}$  to  $182 \mu\text{g}_{\text{EK}} \cdot \text{L}^{-1} \cdot \text{h}^{-1}$  were received [89, 90]. With the isolation and purification approach developed in this project, a formulation rate of  $214 \mu\text{g}_{\text{EK}} \cdot \text{L}^{-1} \cdot \text{h}^{-1}$  was determined, which means a maximum increase by a factor of  $\sim 7$ .

By introducing several modifications in the downstream process of an existing production procedure described by Collins-Racie and co-workers [7], the diversity of bioreaction engineering could be demonstrated. Enzyme yield was greatly improved making a commercial supply of the biocatalyst unnecessary and thereby decreasing production costs. Furthermore, the new procedure possess some more significant advantages, such as 1) allowing fast and simple buffer change, 2) avoiding pressure limitations, 3) decrease process time and therefore 4) limit the effect of spontaneous autocatalysis and diminish the amount of lost enterokinase during the purification process.

## **9.2 Immobilization of enterokinase**

To efficiently utilize enterokinase in fusion protein cleavage, the biocatalyst needs to be recycled or re-used either by holding back the enzyme by a membrane or by immobilizing it on or in a carrier material. Withholding the biocatalyst by a membrane cannot be applied in this reaction due to the specific molecular weights of the involved proteins, with the enzyme being smaller than the fusion protein and having the same size as one of the product proteins. Therefore, it was mainly focused on the immobilization of enterokinase using different carrier materials. By immobilizing enterokinase either on Estapor magnetic microspheres or hexamethylamino Sepabeads<sup>®</sup>, supreme remaining activities of 60 % were received, compared to the few attempts yielding only 30 % by coupling the enzyme to glyoxyl agarose beads [109]. With the latter approach, the cleavage of a fusion protein producing human growth hormone was carried out in only one cycle.

A stabilizing effect was not achieved using the amino-modified magnetic microspheres possibly due to refolding after binding to the carrier. In contrast to the magnetic particles, enterokinase was stabilized by binding to hexamethylamino Sepabeads<sup>®</sup>. An additional treatment with 2-mercaptoethanol resulted in a significant 6-fold increase in half-life time

compared to the free enzyme without influencing the remaining activity. When stored at 4 °C, we achieved a supreme stabilizing effect, displayed by a half-life time greater than 330 days. This allows large-scale immobilization setups and long-time storage of the enzyme-support preparation.

The immobilized enzyme on hexamethylamino Sepabeads® could successfully be applied to fusion protein cleavage showing the decrease in MUC1-IgG2a Fc and the development of the desired product protein MUC1. Thereby, it was proved that the carrier material (hexamethylamino Sepabeads®) is suitable for immobilizing the small protein enterokinase and allowing the large fusion protein to enter the pores and to be cleaved by the enzyme.

In conclusion, enterokinase was successfully immobilized to a specific carrier material, making it possible to simply remove the biocatalyst from the reaction mixture. This allows further utilization of the immobilized enzyme to continuous or repetitive cleavage reactions.

### **9.3 Comparison of CSTR and repeated utilization of immobilized enterokinase**

The developed enzyme-support preparation was applied in the cleavage of MUC1-IgG2a Fc either in a continuous process or in repeated reactions. With a continuous reaction setup, a conversion of 60 % for 1.5 residence times was obtained, before an unexpected drop in conversion was observed. Within the collected fraction, no enzyme activity was measured, showing that the biocatalyst was either still bound to the carrier material or was inactivated. Enzyme inactivation may result as a consequence of the physical stress induced by the constant stirring of the reaction solution and the development of shear forces. Additionally, high substrate concentrations and the long reaction times might have also contributed to enzyme inactivation. Furthermore, sample evaluation is a time-consuming procedure making an *online*-monitoring of the continuous process difficult. Due to insufficient conversion and the difficulties in monitoring the reaction, the continuous process is not a suitable reaction setup for the cleavage of MUC1-IgG2a.

Another reaction setup investigated involved the application of the immobilized enterokinase in repeated cleavage reactions. The cleavage of MUC1-IgG2a Fc proceeded until full conversion is achieved. The reaction mixture is then removed from the enzyme-support preparation followed by the addition of new substrate solution. With this procedure, a maximum of 18 repeated cycles of fusion protein cleavage using the same enzyme support preparation were performed. A decrease in conversion was observed, which correlated with enzyme inactivation. However, 100 % conversion was achieved in at

least 3 batch reactions within 24 h. Taking enzyme inactivation into account, process time has to be increased to receive full conversion with every reaction cycle. Thus, it was proven that the enzyme-support preparation is stable under process conditions and can be recycled within the reaction.

Up to now, Suh and co-workers described the application of enterokinase immobilized in glyoxyl agarose beads for the cleavage of a fusion protein for the production of human growth hormone [109]. In this case, the enzyme-support preparation, however, was used in only one cycle. According to this, the results presented here demonstrate for the first time that enterokinase can be re-used in a maximum of 18 reactions for fusion protein cleavage after being immobilized on hexamethylamino Sepabeads®.

The pharmaceutical industry focuses mainly on the use of fusion proteins for the production of biopharmaceuticals. To receive the therapeutically important protein, the fusion partner needs to be removed either chemically or enzymatically. In the latter case, higher specificity is obtained and milder reaction conditions can be applied. Enzymatic reactions, however, are generally more expensive than chemical reactions due to the costs for the biocatalyst, which add to the costs for the downstream process. Therefore, an enzymatic reaction for fusion protein cleavage has to fulfill some criteria:

- 1) full conversion,
- 2) efficient utilization of the biocatalyst,
- 3) simple downstream process, and
- 4) high purity of the final product.

The efficient utilization of the biocatalyst can be achieved by recycling the enzyme and re-using it in a number of cleavage reactions. By removing the immobilized biocatalyst from the reaction mixture in addition to full conversion, the downstream process is simplified and a high purity of the product can be obtained.

Finally, the continuous process and the repeated utilization of immobilized enterokinase in fusion protein cleavage are compared with regard to the criteria important for industrial application (Table 9-1). The repeated utilization of the enzyme-support preparation is the method of choice for fusion protein cleavage by immobilized enterokinase due to a more efficient utilization of the biocatalyst accompanied by a sufficient stability under process conditions. Full conversion can be achieved taking enzyme inactivation into account.

**Table 9-1 Comparison of the continuous process and the repeated utilization of immobilized enterokinase.**

	<i>Continuous process</i>		<i>Repetitive batch</i>	
Full conversion	60 %	X	100%	✓
Enzyme utilization ( <i>ttn</i> )	6000	✓	33500	✓
Further information	Process monitoring difficult Moderate enzyme stability under process conditions		Process time needs to be prolonged according to enzyme inactivation	

#### **9.4 Comparison of soluble and immobilized enterokinase in fusion protein cleavage**

As stated in the beginning of this chapter, an optimized procedure for the cleavage of fusion proteins had to be developed with emphasis on efficient enzyme utilization. The latter does not necessarily mean to immobilize the biocatalyst. Of course, several advantages arise when using enzyme-support preparations, but the efficiency has to be compared to the soluble enzyme under optimized reaction conditions. The immobilized biocatalyst has to be re-used adequately to cope with the reduced enzyme activity, generally received after immobilization, and the additional work load necessary.

In Table 9-2, different reaction processes for the cleavage of MUC1-IgG2a Fc using either soluble or immobilized enterokinase were compared. The existing method was firstly described by Bäckström and co-workers [21], in which under the given reaction conditions, 100 % conversion and a total turnover number of 80 was obtained. After characterizing enterokinase and determining the reaction parameters for the substrate MUC1-IgG2a Fc, the cleavage reaction was performed under optimized reaction conditions using soluble as well as immobilized biocatalyst. In case of soluble enterokinase, commercially available enterokinase and isolated enzyme were compared. The cleavage reaction was performed under the given reaction conditions reaching 100 % conversion in both cases. With enterokinase commercially purchased a *ttn* of 400 was achieved, whereas a *ttn* of only 200 was obtained with isolated enterokinase. This, however, can be explained by the different substrate concentrations used. As it was shown in Figure 5-2 in section 5.3, enzyme activity increases with increasing concentration until reaching 5  $\mu$ M, when inhibitory effects negatively influence enzyme

activity. Thus, the calculated total turnover number was expected to be higher for the commercial enzyme compared to the isolated enterokinase. For the immobilized biocatalyst no substrate inhibition was observed as it was demonstrated in Figure 6-12 and Figure 6-13 of section 6.6. Thus, higher substrate concentrations can be applied in the cleavage reaction using less biocatalyst. This in turn significantly increased enzyme utilization reaching total turnover numbers of 3800 in a single reaction or 33500 in repetitive reaction cycles.

By adjusting the reaction conditions and considering inhibitory effects, enzyme utilization was improved 3-fold for isolated enterokinase or 5-fold for commercially purchased enzyme compared to the method described by Bäckström *et al.* [21]. By immobilizing enterokinase, substrate inhibition was avoided further increasing the total turnover number by a factor of 48 in a single batch reaction. As it was expected, a supreme rise in the total turnover number by a factor of 419 was determined when using the immobilized enterokinase in repeated batches under the given reaction conditions.

To finally conclude, the cleavage reaction of MUC1-IgG2a Fc by enterokinase was characterized and the optimal reaction parameters have been determined for soluble and immobilized biocatalyst. With the developed immobilization technique a suitable compromise between reduced enzyme activity, enzyme stabilization and additional effort was found. An optimized procedure for the cleavage of MUC1-IgG2a Fc using either soluble or immobilized enterokinase was developed significantly increasing enzyme utilization.



Table 9-2 Comparison of the reaction processes for the cleavage of MUC1-IgG2a Fc using soluble or immobilized enterokinase.

	Bäckström (EKMax™)	EKMax™	Immobilized EK (E. coli BL21)	
			Single Batch	Repeated Batches
EK <sup>#2</sup>	2.35 µg 64 U*mL <sup>-1</sup> 1.0 mg*mL <sup>-1</sup>	0.12 µg 3.2 U*mL <sup>-1</sup> 0.23 mg*mL <sup>-1</sup>	0.11 µg 3.0 U*mL <sup>-1</sup> 0.12 mg*mL <sup>-1</sup>	0.06 µg 1.1 U*g <sub>carrier</sub> <sup>-1</sup> 1.6 mg*mL <sup>-1</sup>
MUC1-IgG2a Fc	50 mM Tris-HCl, pH 8.0 1 mM CaCl <sub>2</sub> 37°C	50 mM Tris-HCl, pH 8.0 25°C, 1400 rpm	50 mM Tris-HCl, pH 8.0 25°C, 1400 rpm	50 mM Tris-HCl, pH 8.0 25°C, 1400 rpm
Reaction time / h	Not known	4	10	24
Space-time yield / g*(L*d) <sup>-1</sup>	0.48 <sup>#1</sup>	0.25	0.28	0.32
Conversion / %	100	100	100 <sup>#3</sup>	100 <sup>#3</sup>
t <sub>tn</sub>	80	400	200	3800 <sup>#4</sup>
Improvement		<b>5x</b>	<b>3x</b>	<b>48x</b> <b>419x</b>

#1 The exact process time is not known.  
 #2 Activities were determined using GD<sub>4</sub>K-2NA as substrate.  
 #3 Conversions of 100% are achieved by adjusting the process time according to enzyme inactivation.  
 #4 Total turnover numbers was determined by taking the amount of produced MUC1 present in the reaction solution into account and neglecting MUC1 adsorbed to the carrier material.

## **9.5 Product Purification**

For the purification of MUC1-IgG2a Fc and the cleaved MUC1, Bäckström and co-workers use ion exchange chromatography [21]. Due to the similar amino acid composition of MUC1-IgG2a Fc and MUC1, both proteins possess a similar pI in the range of 7.0. This makes a complete cleavage of the fusion protein necessary to make protein separation possible. In this project, the purification procedure described by Bäckström was used receiving a similar chromatogram for elution. Despite this, analysis using SDS-PAGE revealed two undesired proteins at 30 kDa and 43 kDa. Since these proteins were eluted with the same salt gradient, it has to be assumed that these proteins possess a similar pI as MUC1. Therefore, a change in pH of the elution buffer might not change the elution pattern. By using ion exchange chromatography, MUC1 with a purity of 60 % could be produced, which is not yet sufficient for further research or pharmaceutical applications.

To improve the purity, a filtration step using a membrane with a 100 kDa cut-off was applied. Unfortunately, the product solution was more concentrated instead of further purified. The two undesired proteins do not just have a similar pI, but must also have sterically large structures preventing the diffusion through the pores of the membrane. When applying a membrane with a cut-off of 300 kDa not only the undesired proteins may diffuse through the membrane, but also the target protein MUC1. Despite the expectations of losing MUC1, the target protein was retained and the undesired proteins were washed out. With the first washing step, less than 5 % of MUC1 were lost, which is neglectable with regard to the improvement in product purity.

In conclusion, product purification was significantly simplified by applying ultrafiltration with a 300 kDa membrane achieving a product purity of as much as 94 %. Disadvantages of ion exchange chromatography, such as a limited loading capacity, a specific pH range, pressure limitations and a long process time, can be circumvented when using ultrafiltration. Furthermore, scaling-up can be accomplished more easily compared to ion exchange chromatography.

## 9.6 Outlook

With this work it could be shown that enterokinase is an efficient and attractive tool for the cleavage of fusion proteins. In an optimized procedure enzyme utilization was successfully improved. Since the pharmaceutical industry focuses on the use of fusion proteins for the production of therapeutically important proteins, well investigated procedures for the cleavage of these fusion proteins are necessary. In contrast to chemicals, proteolytic enzymes, especially enterokinase, possess a very high specificity avoiding unspecific cleavage of the fusion protein and allow the cleavage reaction to occur under mild reaction conditions.

Immobilization generally stabilized the enzyme, which could be demonstrated by the repeated utilization of the enzyme-support preparation. By investigating different techniques for post-translational modifications, the immobilized enterokinase might be further stabilized. This may, subsequently, result in a higher number of repeated reaction cycles and therefore in a further improvement of enzyme utilization. It would also be of interest to investigate different immobilization techniques, for example cross-linking a number of enterokinase molecules. Thereby, an enlargement of the biocatalyst occurs which could then be applied in a membrane reactor.

Although a continuous process seemed only moderately suited for fusion protein cleavage, technical improvements of the reactor setup may lead to the improvement of process parameters. A better mixing, an increased retention time and the use of a higher amount of enzyme-support preparation may lead to full conversion. Furthermore, by applying a different immobilization technique, the enzyme may be bound to the support material more stable to be suited for a continuous process.

In case of product purification, ion exchange chromatography using a mixed mode polymeric ion exchanger, such as PolyCSX (Mallinckrodt Baker BV, The Netherlands) should be investigated. By using polyethylenimine (PEI) as spacer, hydrophilic interactions with proteins are provided. A subsequent modification of PEI with carboxylic acid and sulfonic acid groups results in a mixed mode functionality. Thus, it might be possible to bind proteins via different reactions and different affinities making the separation of protein with similar pIs possible.

In biotechnological research, enterokinase has often been used for the cleavage of fusion proteins for the production of antibodies, coagulation factors, growth hormones, vaccines and insulin. Therefore it would be of great interest to apply immobilized enterokinase in the cleavage of other fusion proteins for the production of therapeutically important proteins. In combination with this, reaction parameters for the new substrates need to be determined.



## CHAPTER 10

---

MATERIALS AND METHODS



## 10 Materials and Methods

### 10.1 Materials

#### 10.1.1 Chemicals, biological materials and other substances

Bio-Rad, Munich Germany	Precision Plus Dual Color Standard
Calbiochem, Bad Soden, Germany	Bovine Serum Albumin (BSA)
Fluka, Steinheim, Germany	2-mercaptoethanol Ammonia Ammonium sulphate D(+)-glucose monohydrate Dipotassium hydrogen phosphate Disodium-EDTA Disodium hydrogen phosphate dihydrate L-tryptophan Magnesium chloride hexahydrate Magnesium sulphate Nickel chloride hexahydrate Peptone from casein Potassium dihydrogen phosphate Sodium benzoate Sodium dihydrogen phosphate Yeast extract
Invitrogen, Carlsbad, USA	<i>E. coli</i> BL21* DE3™ EKMax™ Enterokinase NuPAGE® Antioxidant NuPAGE® MES SDS Running Buffer NuPAGE® Sample Reducing Agent NuPAGE® Transfer Buffer SeeBlue® Plus2 Pre-Stained Standard SilverQuest™ Silver Staining Kit Simply Blue™ SafeStain
Merck KGaA, Darmstadt, Germany	Acetic acid Agar-Agar Aluminium chloride hexahydrate Boric acid Calcium chloride dihydrate Glutardialdehyde (25 %) Glycerine Glycine Hydrochloric acid Imidazole Iron sulphate heptahydrate Manganese sulphate monohydrate Sodium chloride Sodium citrate dihydrate Thiamin dichloride Tris(hydroxymethyl)-aminomethane

Roche AG, Mannheim, Germany	Protease inhibitor “complete EDTA-free” (CAS: 04693132001)
Roth GmbH & Co., Karlsruhe, Germany	Alcianblau 8 GS Carbenicillin disodium salt Isopropylthiogalactoside (IPTG)
Sigma-Aldrich, Taufkirchen, Germany	4-Nitrophenyl phosphate disodium salt hexahydrate (pNPP) Antifoam 204 Bradford Reagent Gly-Asp-Asp-Asp-Asp-Lys-2-naphthylamide Goat-anti-mouse-IgG Goat-anti-mouse-IgG + alkaline phosphatase- conjugate N-(3-dimethylaminopropyl)-N-ethylcarbodiimide SIGMAFAST™ BCIP/NBT
Sloning Biotechnology GmbH, Puchheim, Germany	Plasmid pQE60_DsbA-EK-H6
VWR International GmbH, Langenfeld, Germany	Cobalt(II) chloride hexahydrate Copper(II) sulphate pentahydrate Ethanol Sodium molybdate dihydrate Zinc sulphate heptahydrate
Wyeth Research, Cambridge, USA	<i>Escherichia coli</i> K12 pSEC-DsbA/EK <sub>L</sub>

### 10.1.2 Materials

Abimed	Reaction columns (5 mL, 10 mL)
Bio-Rad, Munich, Germany	Profinity IMAC Uncharged Resin
Greiner Bio-One GmbH, Solingen, Germany	Polypropylene centrifuge tubes
Invitrogen, Carlsbad, CA, USA	NuPAGE® Novex 4-12 % Bis-Tris Gel, 1.0 mm PVDF membrane, 0.2 µm pore size
Merck Chimie SAS, France	Estapor Microspheres M2 (070/40 & 070/60)
Millipore GmbH, Schwalbach, Germany	Ultracell, regenerated cellulose YM-5, YM-30
Nunc Immunologie	96 Well Immuno Plates, Transparent, F96, MaxiSorp
Pall Life Sciences, Hauppauge, NY, USA	Ultrasette™ Lab Tangential Flow Device 100 kDa, 30 kDa
QIAGEN GmbH, Hilden, Germany	QIAprep Spin Miniprep Kit
Resindion	Sepabeads® EC-HA203
Schott AG, Mainz, Germany	Fermentation shaking flasks (1 L)



### 10.1.3 Equipments

Agilent Technologies, Inc., Santa Clara, USA	Autosampler HPLC system	ALS G1329A Agilent Series 1100
Beckman Coulter Inc., Fullerton, USA	Centrifuge Centrifugation device	Avanti centrifuge J-20XD Polypropylene centrifuge bottles
Bio-Rad, Munich, Germany	HPLC column	Aminex HPX-87H
Branson, Danbury, USA	Ultrasonic device	Sonifier W-250
Broadley James Corporation, Irvine, USA	pH-electrode	
Chemap AG, Volketswil, Switzerland	Chemap Fermentation Plant (30 L)	
Deutsche Metrohm GmbH & Co., Filderstadt, Germany	pH meter	pH meter 632
Eppendorf, Hamburg, Germany	Glucose Analyser Thermostat	EBIO compact Thermostat plus
Federgari, Pavia, Italy	Autoclave	FVA/3
GE Healthcare, Munich, Germany	FPLC-System	Äkta Purifier 10 Fraction collector Frac-950 Monitor pH/C-900 Autosampler A-900
	Ion exchange column	HiTrap QFF (1 mL) HiPrep 16/10 QFF
GMB Glasmechanik AG, Basel, Switzerland	Cryostat	K20
Invitrogen, Carlsbad, CA, USA	Electrophoretic chamber	XCell SureLock™ Mini-Cell CE mark
Isotopenmessgeräte GmbH, Straubenhardt, Germany	Scanning system for gels and membranes	Raytest Stella®
Kendro Laboratory Products, Osterode, Germany	Centrifuge	Multifuge 3S-R Biofuge pico
Mechanical workshop, Research Centre Juelich, Juelich, Germany	“Batch binding chamber” Ultrafiltration cell (3 L)	
Mettler Toledo, Urdorf, Switzerland	O <sub>2</sub> -electrode	
Perkin Elmer, Rodgau, Germany	Victor <sup>2</sup> 1420 Multilabel Counter	Fluorescence reader
Sartorius, Goettingen, Germany	Scales	BP 2100S BP 211D
	Shaking incubator	Certomat BS1
Shimadzu, Duisburg, Germany	Photometer	UV-1700 PharmaSpec Spectrophotometer UV-150- 02

## 10.2 Methods

### 10.2.1 Expression hosts

#### a) Mammalian cells

Recombinant Chinese Hamster Ovarian (CHO) K1 cells were used for the expression of MUC1-IgG2a Fc. These cells were transfected with the expression vector MUC1-IgG2a-pcDNA3 (Figure 10-1) and integrated the genomic DNA for MUC1-IgG2a in its genome. The glycoprotein MUC1 is linked via an enterokinase recognition sequence to the Fc-region of immunoglobulin G 2a (IgG2a Fc). The signal peptide IgG2a Fc transports the fusion protein to the cell culture medium, allowing easy purification.

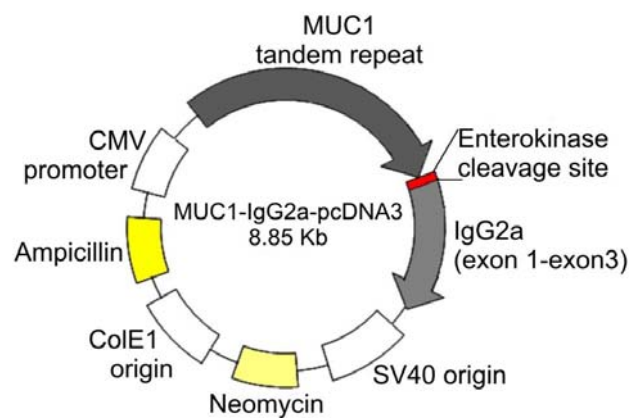


**Figure 10-1 Simplified scheme of the expression vector for the fusion protein MUC1-IgG2a Fc.**

Chinese Hamster Ovarian K1 cells were transfected with the pcDNA3 plasmid.

#### b) Bacterial cells

For the production of enterokinase, the following two expression hosts were used:

***E. coli* K12 GI698** (*F lacIq lacPL8 ampC::lambdacl+*) [7]

***E. coli* BL21\* DE3™** (*F ompT hsdS<sub>B</sub>(r<sub>B</sub><sup>-</sup> m<sub>B</sub><sup>-</sup>) gal dcm rne 131 (DE3)*) (Invitrogen, Carlsbad, USA)

The expression plasmids pSEC-DsbA/EK<sub>L</sub> (Figure 10-2A) encoding the fusion protein DsbA/EK<sub>L</sub> and pQE-60\_DsbA-EK-H6 (Figure 10-2B) encoding DsbA-EK-His were used for transformation. DsbA represents a Thioredoxin homologue, which is responsible for transporting the protein to the periplasmic space of the bacterial cells. The light chain of the enterokinase (EK<sub>L</sub>) is connected to DsbA by a linker sequence and the recognition sequence for enterokinase allowing autocatalytic cleavage. Furthermore, the use of a His-Tag allows the purification of the fusion protein by using affinity chromatography.

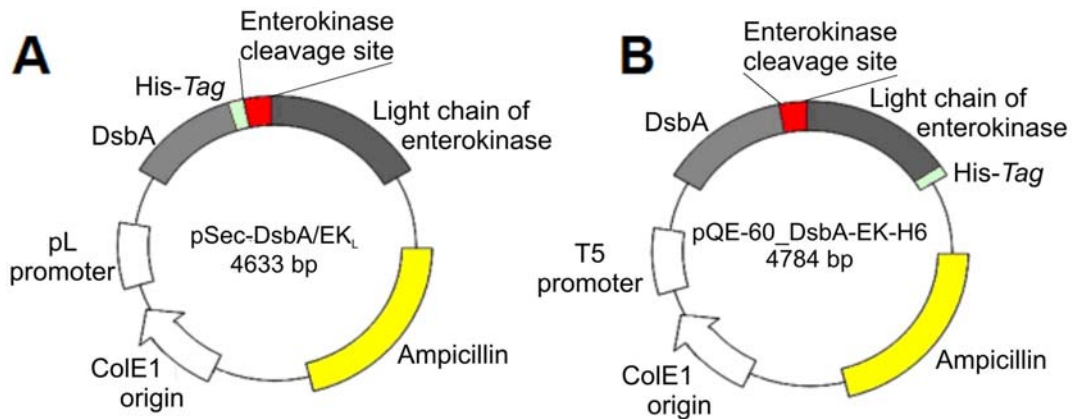


**Figure 10-2** Simplified scheme of the expression plasmids for enterokinase production as fusion protein DsbA/EK<sub>L</sub>.

- A)** Expression of the fusion protein DsbA/EK<sub>L</sub> with His-Tag fused to the fusion partner;  
**B)** Expression of the fusion protein DsbA-EK-H6 with His-Tag fused to enterokinase.

### 10.2.2 Plasmid transformation

The expression plasmid was isolated from *E. coli* K12 according to the vendor's description using the QIAprep Spin Miniprep Kit (QIAGEN GmbH, Hilden, Germany). For transformation, 1 µL plasmid DNA was added to 30-50 µL competent *E. coli* BL21 cells and treated as follows:

Plasmid uptake:	50 min at 4 °C
Nuclease inactivation:	90 sec at 42 °C
Further plasmid uptake:	5 min at 4 °C
Repair of cell membrane and development of antibiotic resistance	adding 500 µL LB-medium (antibiotic-free), incubation for 1 h at 37 °C, 350 rpm (Thermostat plus, Eppendorf, Hamburg, Germany)

For the selection of positively transformed cells, 100 µL of the bacterial suspension was plated onto LB-medium agar plates containing 0.1 g·L<sup>-1</sup> carbenicillin and incubated for 16 h at 37 °C.

### 10.2.3 Fermentation of recombinant *E. coli*

Fermentation of *E. coli* K12 GI698 and *E. coli* BL21\* DE3 were done on a 20 L-scale using minimal medium M9. After fermentation, the cells were harvested by centrifugation and stored at -20 °C. Carbenicillin was added to the medium to select cells containing the vector pSEC-DsbA/EK<sub>L</sub> coding for enterokinase.

A pre-culture was inoculated with a cryo-culture (50 % (v/v) glycerine) of positively selected cells (see 10.2.2) and incubated for at least 12 h at 30 °C with 160 rpm (Certomat BS1, Sartorius, Goettingen, Germany). The main culture of 20 L was inoculated

with about 2 L of pre-cultured cells (10 % v/v). The compositions of the used media are summarized in Table 10-1.

**Table 10-1 Composition of the used media for the fermentation of *Escherichia coli*.**

<i>Component</i>	<i>Concentration / g*L<sup>-1</sup></i>	
LB-Medium (Cryo-culture)		
Peptone	10	
Yeast extract	5	
Sodium chloride	10	
Carbenicillin	0.1	
Minimal media – M9		
	Pre-culture	Main culture
Potassium dihydrogen phosphate	3	3
Dipotassium hydrogen phosphate	12	
Ammonium sulphate	5	5
Magnesium sulphate	0.6	2
Sodium chloride	1	1
Calcium chloride dihydrate	0.015	0.015
Thiamin dichloride	0.0075	0.0075
Iron citrate stock solution	15 mL L <sup>-1</sup>	15 mL L <sup>-1</sup>
Trace elements stock solution	1 mL L <sup>-1</sup>	1 mL L <sup>-1</sup>
Glucose	5	30
Carbenicillin	0.1	0.1
Iron citrate stock solution (150x)		
Iron sulphate heptahydrate	7.5	
Sodium citrate dihydrate	100	
Trace elements stock solution (1000x)		
Aluminium chloride hexahydrate	0.75	
Cobalt chloride hexahydrate	0.6	
Copper sulphate pentahydrate	2.5	
Boric acid	0.5	
Manganese sulphate monohydrate	17.1	
Sodium molybdate dihydrate	3	
Nickel chloride hexahydrate	1.7	
Zinc sulphate heptahydrate	15	

In the beginning of the fermentation, the oxygen supply was guaranteed by an aeration rate of 10 L\*min<sup>-1</sup> and the mixing of the fermentation broth with 400 rpm (Chemap Fermentation Plant). The decreasing oxygen concentration with ongoing fermentation time was compensated by increasing the mixing rate to a maximum of 1000 rpm (Chemap Fermentation Plant) and later by increasing the aeration rate. The pH was constantly adjusted to 6.7 with 25 % ammonia. After reaching a specific optical density of ~20, the initial fermentation temperature of 37 °C was decreased to 25 °C. After an adaptation time of 1 h, the expression in *E. coli* K12 cells was induced with 0.4 g\*L<sup>-1</sup> L-tryptophan.

According to the utilization of glucose, an additional supply with a glucose stock solution ( $500 \text{ g}\cdot\text{L}^{-1}$ ) was initiated in a fed-batch mode. To avoid excessive foam formation 1 % (v/v) Antifoam 204 (Sigma-Aldrich, Taufkirchen, Germany) were added to the fermentation broth. A summary of the fermentation protocol is given in Figure 10-3.

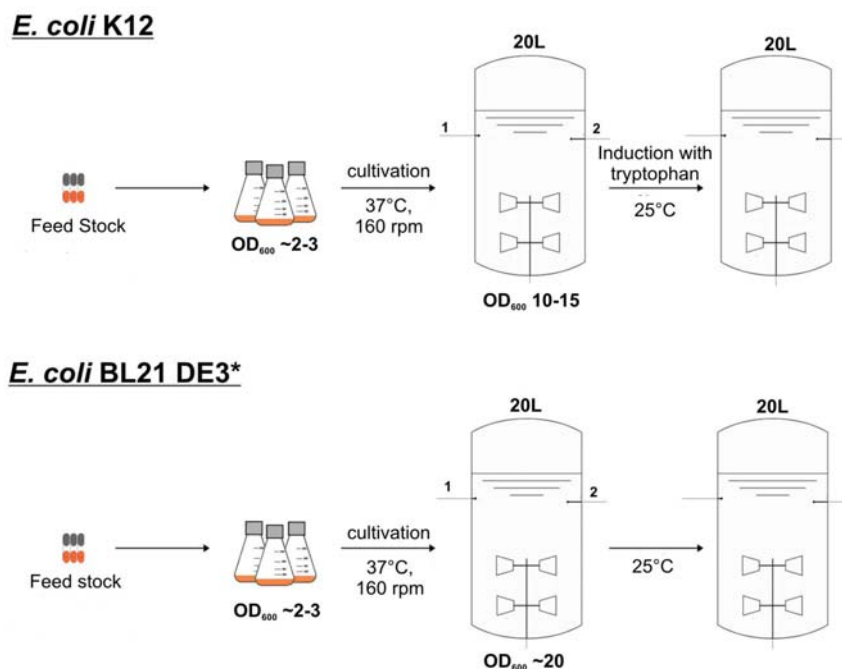


**Figure 10-3 Summary of the fermentation procedure for the production of enterokinase.**

All process parameters, such as pH,  $pO_2$ , mixing rate and aeration rate, were recorded by the Software LabView (v.7.1, National Instruments).

After fermentation, the cells were harvested by centrifugation at 8000 rpm (Avanti centrifuge J-20XD) for 20 min at 4 °C. While discarding the supernatant, the cells were stored in 50 mL fractions at -20 °C until further usage.

### 10.2.4 Fermentation of CHO-K1

Cultivation of CHO K1 was performed in corporation with the Cell Culture Group at the Institute of Biotechnology 2, Research Centre Juelich GmbH.

Starting from a cryo culture of the working cell bank,  $1 \cdot 10^7$  viable cells are used as inoculum for a T75 T-flask having a final cell concentration of about  $1 \cdot 10^6$  viable cells/mL. Cultivation was performed at 37 °C and 5-8 %  $CO_2$ . The cells were diluted with fresh medium to  $3 \cdot 10^5$  viable cells/mL in repeated passages while filling up the T-flask. A T-flask with  $1 \cdot 10^6$  viable cells/mL was then used for inoculation of a spinner flask (Schott, Germany) having a starting cell density of  $3 \cdot 10^5$  viable cells/mL, thereby entering a dynamic culture system. As before with the T-flask, the cells were diluted to  $3 \cdot 10^5$  viable

cells/mL with medium while filling up the spinner flask, which is then used as inoculum for 3-5 L glass reactor (Applicon Biotek, Kunellwald, Germany).

#### CELL CULTURE MEDIUM

Pro CHO4-CDM (Lonza, Switzerland)

- + 0.6 g\*L<sup>-1</sup> glutamine (Gibco, Invitrogen Corporation, Scotland)
- + 1.68 g\*L<sup>-1</sup> sodium bicarbonate (Gibco, Invitrogen Corporation, Scotland)
- + 0.0076 g\*L<sup>-1</sup> thymidine (Fluka, Germany)
- + 0.0136 g\*L<sup>-1</sup> hypoxanthine (Serva, Germany)
- + 0.33 g\*L<sup>-1</sup> G418-sulphate in stock culture (Gibco, Invitrogen Corporation, Scotland)

The culture media of three perfusion cultures were obtained for the isolation of the fusion protein MUC1-IgG2a Fc. Further information about the course of the cultivation is given in the appendix 11.1.

### 10.2.5 Determination of fermentation process parameters

#### Optical density (OD)

For the observation of growth behavior, the optical density was determined by measuring the increase in turbidity of the culture medium at a wavelength of 600 nm.

#### Dry cell weight (DCW)

The cell dry weight was determined by centrifuging 25 mL culture medium at 5000 rpm (Multifuge 3S-R, Kendro Laboratory Products, Osterode, Germany) for 10 min at 4 °C in a 50 mL falcon tube. The received cell pellet was dried at 60 °C until reaching a constant weight. After cooling, the difference in weight between a cell pellet containing falcon tube and an empty falcon tube was determined, giving the cell dry weight.

#### Glucose concentration

Using a glucose analyzer (Eppendorf, Hamburg, Germany), the glucose concentration in the cell-free medium was determined. For the measurement within a range of 0 to 5 g<sub>glucose</sub>\*L<sup>-1</sup>, the samples were diluted with buffer (pH 7.3).

<b>Analyzing buffer:</b>	6.27 g*L <sup>-1</sup>	disodium hydrogen phosphate
	1.15 g*L <sup>-1</sup>	sodium dihydrogen phosphate
	1.5 g*L <sup>-1</sup>	sodium benzoate
	0.5 g*L <sup>-1</sup>	disodium-EDTA
	2.5 g*L <sup>-1</sup>	sodium chloride

### Acetate concentration

Cell-free culture medium is used for the analytical determination of the acetate concentration by a chromatographic separation of organic acids. For quantification, an external one-point calibration with a standard concentration of 1 mM was carried out. Prior to measurement, all samples were diluted 1:10 with deionized water.

The received data was process with the Software Chromeleon 6.8 (Dionex).

#### SPECIFICATION OF HPLC ANALYSIS

Injection volume	100 $\mu$ L
Column	Aminex HPX-87H, 300 x 7.8 mm
Mobile phase	0.1 M sulphuric acid (H <sub>2</sub> SO <sub>4</sub> )
Flow rate	0.5 mL min <sup>-1</sup>
Wavelength	215 nm

### 10.2.6 Cell disruption

The biomass received after fermentation was slowly thawed and resuspended in lysis buffer having a wet cell weight of about 15-30 % (w/v). For minimizing unspecific binding during the purification process, imidazole was added to the lysis buffer in a low concentration. Additionally, protease inhibitors were added to the cell suspension to avoid proteolysis during cell disruption.

Cells were disrupted using ultrasound in a 30 mL flow-through ultrasound cell with a flow rate of 2 mL\*min<sup>-1</sup>.

#### SPECIFICATION OF THE ULTRASOUND PROCEDURE

Time of ultrasound	8 sec
Time of pause	4 sec
Temperature	2 °C

The received suspension was centrifuged for 40 min at 13,000 rpm (JA14, Avanti centrifuge J-20XD, Beckman Coulter Inc., Fullerton, USA) and 4 °C for separating cell debris and soluble protein. The protein solution in the supernatant was applied to affinity chromatography as described in 10.2.7.

### 10.2.7 Affinity chromatography for EK isolation

The fusion protein DsbA/EK<sub>L</sub> contains a His-Tag by which the protein can be specifically separated from the remaining proteins. For binding the desired protein, immobilized metal affinity chromatography (IMAC) was used. The applied material (Profinity™ IMAC Uncharged Resin, BioRad, Munich, Germany) was loaded with nickel-ions according to the vendor's description.

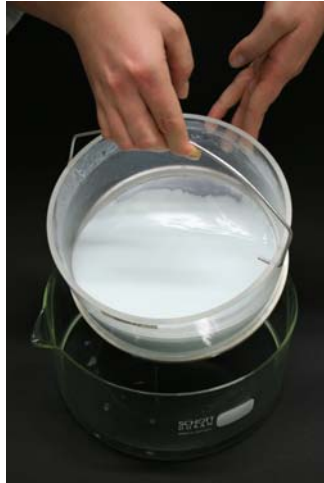


**Figure 10-4** Batch binding cell containing  $\text{Ni}^{2+}$ -IDA sepharose for the purification of the fusion proteins DsbA/EK<sub>L</sub> and DsbA-EK-H6.

The entire procedure was carried out in a batch binding cell (Figure 10-4) located on a rotational shaker at 50 rpm (Polymax 1040, Heidolph Instruments GmbH & Co. KG, Schwabach, Germany).

PROCEDURE OF AFFINITY CHROMATOGRAPHY

Resin equilibration with buffer B1	500 mL, 20 min, 3 times
Protein binding	45 min
Washing with buffer B2	500 mL, 15 min, 5 times
Elution with buffer B3	500 mL, 30 min
Washing with deionized water	500 mL, 15 min

The fractions of the elution as well as of the last washing step with deionized water were pooled, further purified and concentrated by ultrafiltration with a membrane having a 5 kDa cut-off. In parallel, the buffer was changed to standard reaction buffer B4. Further purification of the enterokinase solution was achieved by ion exchange chromatography (10.2.8).

**Table 10-2** Buffer compositions for affinity chromatography.

<i>Buffer</i>	<i>Component</i>	<i>Concentration / g*L<sup>-1</sup></i>
B1 (equilibration)	Tris-HCl, pH 8.0	2.40
	Sodium chloride	11.60
B2 (washing)	Tris-HCl, pH 8.0	2.40
	Sodium chloride	11.60
	Imidazole	2.04
B3 (elution)	Tris-HCl, pH 8.0	2.40
	Sodium chloride	11.60
	Imidazole	13.6
B4 (standard reaction buffer)	Tris-HCl, pH 8.0	6.06
	Calcium chloride*dihydrate	0.15



For detailed analysis, samples were taken after each step of performance for investigations with SDS-PAGE (10.2.15) and enzyme activity testing (10.2.9).

### 10.2.8 Ion exchange chromatography for protein purification

Using an ÄKTApurifier system and a sepharose QFF column (HiPrep 16/10 QFF), target proteins, such as MUC1-IgG2a Fc and enterokinase were further purified. By choosing a pH value approximately 1-1.5 values above the pI of the protein allows the charged target protein to bind to the column material. Applying a salt gradient with NaCl the protein was be eluted from the resin. The received chromatograms of the purified proteins are listed in the appendix (11.2).

**Buffer A:** 50 mM Tris-HCl, pH 8.4

**Buffer B:** 50 mM Tris HCl, pH 8.4  
0.5 M NaCl

#### SPECIFICATION OF RUNNING CONDITIONS

Column equilibration	0.70 CV, 2.5 mL*min <sup>-1</sup> , 100 % Buffer A
Sample injection	1.00 CV, 1.0 mL*min <sup>-1</sup>
Washout unbound sample	0.50 CV, 1.0 mL*min <sup>-1</sup> , 100 % Buffer A
Gradient for Elution	2.50 CV, 2.5 mL*min <sup>-1</sup> , 0-30 % Buffer B 2.50 CV, 2.5 mL*min <sup>-1</sup> , 30 % Buffer B 3.75 CV, 2.5 mL*min <sup>-1</sup> , 30-100 % Buffer B
Column washing	2.00 CV, 2.5 mL*min <sup>-1</sup> , 100 % Buffer B
Column equilibration	2.50 CV, 2.5 mL*min <sup>-1</sup> , 100 % Buffer A

### 10.2.9 Determination of enzyme activity

Enzyme activity was determined fluorometrically using the synthetic substrate Gly-Asp-Asp-Asp-Asp-Lys-2-naphthylamide (GD<sub>4</sub>K-2NA) [114]. The liberated fluorophore 2-naphthylamine (2NA) was determined with a fluorescence spectrophotometer (Victor<sup>2</sup> 1420 Multilabel Counter, Perkin Elmer, Rodgau, Germany) using an excitation filter of 350 nm and an emission wavelength of 460 nm. For calibration a standard solution of 2NA was used. If not stated otherwise, all measurements were performed at 25 °C. The reaction setup was as described in Table 10-3.

**Table 10-3 Reaction setups for activity determination of enterokinase.**

	<i>EK (Invitrogen, Carlsbad, USA)</i>	<i>Isolated EK</i>	<i>Immobilized EK</i>
Standard reaction buffer	70 $\mu$ L	200 $\mu$ L	750 $\mu$ L
1 mM GD <sub>4</sub> K-2NA	25 $\mu$ L	25 $\mu$ L	250 $\mu$ L
Enzyme solution	5 $\mu$ L	25 $\mu$ L	
Total reaction volume	100 $\mu$ L	250 $\mu$ L	1000 $\mu$ L
Measuring volume	100 $\mu$ L	250 $\mu$ L	100 $\mu$ L

**Standard reaction buffer:** 50 mM Tris-HCl, pH 8.0

One unit is defined as the amount of enzyme reducing one micromole of GD<sub>4</sub>K-2NA per minute under the described conditions.

### 10.2.10 Determination of reaction kinetics

Enterokinase was characterized either as soluble enzyme as well as immobilized on the specific carriers.

#### Substrate GD<sub>4</sub>K-2NA

All investigations concerning enzyme characterization for the substrate GD<sub>4</sub>K-2NA were performed using EKMAX™ (Invitrogen, Carlsbad, USA).

#### TEMPERATURE DEPENDENCY

Soluble and immobilized enzyme was incubated at different temperatures (20, 25, 30, 33, 35, 37 and 40 °C) in standard reaction buffer, pH 8.0. Periodically withdrawn samples were assayed for activity as described earlier. The storage stability is given as half-life time after which half the original activity remains assuming exponential decay.

#### PH DEPENDENCY

Soluble and immobilized enzyme was incubated in standard reaction buffer with different pH (pH 5.0-9.0) at 25 °C. Periodically withdrawn samples were assayed for activity as described earlier.

#### Substrate MUC1-IgG2a Fc2a

All reaction setups involving the fusion protein MUC1-IgG2a Fc were performed under sterile and protease-free conditions. Enterokinase isolated from the expression host *E. coli* BL21\* DE3 was used the following investigations.

#### TEMPERATURE DEPENDENCY

Soluble ( $0.19 \text{ U}\cdot\text{mL}^{-1}$ ) and immobilized enzyme ( $0.35 \text{ U}\cdot\text{mL}^{-1}$ ) were added to  $0.233 \text{ mg}\cdot\text{mL}^{-1}$  MUC1-IgG2a Fc (for free EK) or  $1.12 \text{ mg}\cdot\text{mL}^{-1}$  MUC1-IgG2a Fc (for immobilized EK) and incubated in standard reaction buffer, pH 8.0 at different temperatures (20, 25, 30, 33, 35, 37 and 40 °C). Periodically withdrawn samples were assayed by SDS-PAGE and Western Blot analysis.

#### PH DEPENDENCY

Soluble ( $0.19 \text{ U}\cdot\text{mL}^{-1}$ ) and immobilized enzyme ( $0.35 \text{ U}\cdot\text{mL}^{-1}$ ) were added to  $0.233 \text{ mg}\cdot\text{mL}^{-1}$  MUC1-IgG2a Fc (for free EK) or  $1.12 \text{ mg}\cdot\text{mL}^{-1}$  MUC1-IgG2a Fc (for immobilized EK) and incubated in standard reaction buffer with different pH (pH 5.0-9.0) at 25 °C. Periodically withdrawn samples were assayed by SDS-PAGE and Western Blot analysis.

MUC1-IgG2a Fc was separately incubated without enterokinase under the same conditions for investigating the stability of the fusion protein.

#### **10.2.11 Immobilization on Sepabeads®**

The carrier material (pore diameter: 80-150  $\mu\text{m}$ , mean particle diameter: 200-240  $\mu\text{m}$ , functional group density: min.  $0.7 \text{ mmol}\cdot\text{g}^{-1}$ ) was washed with 20 mM sodium phosphate buffer, pH 8.0. 100 mg of support were suspended in sodium phosphate buffer, pH 8.0, containing different amounts of glutardialdehyde (GDA) and were incubated for 1 hour under constant shaking. After intense washing of the support in sodium phosphate buffer, the carrier was mixed with enzyme solution ( $5 \mu\text{g}\cdot\text{mL}^{-1}$ , Invitrogen, Carlsbad, USA) and incubated for 16 hours at 4 °C. Afterwards the enzyme-support preparation was thoroughly washed and the activity was determined as described before.

#### **10.2.12 Immobilization on Estapor paramagnetic microspheres**

100  $\mu\text{L}$  of the carrier suspension (particle diameter: 1.0-2.0  $\mu\text{m}$ , ferrite content 35-45 %) were washed with 10 mM sodium phosphate buffer, pH 6.0. Afterwards, activation of the functional groups was carried out in the same buffer containing N-(3-dimethylaminopropyl)-N-ethylcarbodiimide (EDCA) in a final concentration of  $20 \text{ mg}\cdot\text{mL}^{-1}$  or varying concentrations of glutardialdehyde for 1 hour under constant shaking at 23 °C.  $5 \mu\text{g}\cdot\text{mL}^{-1}$  of enterokinase (Invitrogen, Carlsbad, Germany) were added to the washed, activated paramagnetic microspheres and incubated for 16 hours at 4 °C. The enzyme-support preparation was washed and activity was determined as described before.

### 10.2.13 Post-treatment: Blocking the remaining functional groups

In case of the Estapor paramagnetic microspheres, the remaining functional groups were either blocked with 1 % 2-mercaptoethanol for 40 min or 100 mM glycine for 20 to 40 minutes.

A post-treatment with either 1 % 2-mercaptoethanol or 1 M glycine for 50 min was initiated after the immobilization on hexamethylamino Sepabeads®.

### 10.2.14 Purification of MUC1-IgG2a Fc

The fusion protein MUC1-IgG2a Fc is produced by recombinant CHO K1 cells, which excrete the protein into the cell culture medium. The collected, almost cell-free medium is applied to a purification system (Figure 10-5) consisting of two membrane modules (Pall Life Sciences) with either a 100 kDa or a 30 kDa cut-off. Using this method, the fusion protein is purified and concentrated in one step.

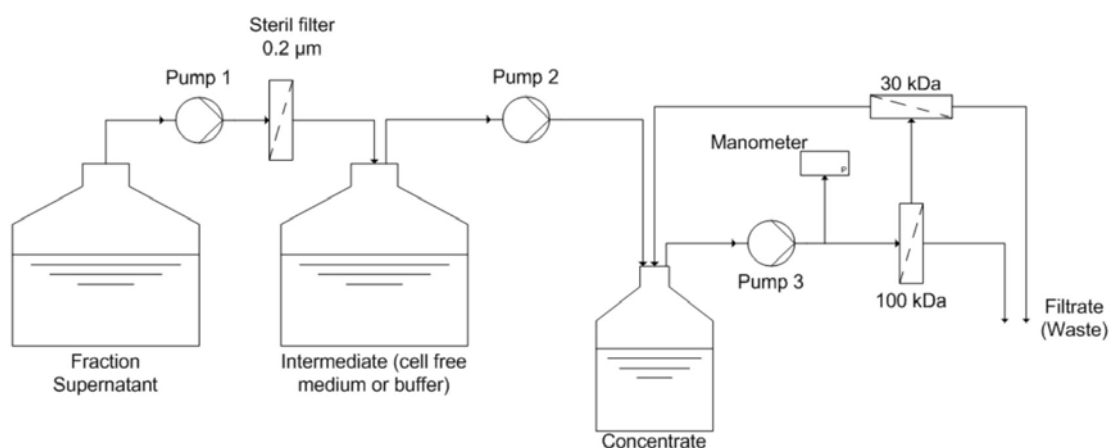


**Figure 10-5** Technical drawing of the 2-membrane module used for the isolation and purification of MUC1-IgG2a Fc from the cell culture medium.

Further purification of received protein solution was necessary. Therefore, ion exchange chromatography, as described in 10.2.8, was carried out. Afterwards, the pure fusion protein solution was concentrated using an ultrafiltration cell (mechanical workshop, Research Centre Juelich GmbH) with a membrane cut-off of 30 kDa.

### 10.2.15 SDS-PAGE

For the analysis of the entire protein content in a sample, a sodium dodecyl sulphate polyacrylamid gel electrophoresis (SDS-PAGE) under reducing conditions was carried out. NuPAGE 4-12 % Bis-Tris gels were used. The SDS-PAGE was performed according to the vendor's description (Invitrogen, Carlsbad, USA). As molecular size standards, either the SeeBlue Plus2® prestained standard (Invitrogen, Carlsbad, USA) or the

Precision Plus Dual Color Standard (BioRad, Munich, Germany) were used. After the electrophoresis the gels were stained depending on the proteins to be detected (see 10.2.16)

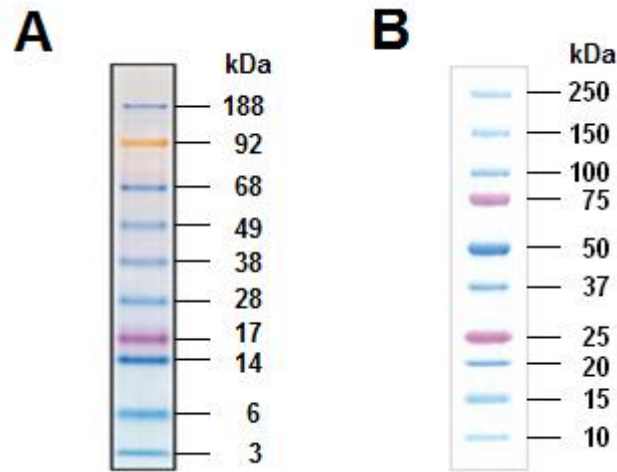


**Figure 10-6 Size marker used for protein identification.**  
A) Invitrogen – SeeBlue Plus2® prestained standard;  
B) BioRad – Precision Plus Dual Color Standard.

## 10.2.16 Gel staining techniques

### Comassie staining

For the detection of enterokinase and the fusion protein DsbA/EK<sub>L</sub>, Simply Blue™ SafeStain (Invitrogen, Carlsbad, USA) was used. The SDS-gels were stained according to the vendor's instructions.

### Silver staining

Using the silver staining method allows the detection of very small traces of protein. This method was carried out by using the SilverQuest™ Silver Staining Kit (Invitrogen, Carlsbad, USA) according to the vendor's instructions.

This staining method was applied for the detection of MUC1-IgG2a Fc and IgG2a Fc as well as enterokinase.

### Alcian blue staining

Alcian blue specifically visualizes glycosylated proteins such as MUC1-IgG2a Fc and MUC1. A 0.125 % alcian blue solution in 10 % acetic acid and 25 % ethanol was applied to the gel for 1 h under shaking conditions. Destaining was performed by incubating the gel 2 times for 30 min in 10 % acetic acid and 25 % ethanol followed by washing the gel for 1 h in deionized water.

### 10.2.17 Western Blot for MUC1-IgG2a Fc

For the detection of MUC1-IgG2a Fc, Western blotting was performed after SDS-PAGE with unstained gels. Therefore, the protein was transferred to a polyvinylidene difluoride (PVDF) membrane. The following immunodetection was done using goat-anti-mouse-IgG-AP antibody. The visualization of the specifically bound antibodies was achieved by applying a solution of BCIP/NBT to the membrane. The entire experimental procedure can be found in the appendix (11.3).

### 10.2.18 ELISA for MUC1-IgG2a Fc

The enzyme-linked immunosorbent assay (ELISA) is mainly used for the determination of specific protein concentrations starting as low as  $0.2\text{-}1.0\ \mu\text{g}\cdot\text{mL}^{-1}$ . Using this method, the concentration of MUC1-IgG2a Fc was determined. The IgG2a Fc specifically binds to the coating antibody (goat-anti-mouse-IgG), which was loaded onto the multi-well plate. By the binding of the conjugate antibody (goat-anti-mouse-IgG-AP) connected to alkaline phosphatase (AP), IgG2a-Fc can be detected specifically. The amount of bound enzyme is proportional to the amount of bound MUC1-IgG2a Fc.

By adding the substrate solution (p-Nitrophenol phosphate – pNPP), an enzymatic cleavage of the phosphate residue occurs causing a coloration of the investigated solutions into yellow, representing the developed nitrophenol. This can be detected photometrically with a wavelength of 405 nm. The intensity of the coloration is proportional to the concentration of the conjugate antibody.

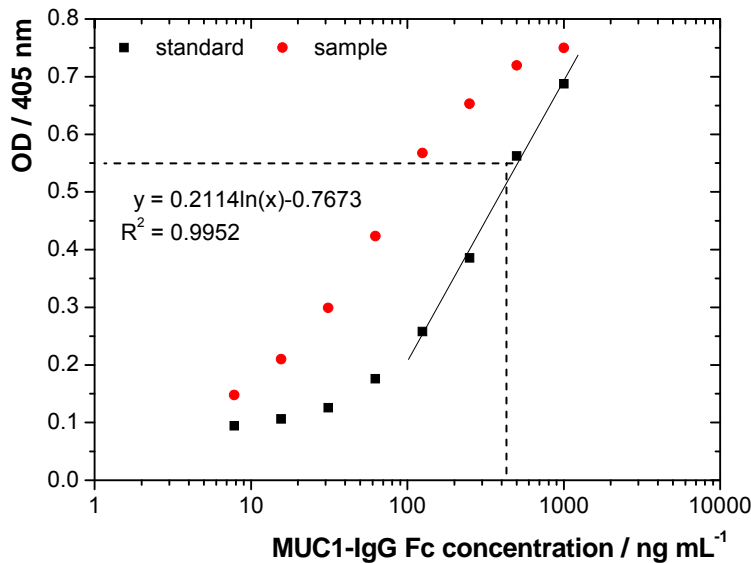


Figure 10-7 Example for data analysis of the ELISA.

The received data of the investigated samples and the data for the standard samples have to be blotted using a logarithmic scaling (Figure 10-7). Using the slope of the linear regression and taking the dilutions of the samples into account, the concentration of the single samples can be calculated. The entire experimental procedure can be found in the appendix (11.4)

#### DETERMINATION OF THE LINEAR REGRESSION

$$y = m * \ln(x) - b$$

y	optical density of the standard
m	slope of the standard linear regression
x	standard concentration / $\mu\text{g} \cdot \text{mL}^{-1}$
b	intersection of standard linear regression with y-axis

#### DETERMINATION OF SAMPLE CONCENTRATION

$$c_{\text{sample}} = \exp\left(\frac{OD_{\text{sample}} + b}{m}\right)$$

$c_{\text{sample}}$	product concentration / $\mu\text{g} \cdot \text{mL}^{-1}$
$OD_{\text{sample}}$	optical density of sample
b	intersection of standard linear regression with y-axis
m	slope of the standard linear regression

### 10.2.19 Analytical investigations

Analytical investigations of the cleavage reaction of MUC1-IgG2a Fc by either free or immobilized enterokinase was finally done using the automation Raytest "Stella", a scanning system for gels and membranes (Isotopenmessgeräte GmbH, Straubenhardt, Germany). After staining, the gels were scanned and analyzed using the software AIDA Analyzer v.4.18, by which each stained protein band is scanned and analyzed according to the number of pixels. Using a standard for each gel, the measured pixels can be blotted over the concentration of the protein. All measurements were subjected to MUC1 as standard protein. In figure 10-8, an example of evaluation of the gel data and the resulting standard curve is given as example.

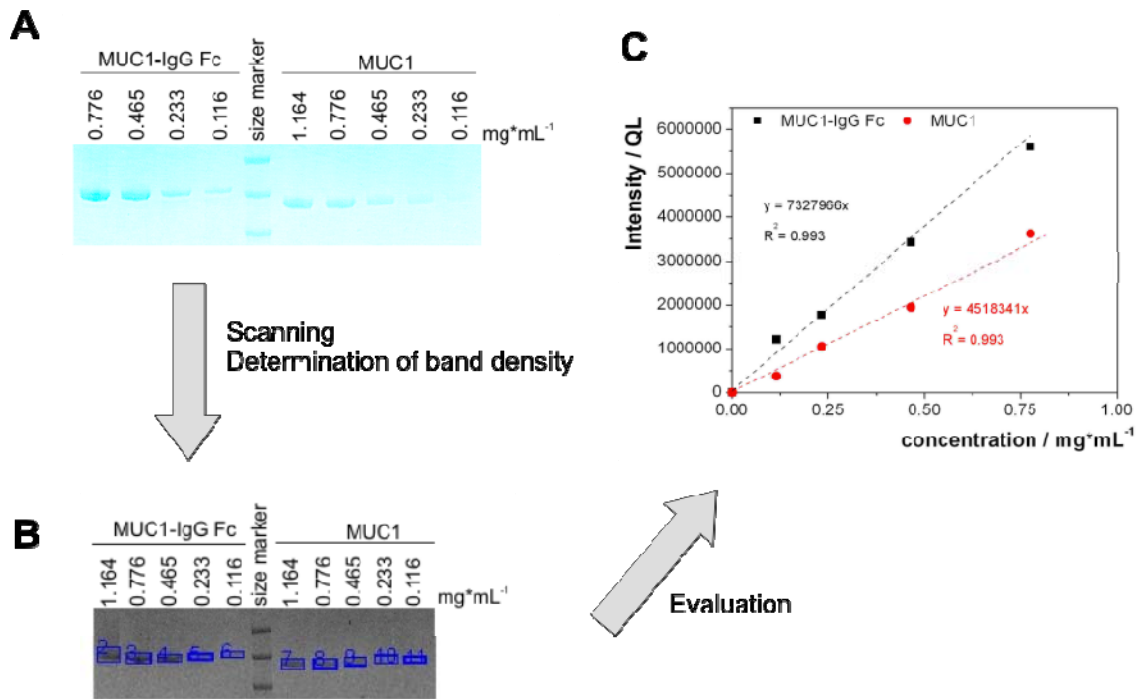


**Figure 10-8 Applied analytical method for investigating the cleavage reaction of MUC1-IgG2a Fc using enterokinase.**

- A)** SDS-PAGE followed by Alcian blue staining for the visualization of glycosylated proteins,
- B)** Scanning of the gel and determination of intensity of desired protein band, and
- C)** plotting intensity of protein band over protein concentration.

Other analytical methods, such as RP-HPLC, SEC, CE and IEC were also tested, but a sufficient analytical separation of MUC1-IgG2a Fc and MUC1 could not be achieved. Results received during the development of the analytical method are presented in the appendix (11.5).

### 10.2.20 Continuous cleavage reaction

For a continuous cleavage of the fusion protein MUC1-IgG2a Fc, 2.2 U\*g<sub>Sepabeads</sub><sup>-1</sup> enterokinase were immobilized according to the method described in 10.2.11 using 4 g Sepabeads® EC-HA203. Prior to this, the entire setup was sterilized using 1 % NaNO<sub>3</sub> followed by extensive washing with sterilized standard reaction buffer. The glass reaction vessel was maintained at 25 °C using a water bath and was stirred with 700 rpm. The substrate solution containing 2.32 mg\*mL<sup>-1</sup> MUC1-IgG2a Fc was cooled to 4 °C to avoid protein degradation by proteases, although being treated under sterile conditions at all times. The enzyme-support preparation was saturated by inducing two repeated batch reactions. By applying a flow rate of 1.7 mL\*h<sup>-1</sup>, a continuous flow was initiated. Fractions were collected for 90 minutes and analyzed according to 10.2.19.



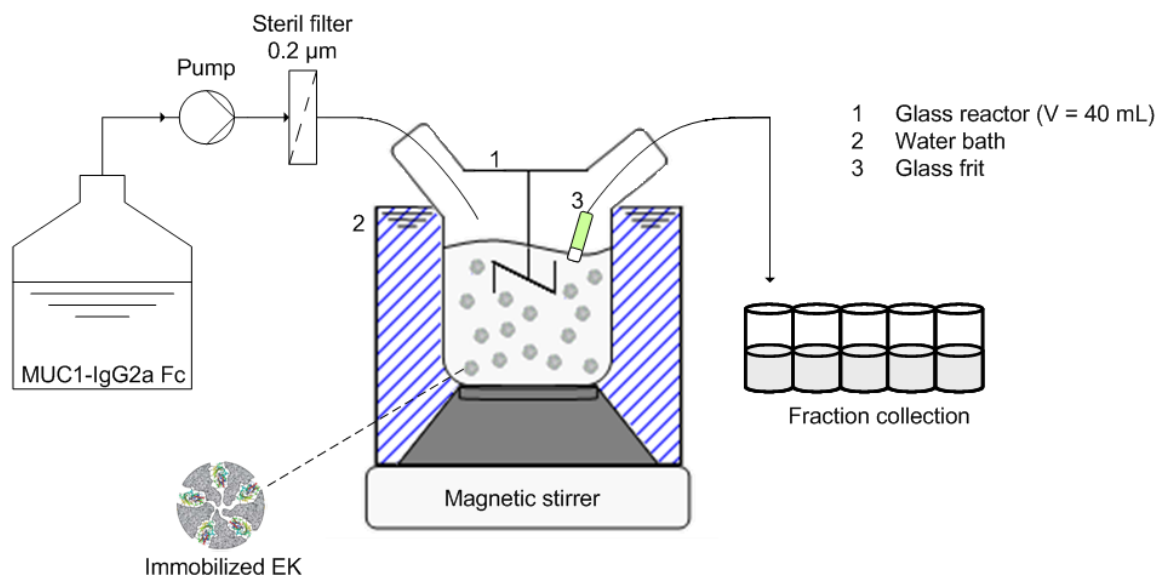


**Figure 10-9** Reactor scheme for continuous cleavage reaction of MUC1-IgG2a Fc by immobilized enterokinase.

### 10.2.21 Repetitive batch reactions

For repetitive batch experiments,  $1.1 \text{ U} \cdot \text{g}_{\text{Sepabeads}}^{-1}$  were immobilized according to the method stated in section 10.2.11. The setups were performed in duplicates. To start the reaction  $1.16 \text{ mg} \cdot \text{mL}^{-1}$  MUC1-IgG2a Fc were added to the immobilized enterokinase under sterile conditions. The cleavage reaction proceeded at  $25 \text{ }^\circ\text{C}$  and 1400 rpm. Regularly withdrawn samples were analyzed using the method described in section 10.2.19. After 24 h, the reaction was stopped by removing the protein solution. Prior to the next batch reaction, the same enzyme-support preparation was washed with 50 mM Tris-HCl, pH 8.0.

### 10.2.22 Product recovery and purification

Two procedures have to be applied for the recovery of MUC1, which is present as soluble fraction in the reaction mixture and as protein adsorbed to Sepabeads<sup>®</sup> EC-HA203.

#### SOLUBLE FRACTION

The reaction solution was removed from the enzyme-support preparation and applied to ultrafiltration using a XM300 membrane. The retentate was washed with sterile deionized water.

#### ADSORBED PROTEIN

The enzyme-support preparation was washed with cold 1 M NaCl. The received protein solution was washed and the buffer was changed to standard reaction buffer before

applying the solution to ultra-filtration. Again, the retentate was washed with sterile deionized water.

The purity of the received product solution was analyzed using the methods described in section 10.2.19. The fractions were lyophilized and stored at -20 °C.

## APPENDIX

---



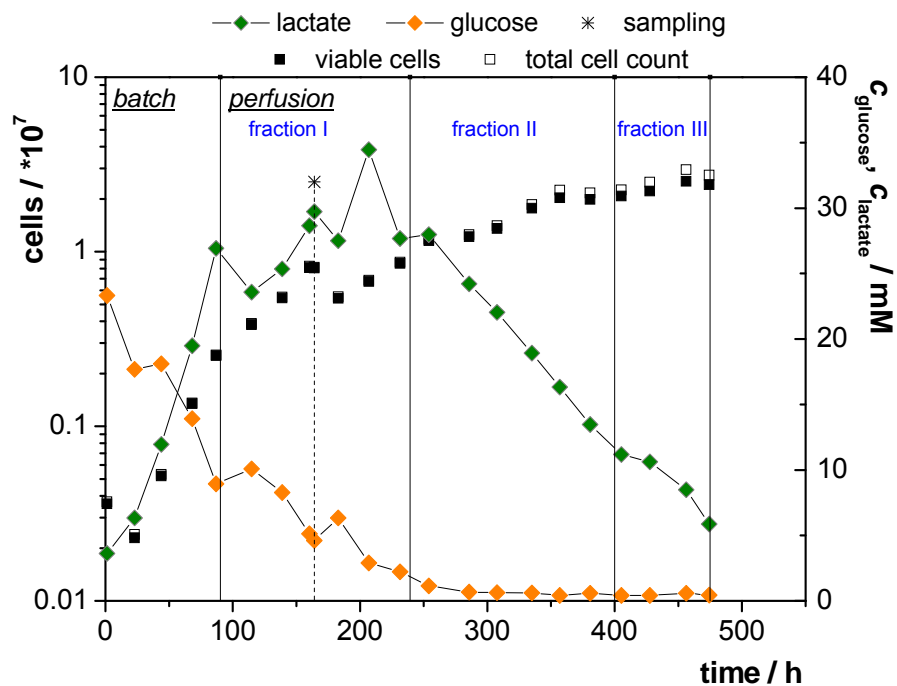
## 11 Appendix

### 11.1 Perfusion cultures of CHO-K1

CHO-K1 cells produce MUC1-IgG2a Fc throughout the cultivation. Maximum production rate was observed with limiting glucose concentration and the decrease in lactate concentration in the cell culture medium.

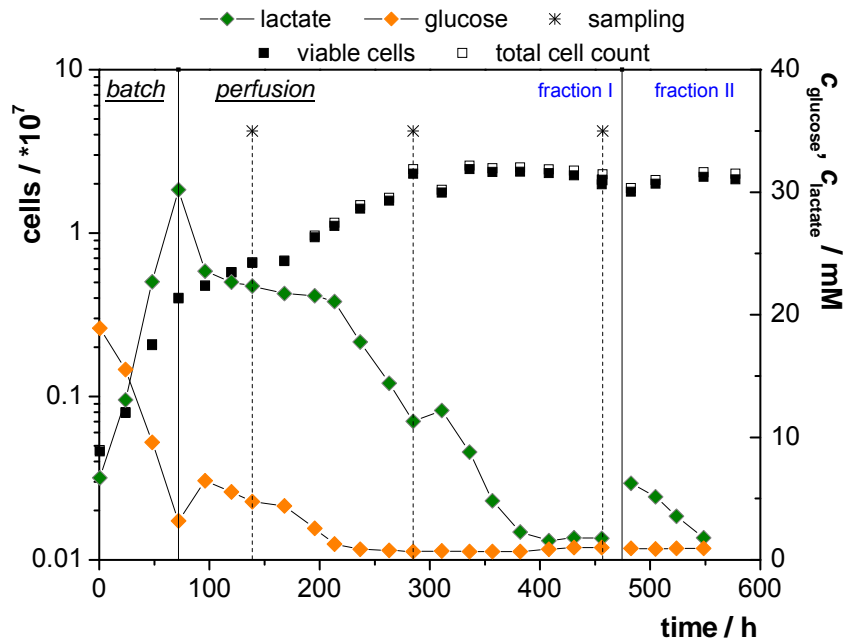
The concentrated solutions containing MUC1-IgG2a Fc were applied to ion exchange chromatography according to 10.2.8. Different fractions were collected and concentrated with an ultra-filtration membrane with a cut-off of 100 kDa, receiving the fractions described in section 3.2.

FERMENTATION 1: R CWPer3



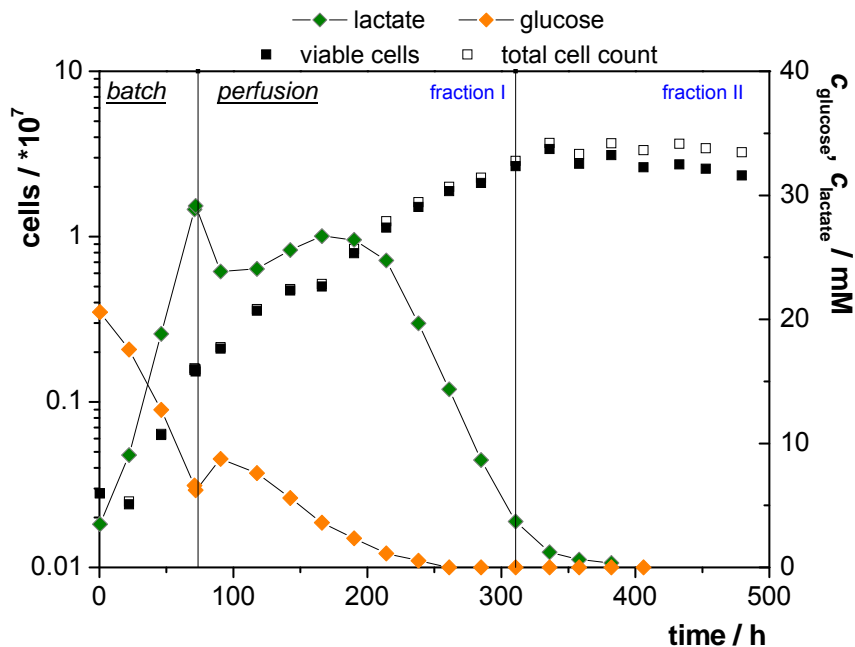
Fraction II and III were used for the isolation and purification of MUC1-IgG2a Fc using the 2-membrane module described in section 10.2.14.

## FERMENTATION 2: R CWPer4



Fraction I and II were used for the isolation and purification of MUC1-IgG2a Fc using the 2-membrane module described in section 10.2.14.

## FERMENTATION 3: RMUC1 Prot2



Fraction I was used for the isolation and purification of MUC1-IgG2a Fc using the 2-membrane module described in section 10.2.14.

## 11.2 Chromatograms of purified proteins by IEC

All proteins used in this project were purified with ion exchange chromatography (HiPrep 16/10 QFF) according to the method described in 10.2.8. Chromatograms for each protein involved in this reaction are given in Figure 11-1.

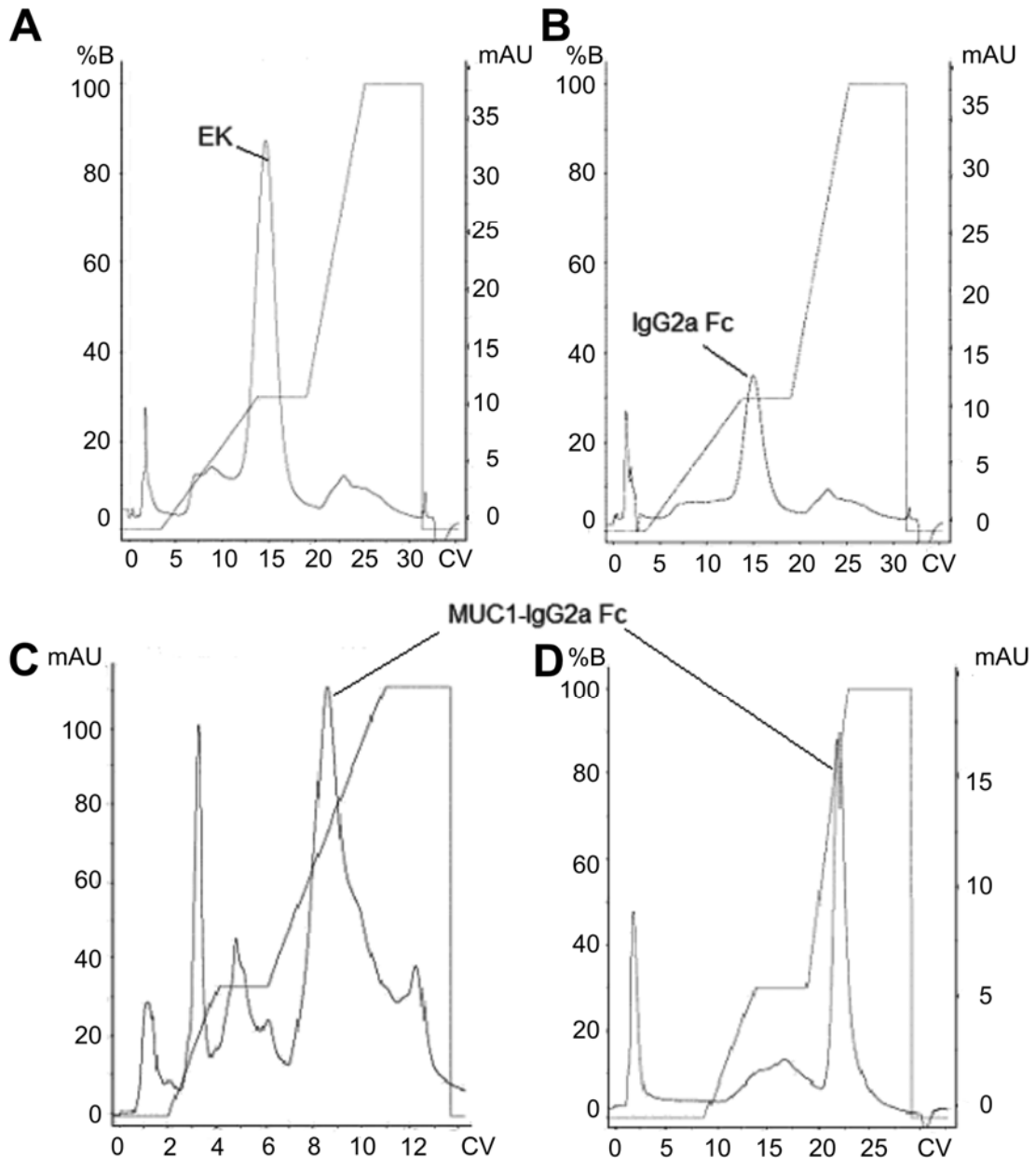


**Figure 11-1** Chromatograms received after ion exchange chromatography using HiPrep 16/10 QFF sepharose.

- A)** enterokinase,
- B)** IgG2a Fc,
- C)** non-purified MUC1-IgG2a Fc,
- D)** purified MUC1-IgG2a Fc.

### 11.3 Immunoblotting for MUC1-IgG2a Fc

#### Transfer of proteins from a SDS-gel to a PVDF membrane

**Transfer Buffer:**                    50 mL 20x NuPAGE® Transfer Buffer  
    850 mL deionized water  
    100 mL methanol

- Incubate filter papers and sponges in transfer buffer
- Incubate membrane in methanol (increases protein capacity)
- Remove plastic from the gel and incubate it in transfer buffer
- Put the blotting chamber together according to Figure 11-2
- Insert blotting chamber in gel chamber and fill with transfer buffer
- 30 V for 60 min

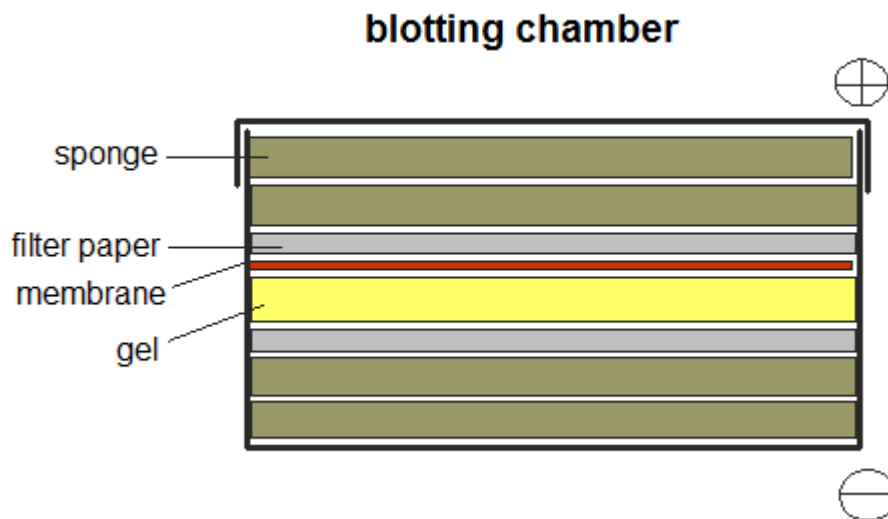


**Figure 11-2** Stacking scheme of blotting chamber for the transfer of proteins from SDS-gel to PVDF membrane.

#### Solutions

**Blocking/Washing Buffer (BWB):**                    6.060 g Tris-HCl (pH 7.4)  
     2.920 g NaCl  
     0.254 g MgCl<sub>2</sub>\*6H<sub>2</sub>O  
     2.5 mL Tween 20

**Antibody solution:**                    20 mL BWB + 40 µL anti-mouse IgG-AP (Sigma 5153)

**APase buffer:**                    1 tablet in 20 mL deionized water (Sigma 2770)

**Substrate solution:**                    1 tablet Sigma fast BCIP/NBT (Sigma 5655) in 10 mL deionized water

**Stop solution:**                    1x PBS  
     20 mM EDTA pH 7.2



Development of the membrane

- Incubate membrane 1 h at 37 °C under slight shaking conditions in BWB
- Incubate membrane 1 h at 37 °C under slight shaking conditions in antibody solution
- Wash membrane twice for 15 min with BWB
- Equilibrate membrane for 3 min in APase buffer
- Incubate membrane in substrate solution until protein bands are clearly visible
- Shortly wash membrane in deionized water
- Incubate membrane for 1 min in stop solution

## 11.4 ELISA for MUC1-IgG2a Fc

### Solutions:

<b>S1 :</b>	PBS 10x	80.0 g*L <sup>-1</sup> 11.5 g*L <sup>-1</sup> 2.0 g*L <sup>-1</sup> 2.0 g*L <sup>-1</sup>	sodium chloride disodium hydrogen phosphate potassium chloride potassium dihydrogen phosphate
	PBS 1x		dilute 10 x PBS with deionized water
<b>S2:</b>	Blocking buffer		Dissolve 1 % BSA (w/v) in 1x PBS
<b>S3:</b>	Washing buffer		Dissolve 0.05 % (v/v) Tween20 in 1x PBS
<b>S4:</b>	Coating antibody (Sigma M-8642)		Dissolve 1 mg goat-anti-mouse-IgG in 25 mL 1x PBS (40 µg*mL <sup>-1</sup> ) Aliquot á 1 mL and store at -20 °C Before use, dilute with 1x PBS to 3 µg*mL <sup>-1</sup>
<b>S5:</b>	Diluting buffer		Dissolve 0.1 % (v/v) BSA in 1x PBS
<b>S6:</b>	Standard Solution		Dilute 1 mg*mL <sup>-1</sup> MUC1-IgG2a Fc Standard with S5 to 1 µg*mL <sup>-1</sup>
<b>S7:</b>	Conjugate antibody (Sigma A-5153)		Goat-anti-mouse-IgG + alkaline phosphatase-conjugate Dilute 1:1000 with S5
<b>S8:</b>	Substrate solution (pNPP) (Sigma N-2770)		Dissolve 1 Tris buffer tablet in 20 mL deionized water Dissolve 1 pNPP tablet in Tris buffer

### Procedure:

- Coating of multi-well plate with 100 µL coating antibody (S4), seal plate with plate sealer and incubate over night at 25 °C
- Wash plate 3x with 200 µL S3
- Block unspecific binding sites by adding 200 µL S2, seal plate with plate sealer and incubate for 2 h at 37 °C
- Wash plate 3x with 200 µL S3
- Measure coated multi-well plate at 405 nm with fluorometric spectrophotometer (Victor<sup>2</sup> 1420 Multilabel Counter, Perkin Elmer, Rodgau, Germany) as a negative reference
- Dilute Standard and samples with S5
- Add 100 µL of S5 in B1-B12 to H1-H12, leave row A empty
- Add 200 µL of standard solution (S6) to A1 and A2, and S5 to A12

- Add 200  $\mu$ L of diluted samples in the remaining wells (each as duplets)
- Pipette 100  $\mu$ L from row A to row B and mix, continue diluting the entire plate according to this procedure until row H, 100  $\mu$ L of row H will be discarded
- Seal plate with plate sealer and incubate for 1 h at 37 °C
- Wash plate 3x with 200  $\mu$ L S3
- Add 100  $\mu$ L freshly prepared conjugate antibody (S7), seal plate with plate sealer and incubate for 1 h at 37 °C
- Wash plate 3x with 200  $\mu$ L S3
- Wash plate with 200  $\mu$ L deionized water
- Add 100  $\mu$ L freshly prepared substrate solution (S8) and directly measure absorbance at 405 nm
- Repeat measurement after 10 to 30 min until reaching an extinction of 0.7 to 0.8 for the standard samples

## 11.5 The challenge of analytical protein separation

For investigating the cleavage reaction of MUC1-IgG2a Fc by enterokinase, an analytical method needed to be developed, which guarantees sufficient separation of the involved proteins. It has to be considered, however, that the product proteins, MUC1 and IgG2a Fc, derive from the substrate protein, MUC1-IgG2a Fc. Thus, the properties of the proteins to be separated analytically possess similar properties with regard to size and amino acid composition. The most important characteristics of the proteins are summarized in Table 11-1.

**Table 11-1 Properties of proteins involved in the cleavage reaction.**

	<i>MUC1-IgG2a Fc</i>	<i>MUC1</i>	<i>IgG2a Fc</i>	<i>EK</i>
Origin	recombinant (CHO K1)	<i>human</i>	<i>murine</i>	recombinant ( <i>E. coli</i> )
Size (kDa)	170	140	30	26
hydrophobic AA	310	208	102	79
hydrophilic AA	492	343	149	102

With the main focus on developing a continuously operated process, a fast and efficient analytical method was necessary. Therefore, the most commonly used techniques, such as RP-HPLC, IEC, SEC and CE have been investigated extensively using different columns. To improve peak separation, several parameters have been varied. Nevertheless, a sufficient separation of the proteins was not achieved. Analytical investigations were finally performed by separating the proteins by gel electrophoresis.

### VARIED PARAMETERS ACCORDING TO COLUMN SPECIFICITY

pH	flow rate
temperature	mobile phase
injection volume	gradient

## ANALYTICAL TECHNIQUES AND COLUMNS

**1) Capillary electrophoresis**

SDS-coated capillary - Beckman (Fullerton, CA, USA)  
(65 cm, 100 µm I.D.)

**2) Size exclusion chromatography**

MZ-Gel SDplus (co 200 kDa)- MZ-Analysentechnik, Mainz, Germany

Superdex 200 - GE Healthcare, Munich, Germany

TSK gel G3000 SWXL - Tosoh, Tokyo, Japan

**3) RP-HPLC**

Jupiter 5u C18 300 - Phenomenex Ltd., Aschaffenburg, Germany

Jupiter 5u C4 300 - Phenomenex Ltd., Aschaffenburg, Germany

Multospher 300-5 C4 - Macherey & Nagel, Düren, Germany

Multo HighBio 300-5 C4 - Macherey & Nagel, Düren, Germany

Nucleosil 300-5 C8 - Chromatographieservice GmbH, Langerwehe, Germany

Nucleosil 300-5 C4 - Chromatographieservice GmbH, Langerwehe, Germany

**4) Ion exchange chromatography**

Mono Q - GE Healthcare, Munich, Germany

Source 15Q - GE Healthcare, Munich, Germany

HiTrap QFF 16/10 - GE Healthcare, Munich, Germany



## REFERENCES

---





## 12 References

- 1 Liese, A., Seelbach, K. and Wandrey, C. (2006) *Industrial Biotransformations*. Wiley-VCH, Weinheim
- 2 Kunitz, M. (1939) Purification and concentration of enterokinase. *Journal of General Physiology* **22**, 447-450
- 3 Kunitz, M. (1939) Formation of trypsin from crystalline trypsinogen by means of enterokinase. *Journal of General Physiology* **22**, 429-446
- 4 Martinez, A., Knappskog, P. M., Olafsdottir, S., Doskeland, A. P., Eiken, H. G., Svebak, R. M., Bozzini, M., Apold, J. and Flatmark, T. (1995) Expression of recombinant human phenylalanine hydroxylase as fusion protein in *Escherichia coli* circumvents proteolytic degradation by host cell proteases - Isolation and characterization of the wild-type enzyme. *Biochemical Journal* **306**, 589-597
- 5 Smith, D. B. and Johnson, K. S. (1988) Single-step purification of polypeptides expressed in *Escherichia coli* as fusions with glutathione S-transferase. *Gene* **67**, 31-40
- 6 Bricteux-Grégoire, S., Schyns, R. and Florin, M. (1972) Phylogeny of trypsinogen activation peptides. *Comparative Biochemistry and Physiology* **42**, 23-39
- 7 Collins-Racie, L. A., McColgan, J. M., Grant, K. L., DiBlasio-Smith, E. A., McCoy, J. M. and La Vallie, E. R. (1995) Production of recombinant bovine enterokinase catalytic subunit in *Escherichia coli* using the novel secretory fusion partner DsbA. *Biotechnology* **13**, 982-987
- 8 Hopp, T. P., Prickett, K. S., Price, V. L., Libby, R. T., March, C. J., Cerretti, D. P., Urdal, D. L. and Conlon, P. J. (1988) A short polypeptide marker sequence useful for recombinant protein identification and purification. *Biotechnology* **6**, 1204-1210
- 9 Krasevec, N., Svetina, M., Gaberc-Porekar, V., Menart, V. and Komel, R. (2003) *In vivo* and *in vitro* cleavage of glucoamylase-TNF $\alpha$  fusion protein secreted from *Aspergillus niger*. *Food Technology & Biotechnology* **41**, 345-351
- 10 La Vallie, E. R., DiBlasio, E. A., Kovacic, S., Grant, K. L., Schendel, P. F. and McCoy, J. M. (1993) A thioredoxin gene fusion expression system that circumvents inclusion body formation in the *Escherichia coli* cytoplasm. *Biotechnology* **11**, 187-193
- 11 Sturmfels, A., Götz, F. and Peschel, A. (2001) Secretion of human growth hormone by the food-grade bacterium *Staphylococcus carnosus* requires a propeptide irrespective of the signal peptide used. *Archives of Microbiology* **175**, 295-300
- 12 Wagner, B., Robeson, J., McCracken, M., Watrang, E. and Antczak, D. F. (2005) Horse cytokine/IgG fusion proteins - mammalian expression of biologically active cytokines and a system to verify antibody specificity to equine cytokines. *Veterinary Immunology and Immunopathology* **105**, 1-14
- 13 Voet, D. and Voet, J. G. (1994). Wiley-VCH, Weinheim
- 14 Blow, D. M. (1976) Structure and mechanism of chymotrypsin. *Accounts of Chemical Research* **9**, 145-151
- 15 Kraut, J. (1977) Serine proteases: structure and mechanism of catalysis. *Annual Reviews of Biochemistry* **46**, 331-358
- 16 Anderson, L. E., Walsh, K. A. and Neurath, H. (1977) Bovine enterokinase: purification, specificity, and some molecular properties. *Biochemistry* **16**, 3354-3360
- 17 Liepnieks, J. J. and Light, A. (1979) The preparation and properties of bovine enterokinase. *Journal of Biological Chemistry* **254**, 1677-1683
- 18 Maina, C. V., Riggs, P. D., Grandea, A. G. r., Slatko, B. E., Moran, L. S., Tagliamonte, J. A., McReynolds, L. A. and Guan, C. D. (1988) An *Escherichia coli* vector to express and purify foreign proteins by fusion to and separation from maltose-binding protein. *Gene* **74**, 365-373

## REFERENCES

- 19 Suh, C. W., Choi, G. S. and Lee, E. K. (2003) Enzymic cleavage of fusion protein using immobilized urokinase covalently conjugated to glyoxyl-agarose. *Biotechnology and Applied Biochemistry* **37**, 149-155
- 20 Forsberg, G., Baastrup, B., Rondahl, H., Holmgren, E., Pohl, G., Hartmanis, M. and Lake, M. (1992) An evaluation of different enzymatic cleavage methods for recombinant fusion proteins applied on des-(1-3)-insulin-like growth factor-I. *Journal of Protein Chemistry* **11**, 201-211
- 21 Bäckström, M., Link, T., Olson, F. J., Karlsson, H., Graham, R., Picco, G., Burchell, J., Taylor-Papadimitriou, J., Noll, T. and Hansson, G. C. (2003) Recombinant MUC1 mucin with a breast cancer-like O-glycosylation produced in large amounts in Chinese-hamster ovary cells. *Biochemical Journal* **3**, 677-686
- 22 Dziadek, S., Hobel, A., Schmitt, E. and Kunz, H. (2005) A fully synthetic vaccine consisting of a tumor-associated glycopeptide antigen and a T-cell epitope for the induction of a highly specific humoral immune response. *Angewandte Chemie-International Edition* **44**, 7630-7635
- 23 Dziadek, S., Kowalczyk, D. and Kunz, H. (2005) Synthetic vaccines consisting of tumor-associated MUC1 glycopeptide antigens and bovine serum albumin. *Angewandte Chemie-International Edition* **44**, 7624-7630
- 24 Li, J. L., Staver, M. J., Curtin, M. L., Holms, J. H., Frey, R. R., Edalji, R., Smith, R., Michaelides, M. R., Davidsen, S. K. and Glaser, K. B. (2004) Expression and functional characterization of recombinant human HDAC1 and HDAC3. *Life Sciences* **74**, 2693-2705
- 25 Walsh, G. (2003) Biopharmaceutical benchmarks - 2003. *Nature Biotechnology* **21**, 865-870
- 26 Holmer, A. F. (2002) New biotechnology medicines in development. *Pharmaceutical Research and Manufacturers of America, Washington, D.C.* (<http://www.phrma.org/publications/publications//2002-20-21.601.pdf>; October 2002)
- 27 Dove, A. (2002) Uncorking the biomanufacturing bottleneck. *Nature Biotechnology* **20**, 777-779
- 28 Itakura, K., Hirose, T., Crea, R., Riggs, A. D., Heyneker, H. L., Bolivar, F. and Boyer, H. W. (1977) Expression in *Escherichia coli* of a chemically synthesized gene for the hormone somatostatin. *Science* **198**, 1056-1063
- 29 Goeddel, D. V., Kleid, D. G., Bolivar, F., Heyneker, H. L., Yansura, D. G., Crea, R., Hirose, T., Kraszewski, A., Itakura, K. and Riggs, A. D. (1979) Expression in *Escherichia coli* of chemically synthesized genes for human insulin. *Process of National Academic Sciences USA* **76**, 106-110
- 30 Brake, A. J., Merryweather, J. P., Coit, D. G., Heberlein, U. A., Masiarz, F. R., Mullenback, G. T., Urdea, M. S., Valenzuela, P. and Barr, P. J. (1984)  $\alpha$ -Factor-directed synthesis and secretion of foreign proteins in *Saccharomyces cerevisiae*. *Process of National Academic Sciences USA* **81**, 4642-4646
- 31 Villa-Komaroff, L., Efstratiadis, A., Broome, S., Lomedico, P., Tizard, R., Naber, S. P., Chick, W. L. and Gilbert, W. (1978) A bacterial clone synthesizing proinsulin. *Process of National Academic Sciences USA* **75**, 3727-3731
- 32 (2008) Nobelpreis für Chemie: Eine grün leuchtende Revolution. In *Süddeutsche Zeitung* 08.10.2008, München
- 33 Hagopian, A. and Eylar, E. H. (1968) Glycoprotein biosynthesis: studies on the receptor specificity of the polypeptidyl: N-acetylgalactosaminyl transferase from bovine submaxillary glands. *Archives of Biochemistry and Biophysics* **128**, 422-433
- 34 Varki, A. (1996) "Unusual" modifications and variations of vertebrate oligosaccharides: Are we missing the flowers for the trees? *Glycobiology* **6**, 707-710
- 35 Brockhausen, I. and Kuhns, W. (1997) Role and metabolism of glycoconjugate sulfation. *Trends Glycoscience and Glycotechnology* **9**, 379-398

## REFERENCES

- 36 Löffler, A., Doucey, M. A., Jansson, A. M., Müller, D. R., deBeer, T., Hess, D., Meldal, M., Richter, W. J., Vliegenthart, J. F. G. and Hofsteenge, J. (1996) Spectroscopic and protein chemical analysis demonstrate the presence of C-mannosylated tryptophan in intact human RNase 2 and its isoforms. *Biochemistry* **35**, 12005-120014
- 37 Baynes, J. W. and Wold, F. (1976) Effect of glycosylation in the *in vivo* circulating half-life ribonuclease. *Journal of Biological Chemistry* **251**, 6016-6024
- 38 Hebert, D. N., Zhang, J. X., Chen, W., Foellmer, B. and Helenius, A. (1997) The number and location of glycans on influenza hemagglutinin determine folding and association with calnexin and calreticulin. *Journal of Cell Biology* **139**, 613-623
- 39 Shimiza, M. and Yamauchi, K. (1982) Isolation and characterization of mucin-like glycoprotein in human milk fat globule membrane. *Journal of Biochemistry* **91**, 515-524
- 40 Hanisch, F. G. and Müller, S. (2000) MUC1: the polymorphic appearance of a human mucin. *Glycobiology* **10**, 439-449
- 41 Gendler, S. J., Taylor-Papadimitriou, J., Duhig, T., Rothbar, J. and Burchell, J. (1988) A highly immunogenic region of human polymorphic mucin expressed by carcinomas is made up of tandem repeats. *Journal of Biological Chemistry* **263**, 12820-12823
- 42 Gendler S, L. C., Taylor-Papadimitriou J, Duhig T, Peat N, Burchell J, Pemberton EN, Lalani E, Wilson D (1990) Molecular cloning and expression of human tumor polymorphic epithelial mucins. *Journal of Biological Chemistry* **265**, 15286-15293
- 43 Wesseling, J., Vandervalk, S. W., Vos, H. L., Sonnenberg, A. and Hilkens, J. (1995) Episialin (Muc1) Overexpression Inhibits Integrin-Mediated Cell-Adhesion to Extracellular-Matrix Components. *Journal of Cell Biology* **129**, 255-265
- 44 Regimbald, L. H., Pilarski, L. M., Longenecker, B. M., Reddish, M. A., Zimmermann, G. and Hugh, J. C. (1996) The breast mucin MUC1 as a novel adhesion ligand for endothelial intercellular adhesion molecule 1 in breast cancer. *Cancer Research* **56**, 4244-4249
- 45 Kam, J. L., Regimbald, L. H., Hilgers, J. H. M., Hoffman, P., Krantz, M. J., Longenecker, B. M. and Hugh, J. C. (1998) MUC1 synthetic peptide inhibition of intercellular adhesion molecule-1 and MUC1 binding requires six tandem repeats. *Cancer Research* **58**, 5577-5581
- 46 Taylor-Papadimitriou, J., Burchell, J., Miles, D. W. and Dalziel, M. (1999) MUC1 and cancer. *Biochimica Et Biophysica Acta-Molecular Basis of Disease* **1455**, 301-313
- 47 Pandey, P., Kharbanda, S. and Kufe, D. (1995) Association of the Df3/Muc1 Breast-Cancer Antigen with Grb2 and the Sos/Ras Exchange Protein. *Cancer Research* **55**, 4000-4003
- 48 Schroten, H., Hanisch, F. G., Plogmann, R., Hacker, J., Uhlenbruck, G., Nobis-Bosch, R. and Wahn, V. (1992) Inhibition of adhesion of S-fimbriated *Escherichia coli* to buccal epithelial cells by human milk fat globule membrane components: a novel aspect of the protective function of mucins in the nonimmunoglobulin fraction. *Infectious Immunology* **60**, 2893-2899
- 49 de Bono, J. S., Rha, S. Y., Stephenson, J., Schultes, B. C., Monroe, P., Eckhardt, G. S., Hammond, L. A., Whiteside, T. L., Nicodemus, C. F., Cermak, J. M., Rowinsky, E. K. and Tolcher, A. W. (2004) Phase I trial of a murine antibody to MUC1 in patients with metastatic cancer: Evidence for the activation of humoral and cellular antitumor immunity. *Annals of Oncology* **15**, 1825-1833
- 50 Sangha, R. and North, S. (2007) L-BLP25: a MUC1-targeted peptide vaccine therapy in prostate cancer. *Expert Opinion in Biological Therapy* **7**, 1723-1730
- 51 Girling, A., Bartkova, J., Burchell, J., Gendler, S., Gillett, C. and Taylor-Papadimitriou, J. (1989) A core protein epitope of the polymorphic epithelial mucin detected by the monoclonal antibody SM-3 is selectively exposed in a range of primary carcinomas. *International Journal of Cancer* **43**, 1072-1076

## REFERENCES

- 52 Burdick, M. D., Harris, A., Reid, C. J., Iwamura, T. and Hollingsworth, M. A. (1997) Oligosaccharides expressed on MUC1 produced by pancreatic and colon tumor cell lines. *Journal of Biological Chemistry* **272**, 24198-24202
- 53 Hanisch, F. G., Peter-Katalinic, J., Egge, H., Dabrowski, U. and Uhlenbruck, G. (1990) Structures of acidic O-linked polylactosaminoglycans on human skim milk mucins. *Glycoconjugate Journal* **7**, 524-525
- 54 Hanisch, F. G., Uhlenbruck, G., Peter-Katalinic, J., Egge, H., Dabrowski, J. and Dabrowski, U. (1989) Structures of neutral O-linked polylactosaminoglycans on human skim milk mucins. A novel type of linearly extended poly-N-acetyllactosamine backbones with Galbeta(1-4)GlcNAc beta(1-6) repeating units. *Journal of Biological Chemistry* **264**, 872-873
- 55 Lloyd, K. O., Burchell, J., Kudryashov, V., Yin, B. W. T. and Taylor-Papadimitriou, J. (1996) Comparison of O-linked carbohydrate chains in MUC-1 mucin from normal breast epithelial cell lines and breast carcinoma cell lines. *Journal of Biological Chemistry* **271**, 33325-33334
- 56 Miles, D. W. and Taylor-Papadimitriou, J. (1999) Therapeutic aspects of polymorphic epithelial mucin in adenocarcinoma. *Pharmacol Therapeut* **82**, 97-106
- 57 Taylor-Papadimitriou, J., Burchell, J. M., Plunkett, T., Graham, R., Correa, I., Miles, D. and Smith, M. (2002) MUC1 and the immunobiology of cancer. *Journal of Mammary Gland Biology and Neoplasia* **7**, 209-221
- 58 Yin, L., Li, Y., Ren, J., Kuwahara, H. and Kufe, D. (2003) Human MUC1 carcinoma antigen regulates intracellular oxidant levels and the apoptotic response to oxidative stress. *Journal of Biological Chemistry* **278**, 35458-35464
- 59 Ho, J. J. L. (2000) Mucins in the diagnosis and therapy of pancreatic cancer. *Current Pharmaceutical Design* **6**, 1881-1896
- 60 Hilkens, J., Ligtenberg, M. J.-L., Vos, H. L. and Litvinov, S. V. (1992) Cell membrane associate mucins and their adhesion modulating property. *Trends in Biochemical Science* **17**, 359-363
- 61 Sangha, R. and Butts, C. (2007) L-BLP25: A peptide vaccine strategy in non-small cell lung cancer. *Clinical Cancer Research* **13**, 465s-4654s
- 62 Briggs, S., Price, M. R. and Tendler, S. J. B. (1993) Fine specificity of antibody recognition of breast carcinoma-associated epithelial mucins: antibody binding to synthetic peptide epitopes. *European Journal of Cancer* **29A**, 230-237
- 63 Burchell, J., Taylor-Papadimitriou, J., Boshell, M., Gendler, S. and Duhig, T. (1989) A short sequence, within the amino acid tandem repeat of a cancer-associated mucin, contains immunodominant epitopes. *International Journal of Cancer* **44**, 691-696
- 64 Xing, P. X., Prenzoska, J. and McKenzie, I. F. (1992) Epitope mapping of anti-breast and anti-ovarian mucin monoclonal antibodies. *Molecular Immunology* **29**, 641-650
- 65 von Mensdorff-Pouilly, S., Verstraeten, A. A., Kenemans, P., Snijdewint, F. G. M., Kok, A., van Kamp, G. J., Paul, M. A., van Diest, P. J., Meijer, S. and Hilgers, J. (2000) Survival in early breast cancer patients is favorably influenced by a natural humoral immune response to polymorphic epithelial mucin. *Journal of Clinical Oncology* **18**, 574-583
- 66 von Mensdorff-Pouilly, S., Gourevitch, M. M., Kenemans, P., Verstraeten, A. A., Litvinov, S. V., van Kamp, G. J., Meijer, S., Vermorken, J. and Hilgers, J. H. M. (1996) Humoral immune response to polymorphic epithelial mucin (MUC1) in patients with benign and malignant breast tumors. *European Journal of Cancer* **32A**, 1325-1331
- 67 Jerome, K. R., Barud, D. L., Bendt, K. M., Boyer, C. M., Taylor-Papadimitriou, J., McKenzie, I. F. C., Bast, R. C. and Finn, O. J. (1991) Cytotoxic T-lymphocytes derived from patients with breast adenocarcinoma recognize an epitope present on the protein core of a human mucin molecule preferentially expressed by malignant cells. *Cancer Research* **51**, 2908-2916

## REFERENCES

- 68 Musselli, C., Livingston, P. O. and Ragupathi, G. (2001) Keyhole limpet hemocyanin conjugate vaccine against cancer: The Memorial Sloan Kettering experience. *Journal of Cancer Research and Clinical Oncology* **127 (Suppl. 2)**, R20-R26
- 69 Link, T. (2003) Glukoselimitierung als Strategie zur Steigerung der Produktion von MUC1 und anderen rekombinanten Glykoproteinen. In *Methematisch-Naturwissenschaftliche Fakultät*, pp. 137, Rheinische Friedrich-Wilhelm Universität, Bonn
- 70 Maroux, S., Baratti, J. and Desnuelle P. (1971) Purification and specificity of porcine enterokinase. *Journal of Biological Chemistry* **246**, 5031-5039
- 71 Tyler, B. (1978) Regulation of Assimilation of Nitrogen-Compounds. *Annual Review of Biochemistry* **47**, 1127-1162
- 72 Rinas, U., Krackehelm, H. A. and Schugerl, K. (1998) Glucose as a substrate in recombinant strain fermentation technology - by-product formation, degradation and intracellular accumulation of recombinant protein. *Applied Microbiology and Biotechnology* **31**, 163-167
- 73 Luli, G. W. and Strohl, W. R. (1990) Comparison of growth, acetate production, and acetate inhibition of *Escherichia coli* strains in batch and fed-batch fermentations. *Applied and Environmental Microbiology* **56**, 1004-1011
- 74 Shiloach, J., Kaufman, J., Guillard, A. S. and Fass, R. (1996) Effect of glucose supply strategy on acetate accumulation, growth, and recombinant protein production by *Escherichia coli* BL21 ( $\lambda$  DE3) and *Escherichia coli* JM109. *Biotechnology and Bioengineering* **49**, 421-428
- 75 Gschaedler, A., Le, N. T. and Boudrant, J. (1994) Glucose and acetate influences on the behavior of the recombinant strain *Escherichia coli* Hb-101 (Gapdh). *Journal of Industrial Microbiology* **13**, 225-232
- 76 Kleman, G. L. and Strohl, W. R. (1994) Acetate metabolism by *Escherichia coli* in high-cell-density fermentation. *Applied and Environmental Microbiology* **60**, 3952-3958
- 77 Han, K., Lim, H. C. and Hong, J. (1992) Acetic acid formation in *Escherichia coli* fermentation. *Biotechnology and Bioengineering* **39**, 663-671
- 78 Holms, W. H. (1986) The central metabolic pathways of *Escherichia coli* - relationship between flux and control at a branch point, efficiency of conversion to biomass, and excretion of acetate. *Current Topics in Cellular Regulations* **28**, 69-105
- 79 Markl, H., Zenneck, C., Dubach, A. C. and Ogbonna, J. C. (1993) Cultivation of *Escherichia coli* to high cell densities in a dialysis reactor. *Applied Microbiology and Biotechnology* **39**, 48-52
- 80 Nakano, K., Rischke, S., Sato, S. and Markl, H. (1997) Influence of acetic acid on the growth of *Escherichia coli* K12 during high-cell-density cultivation in a dialysis reactor. *Applied Microbiology and Biotechnology* **48**, 597-601
- 81 Portner, R. and Markl, H. (1998) Dialysis cultures. *Applied Microbiology and Biotechnology* **50**, 403-414
- 82 Akesson, M., Hagander, P. and Axelsson, J. P. (2001) Avoiding acetate accumulation in *Escherichia coli* cultures using feedback control of glucose feeding. *Biotechnology and Bioengineering* **73**, 223-230
- 83 van de Walle, M. and Shiloach, J. (1998) Proposed mechanism of acetate accumulation in two recombinant *Escherichia coli* strains during high density fermentation. *Biotechnology and Bioengineering* **57**, 71-78
- 84 Shiloach, J. and Fass, R. (2005) Growing *E. coli* to high cell density - A historical perspective on method development. *Biotechnology Progress* **23**, 345-357
- 85 Chmiel, H. (2006) *Bioprozesstechnik*. Elsevier GmbH, Spektrum Akademischer Verlag, München
- 86 Stanbury, P. F. (1995) *Principles of Fermentation Technology*. Butterworth-Heinemann

- 87 Majewski, R. A. and Domach, M. M. (1990) Simple constrained-optimized view of acetate overflow in *Escherichia coli*. *Biotechnology and Bioengineering* **35**, 732-738
- 88 Muttzall, K. (1993) Einführung in die Fermentationstechnik. Behr's Verlag, Hamburg
- 89 Choi, S., Song, H. W., Moon, J. W. and Seong, B. L. (2001) Recombinant enterokinase light chain with affinity tag: Expression from *Saccharomyces cerevisiae* and its utilities in fusion protein technology. *Biotechnology and Bioengineering* **75**, 718-724
- 90 Vozza, L. A., Wittwer, L., Higgins, D. R., Purcell, T. J., Bergseid, M., Collins-Racie, L. A., La Vallie, E. R. and Hoeffler, J. P. (1996) Production of a recombinant bovine enterokinase catalytic subunit in the methylotrophic yeast *Pichia pastoris*. *Biotechnology* **14**, 77-81
- 91 Fehllhammer, H., Bode, W. and Huber, R. (1977) Crystal Structure of Bovine Trypsinogen at 1.8 Å Resolution 2. Crystallographic Refinement, Refined Crystal Structure and Comparison with Bovine Trypsin. *Journal of Molecular Biology* **111**, 415-438
- 92 Antonowicz, I., Hesford, F. J., Green, J. R., Grogg, P. and Hadorn, B. (1980) Application of a new synthetic substrate to the determination of enteropeptidase in rat small intestine and human intestinal biopsies. *Clinical Chimica Acta* **101**, 69-76
- 93 Gasparian, M. E., Ostapchenko, V. G., Schulga, A. A., Dolgikh, D. A. and Kirpichnikov, M. P. (2003) Expression, purification, and characterization of human enteropeptidase catalytic subunit in *Escherichia coli*. *Protein Expression and Purification* **31**, 133-139
- 94 Mikhailova, A. G., Likhareva, V. V., Prudchenko, I. A. and Rumsh, L. D. (2005) Effect of calcium ions on enteropeptidase catalysis. *Biochemistry* **70**, 1129-1135
- 95 Lütz, S., Rao, N. N. and Wandrey, C. (2006) Membranes in biotechnology. *Chemical Engineering & Technology* **29**, 1404-1415
- 96 Mateo, C., Fernández-Lorente, G., Abian, O., Fernández-Lafuente, R. and Guisán, J. M. (2000) Multifunctional epoxy supports: A new tool to improve the covalent immobilization of proteins. The promotion of physical adsorptions of proteins on the supports before their covalent linkage. *Biomacromolecules* **1**, 739-745
- 97 Mateo, C., Abian, O., Fernandez-Lafuente, R. and Guisan, J. M. (2000) Increase in conformational stability of enzymes immobilized on epoxy-activated supports by favoring additional multipoint covalent attachment. *Enzyme and Microbial Technology* **26**, 509-515
- 98 Hildebrand, F. and Lütz, S. (2006) Immobilisation of alcohol dehydrogenase from *Lactobacillus brevis* and its application in a plug-flow reactor. *Tetrahedron: Asymmetry* **17**, 3219-3225
- 99 Schoevaart, R., Wolbers, M. W., Golubovic, M., Ottens, M., Kieboom, A. P. G., van Rantwijk, F., van der Wielen, L. A. M. and Sheldon, R. A. (2004) Preparation, optimization, and structures of cross-linked enzyme aggregates (CLEAs). *Biotechnology and Bioengineering* **87**, 754-762
- 100 Bastida, A., Sabuquillo, P., Armisen, P., Fernández-Lafuente, R., Huguete, J. and Guisán, J. M. (1998) Single step purification, immobilization, and hyperactivation of lipases via interfacial adsorption on strongly hydrophobic supports. *Biotechnology and Bioengineering* **58**, 486-493
- 101 Sheldon, R. A., Schoevaart, R. and van Langen, L. M. (2005) Cross-linked enzyme aggregates (CLEAs): A novel and versatile method for enzyme immobilization (a review). *Biocatalysis and Biotransformation* **23**, 141-147
- 102 Kurlemann, N. and Liese, A. (2004) Immobilization of benzaldehyde lyase and its application as a heterogeneous catalyst in the continuous synthesis of a chiral 2-hydroxy ketone. *Tetrahedron: Asymmetry* **15**, 2955-2958
- 103 Mateo, C., Abian, O., Fernández-Lafuente, R. and Guisán, J. M. (2000) Reversible enzyme immobilization via a very strong and nondistorting ionic adsorption on

REFERENCES

- support-polyethylenimine composites. *Biotechnology and Bioengineering* **68**, 98-105
- 104 Pierre, A. C. (2004) The sol-gel encapsulation of enzymes. *Biocatalysis and Biotransformation* **22**, 145-170
- 105 Veum, L., Hanefeld, U. and Pierre, A. (2004) The first encapsulation of hydroxynitrile lyase from *Hevea brasiliensis* in a sol-gel matrix. *Tetrahedron* **60**, 10419-10425
- 106 De Temino, D. M.-R., Hartmeier, W. and Ansorge-Schumacher, M. B. (2005) Entrapment of the alcohol dehydrogenase from *Lactobacillus kefir* in polyvinyl alcohol for the synthesis of chiral hydrophobic alcohols in organic solvents. *Enzyme and Microbial Technology* **36**, 3-9
- 107 Fonseca, P. and Light, A. (1982) Incorporation of Bovine Enterokinase into Synthetic Phospholipid Vesicles. *Biophysical Journal* **37**, 44-45
- 108 Fonseca, P. and Light, A. (1983) Incorporation of Bovine Enterokinase in Reconstituted Soybean Phospholipid Vesicles. *Journal of Biological Chemistry* **258**, 3069-3074
- 109 Suh, C. W., Park, S. H., Park, S. G. and Lee, E. K. (2005) Covalent immobilization and solid-phase refolding of enterokinase for fusion protein cleavage. *Process Biochemistry* **40**, 1755-1762
- 110 Torres, R., Mateo, C., Fernández-Lorente, G., Ortiz, C., Fuentes, M., Palomo, J. M., Guisan, J. M. and Fernández-Lafuente, R. (2003) A novel heterofunctional epoxy-amino sepabeads for a new enzyme immobilization protocol: Immobilization-stabilization of  $\beta$ -galactosidase from *Aspergillus oryzae*. *Biotechnology Progress* **19**, 1056-1060
- 111 Liao, M.-H. and Chen, D.-H. (2001) Immobilization of yeast alcohol dehydrogenase on magnetic nanoparticles for improving its stability. *Biotechnology letters* **23**, 1723-1727
- 112 López-Gallego, F., Betancor, L., Hidalgo, A., Mateo, C., Guisán, J. M. and Fernández-Lafuente, R. (2004) Optimization of an industrial biocatalyst of glutaryl acylase: Stabilization of the enzyme by multipoint covalent attachment onto new amino-epoxy Sepabeads. *Journal of Biotechnology* **111**, 219-227
- 113 Graham, R. A., Burchell, J. M. and Taylor-Papadimitriou, J. (1996) The polymorphic epithelial mucin: Potential as an immunogen for a cancer vaccine. *Cancer Immunology Immunotherapy* **42**, 71-80
- 114 Antonowicz, I., Hesford, F. J., Green, J. R., Grogg, P. and Hadorn, B. (1980) Application of a New Synthetic Substrate to the Determination of Enteropeptidase in Rat Small-Intestine and Human Intestinal Biopsies. *Clinica Chimica Acta* **101**, 69-76





# CURRICULUM VITAE

---



## 13 Curriculum Vitae

### PERSONAL DATA

Date of Birth 01. January 1981  
Place of Birth Muehlhausen/Thuringia, Germany

### SCIENTIFIC CAREER

10/2008 – Provisional Group Leader: Technical Biocatalysis, Institute of Biotechnology 2, Research Centre Juelich GmbH, Juelich, Germany

### EDUCATION

10/2005 – 09/2008 **Doctoral Thesis**, Research Group: Technical Biocatalysis, Institute of Biotechnology 2, Research Centre Juelich GmbH, Juelich, Germany

Title: Development of a process for the cleavage of a mucin fusion protein enterokinase

11/2003 – 08/2005 **Master of Science in Biomedical Sciences**, University of Applied Sciences Bonn-Rhein-Sieg, Rheinbach, Germany [very good]

Title: The effect of pentoxifylline on the cytoprotective and anti-inflammatory properties of human U937 cells: The role of heme-oxygenase I

Place of Performance: Institute of Biotechnology, Jagiellonian University, Krakow, Poland

09/2000 – 09/2003 Combined studies: **Bachelor of Science in Biology**, University of Applied Sciences Bonn-Rhein-Sieg, Rheinbach, Germany [very good] & **Bachelor of Science – Biosciences with Biomedical Sciences**, Robert-Gordon University, Aberdeen, Scotland, UK [First Class Honours]

Title: RNA-protein interactions of Coxsackievirus B3 3C proteinase with cloverleaf RNA of BEV and PEV

Place of Performance: Institute of Virology, Friedrich-Schiller University, Jena, Germany

09/1991 – 06/2000 **Allgemeine Hochschulreife** (equivalent to A-levels), Albert-Schweitzer Gymnasium, Muehlhausen/Thuringia, Germany [very good]

08/1997 – 06/1998 **High School Diploma**, Student Exchange in Benson Minnesota, USA [very good]

### STUDIES ABROAD

- 02/2005 – 06/2005 Experimental work, master thesis, Institute of Biotechnology, Jagiellonian University, Krakow, Poland
- 09/2002 – 03/2003 Bachelor of Science – Biosciences with Biomedical Sciences, Robert-Gordon University, Aberdeen, Scotland, UK [First Class Honours]

### AWARDS AND SCHOLARSHIPS

- DAAD-Scholarship Research abroad, master thesis in Poland
- BonnConsult Award Award for scientific achievements, bachelor thesis

### ADDITIONAL SCIENTIFIC WORK

- Scientific Assistant, University of Applied Sciences Bonn-Rhein-Sieg, Rheinbach, Germany
- 10/2004 – 01/2005 Organization of a Junior Academy of Science for 6-11 year old highly gifted students
- 11/2003 – 01/2004 Department of Cell Culture and Molecular Genetics
- 03/2002 – 07/2002 Department of General Chemistry
- 10/2001 – 02/2002 Department of General Chemistry

